Optimization and Inference in Networked Dynamical Systems: A Control Theoretic Approach

by

Fakhteh Saadatniaki

A dissertation submitted

In partial fulfillment of the requirements

for the degree of

Doctor of Philosophy

in

Department of Electrical and Computer Engineering

Tufts University

Advisor: Professor Usman Ahmed Khan

May 2019

Abstract

In this thesis, we study problems in the modeling, analysis, and design of complex, distributed, and networked dynamical systems. More specifically, we investigate three distinct problems in networked systems and control theory as follows:

We first address a problem in distributed estimation where a network of agents is tasked to estimate the state of a Continuous-Time, Linear Time-Invariant system under the assumption that no agent possesses enough measurements in its communication range to estimate the entire system state on its own. In this context, we provide a networked Kalman-type estimator that combines prediction and innovation with information fusion among the agents and consider an approach based on designing static estimator gains. The main contribution of this work is to analyze the estimation error using the notions of dissipativity and the input-output approach, enabling us to formulate stability and performance arguments as quasiconvex optimization problems involving linear matrix inequalities. We show that the resulting estimation error is stable and further ensures a given level of performance regarding noise rejection.

Next, we study the optimal control of information epidemics and characterize a variant of the viral marketing phenomenon over heterogeneous social networks. The marketing objective investigated in this framework is product

adoption. In this context, borrowing concepts from the theory of epidemic processes, we model the transitions of the members of the target market between different stages of the adoption process; specifically, we introduce a simple yet insightful 3-compartment setup, i.e., the potential-adopting-dormant-potential model. We then propose an optimal control scheme aiming at simultaneously optimizing the population of the adopting and dormant compartments under given time and resource constraints. We prove the existence of the solution to the optimal control problem and provide both analytical and numerical solutions using the Pontryagin Maximum Principle and Forward-Backward Sweep Method, respectively.

Finally, motivated by various applications from large-scale data science to mobile wireless sensor networks, we aim to solve the distributed optimization problem over multi-agent networks, where each agent has a local function derived from private information. The goal is to have agents collaborate with each other to optimize the sum of these local functions. Existing algorithms mostly deal with the corresponding problems under the assumption that the underlying network topology is strongly-connected, static, and undirected. The contribution of this work lies in the relaxation of such assumptions on the network topology. In particular, we assume that agents communicate according to a time-varying directed graph and present a computationally efficient fast distributed optimization algorithm. Contrary to the existing work, our

proposed algorithm does not require the estimation of the Perron eigenvector of the weight matrices. Instead, the proposed approach, termed as TV-$\mathcal{AB}$, relies on a novel information mixing approach exploiting both row and column-stochastic weights to achieve agreement toward the optimal solution when the underlying graph is directed. We show that TV-$\mathcal{AB}$ converges linearly to the optimal solution when the global objective is smooth and strongly-convex, and the underlying time-varying network exhibits bounded connectivity. We derive the convergence results based on the stability analysis of a linear system of inequalities along with a matrix perturbation argument.

Acknowledgments

The research in this thesis would have been impossible without the encouragement from many others. It is a delight to acknowledge those who have supported me over the last five years.

I would like to express my sincere gratitude to my adviser, Professor Usman Khan, for his continuous support, counsel, and guidance through every stage of my PhD studies. I am grateful for everything you have taught me and I feel incredibly fortunate to have had you as my advisor. I particularly appreciate your fine balance between giving me the freedom to pursue what I was interested in and proposing alternate directions when necessary.

I would like to extend my deepest gratitude to Professor Ronald Lasser, for his mentorship and warm encouragement throughout my PhD career. I very much enjoyed working as your teaching assistant and learned a lot from you.

I am very thankful to my thesis committee members, Professor Aleksander Stanković and Professor Babak Moaveni from Tufts University, and M. Yousof Naderi from Northeastern University, for taking the time to review my thesis. I appreciate the insightful comments and useful suggestions that helped me improve the quality of this work. Meanwhile, I want to thank my colleagues, Sam Safavi, Chenguang Xi, and Ran Xin for investing time and energy discussing ideas with me and transferring their experience and knowledge to me.

To Miriam Santi, George Preble, and Emily Jensen at the Electrical and Computer Engineering Department, thank you for all you have helped me with throughout these years.

Finally, I want to thank my family for their unreserved love and support not only during my time in graduate school but also throughout each and every stage of my life and for their unflagging confidence in me. Words cannot describe what you have done for me, and I can't thank you enough.

Contents

List of Figures

List of Algorithms

Chapter 1

Introduction

1.1 Overview and Outline

The field of Systems and Control Theory originally focused on the modeling, analysis, and design for dynamical systems described by linear or nonlinear differential or difference equations. In the interconnected world of today, however, the focus has shifted towards complex, often distributed and networked, systems. In this thesis, we are interested in systems that capture the dynamics of such multi-agent systems. We take a control theoretic approach to obtain insights and tools for the control of networked systems in the presence of distributed information delivered over a network infrastructure. Specifically, we study problems in distributed estimation, control of spreading processes over networks, and distributed optimization, respectively. In the remainder of this chapter, we briefly introduce each of these problems and provide preliminaries and notations necessary to formulating and approaching these three problems.

1.1.1 Distributed Estimation

Estimation of linear dynamical systems is an active field of research, pioneered by Kalman filtering [1]. However, the increasing complexity of system dynamics, stemming from the high-dimensionality of such systems, and the availability of diverse sensing methodologies push the traditional centralized estimation techniques to the limit and the need for distributed algorithms arises quite naturally. In Chapter 2 of this thesis, we aim to address the distributed estimation of Continuous-Time, Linear Time-Invariant (CT-LTI) systems where a network of agents is tasked to estimate the state under the assumption that no agent possesses enough measurements in its neighborhood to estimate the entire system state on its own. In this context, we provide a networked Kalman-type estimator that combines prediction and innovation with information fusion among the agents and consider an approach based on designing static estimator gains. The main contribution of this work is to analyze the estimation error using the notions of dissipativity and the input-output approach, enabling us to formulate stability and performance arguments as quasiconvex optimization problems involving linear matrix inequalities (LMIs). We show that the resulting estimation error is stable and further ensures a given level of performance regarding noise rejection.

1.1.2 Control of Spreading Processes

In Chapter 3, we study the optimal control of information epidemics and characterize a variant of the viral marketing phenomenon over heterogeneous social networks. The marketing objective investigated in this framework is product adoption. In this context, borrowing concepts from the theory of epidemic processes, we model the transitions of the members of the target market between different stages of the adoption process; specifically, we introduce a simple yet insightful 3-compartment setup, i.e., the potential-adopting-dormant-potential model, which is equivalent to the compartmental model susceptible-infected-recovered-susceptible in epidemiology. We then propose an optimal control scheme aiming at simultaneously optimizing the population of the adopting and dormant compartments under given time and resource constraints. We prove the existence of the solution to the optimal control problem and provide both analytical and numerical solutions using the Pontryagin Maximum Principle and Forward-Backward Sweep Method, respectively.

1.1.3 Distributed Optimization

In Chapter 4 of this thesis, motivated by various applications from large-scale data science to mobile wireless sensor networks, we aim to solve the distributed optimization problem over multi-agent networks, where each agent has access to a local function derived from private information. The goal is to have the agents collaborate with each other to optimize the sum of these local functions. Existing algorithms mostly deal with the corresponding problems under the assumption that the underlying network topology is strongly-connected, static, and undirected. The contribution of this work lies in the relaxation of such assumptions on the network topology. In particular, we assume that agents communicate according to a time-varying directed graph and present a computationally efficient fast distributed optimization algorithm. Contrary to the existing work, our proposed algorithm does not require the estimation of the Perron eigenvector of the weight matrices. Instead, the proposed approach relies on a novel information mixing approach exploiting both row and column-stochastic weights to achieve agreement toward the optimal solution when the underlying graph is directed. We show that our algorithm converges linearly to the optimal solution provided the global objective is smooth and strongly-convex, and the underlying sequence of time-varying directed graphs exhibits bounded connectivity. We derive the convergence results based on the stability analysis of a linear system of inequalities along with a matrix perturbation argument.

1.2 Notations and Preliminaries

In this section, we first introduce the mathematical notation used throughout this work. We then review some of the fundamental concepts regarding graphs and nonnegative matrices, dissipative systems, LMIs, mathematical analysis, and iterative methods necessary to the problems investigated in this work.

1.2.1 Notations

We denote column vectors by lowercase bold letters, $\mathbf{x}$, and matrices by uppercase italics, X. For a vector $\mathbf{x}$, its i^{th} element is denoted by $[\mathbf{x}]_i$, while for a matrix X, its $(i,j)^{\text{th}}$ element is denoted by $[X]_{i,j}$. The superscripts '$\top$' and '$*$' denote transpose and complex-conjugate transpose, respectively.

The $n \times n$ identity matrix, the $n \times m$ zero matrix, and the n-dimensional column vector of all ones are denoted by I_n, $0_{n\times m}$, and $\mathbf{1}_n$, respectively. The indexes are dropped if the context is clear. Similarly, the dependency (t) is dropped for functions of the continuous time variable t to achieve more compact expressions if allowed by the context.

For matrices X and Y, their diagonal aggregation and Kronecker product [2, Definition 4.2.1] are denoted by $\text{diag}[X, Y]$ and $X \otimes Y$, respectively. For a vector $\mathbf{x}$, $\text{diag}[\mathbf{x}]$ denotes a diagonal matrix with elements of $\mathbf{x}$ on the main diagonal. For a square matrix X, $\rho(X)$ denotes the spectral radius, while $\lambda_i(X)$ denotes the i^{th} eigenvalue when X is symmetric. For symmetric matrices, '$\succ$' ('$\succeq$') denotes positive (semi)definiteness, while for a system of linear inequalities written in matrix form $C\mathbf{x} \leq \mathbf{b}$, the inequality sign $\leq$ represents an elementwise comparison.

The notation $\|\cdot\|$ denotes the Euclidean norm for vectors and the spectral norm for matrices, whereas $\|\cdot\|_{\max}$ denotes the l_∞-norm on the set of square matrices. Refer to [3, Chapter 5] for more details.

For a differentiable function $f : \mathbb{R}^p \to \mathbb{R}$, the transpose of its first-order derivative with respect to $\mathbf{x}$ is called the gradient of f and is denoted by $\boldsymbol{\nabla} f(\mathbf{x})$. Its components are the partial derivatives of f: $[\boldsymbol{\nabla} f(\mathbf{x})]_i = \frac{\partial f(\mathbf{x})}{\partial [\mathbf{x}]_i}$, $1 \leq i \leq p$. The extended set of square integrable functions, see e.g., [4, Chapter 4] is denoted by $\mathcal{L}_2^e$ while $\mathbb{R}^+$ is the set of positive real numbers.

For sets $\mathbb{A}$ and $\mathbb{B}$, $\mathbb{A} \times \mathbb{B}$ represents their Cartesian product. In addition, we denote the cardinality, i.e., the number of elements in the set S, by $|S|$.

Definition 1.2.1.1 (Lower Linear Fractional Transformation [5]). *Suppose that matrix G is partitioned into four blocks G_{11}, G_{12}, G_{21}, and G_{22}, such that* *the following expression is well-defined:*

$$\mathcal{F}_l(G, K) = G_{11} + G_{12}K\,(I - G_{22}K)^{-1}\,G_{21}.$$

We denote $\mathcal{F}_l(G, K)$ as the lower Linear Fractional Transformation (LFT) of G with respect to K.

Similarly, $\mathcal{F}_u(G, K) = G_{22}+G_{21}K\,(I - G_{11}K)^{-1}\,G_{12}$ denotes the upper LFT of G with respect to K.

Definition 1.2.1.2 (H_∞ Norm [5]). *For a stable LTI system represented by transfer matrix G, the H_∞ norm is defined as:*

$$\|G\|_\infty \triangleq \sup_{\omega\in\mathbb{R}} \|G(j\omega)\|.$$

1.2.2 Graph Theory

In this section, we present some graph theoretic concepts and basic definitions and preliminaries regarding nonnegative matrices which support the contents in this thesis.

Undirected and Directed Graphs

An undirected graph $\mathcal{G}(\mathcal{V}, \mathcal{E})$ is a collection $\mathcal{V} = \{1, 2, \cdots, n\}$ of nodes/ agents and a collection $\mathcal{E} \subseteq \mathcal{V} \times \mathcal{V}$ of unordered pairs of nodes called edges, i.e., the edges are bidirectional. In contrast, a graph where there exists at least one unidirectional edge is called a directed graph (digraph for short).

Definition 1.2.2.1 (Weighted Adjacency Matrix)**.** *The weighted adjacency matrix of a [di]graph $\mathcal{G}(\mathcal{V},\mathcal{E})$ is a nonnegative matrix $A \in \mathbb{R}^{n\times n}$ such that*

$$\begin{cases} [A]_{i,j} \neq 0, & (j,i) \in \mathcal{E} \\ 0 & \textit{otherwise} \end{cases},$$

where $n = |\mathcal{V}|$. When $[A]_{i,j} \in \{0,1\}$, A is simply referred to as the adjacency matrix of the graph $\mathcal{G}$.

An agent j can send information to an agent i, i.e., $j \longrightarrow i$, if and only if $(j,i) \in \mathcal{E}$.

Definition 1.2.2.2 (Neighborhood of a Node)**.** *Given a digraph $\mathcal{G}(\mathcal{V},\mathcal{E})$ and its [weighted] adjacency matrix A, the in-neighborhood at the i^{th} node is defined as $\mathcal{N}_i^{in} \triangleq \{j|[A]_{i,j} \neq 0\}$ while the out-neighborhood is $\mathcal{N}_i^{out} \triangleq \{j|[A]_{ji} \neq 0\}$.*

Definition 1.2.2.3 (Degree Matrix)**.** *Given a digraph $\mathcal{G}(\mathcal{V},\mathcal{E})$, the in(out) degree matrix $D_{in(out)}$ is a diagonal matrix with the number of in(out) neighbors of agent i on the i^{th} diagonal entry, i.e.,*

$$[D_{in(out)}]_{i,i} = |\mathcal{N}_i^{in(out)}|.$$

For an undirected graph, the adjacency matrix A is symmetric. Therefore, $\mathcal{N}_i^{\text{in}} = \mathcal{N}_i^{\text{out}} = \mathcal{N}_i$ and $D_{\text{in}} = D_{\text{out}} = D$.

Definition 1.2.2.4 ((Strong) Connectivity)**.** *A (di)graph is said to be (strongly) connected if every node is reachable from every other node, i.e., there exists a (directed) path from every node to any other node in the (di)graph.*

1.2.3 Nonnegative Matrices

Definition 1.2.3.1 (Perron Eigenvector)**.** *For a nonnegative square matrix A, the spectral radius $\rho(A)$ is an eigenvalue and the corresponding eigenvector $\boldsymbol{\pi}$ is positive and denoted as the Perron vector: $A\boldsymbol{\pi} = \rho(A)\boldsymbol{\pi}$.*

Definition 1.2.3.2 (Reducibility)**.** *An $n \times n$ matrix A is reducible if there exists an $n \times n$ permutation matrix P such that*

$$P^\top AP = \begin{bmatrix} B & C \\ \mathbf{0}_{n-r,r} & D \end{bmatrix}, \quad 1 \leq r \leq n-1.$$

An $n \times n$ matrix A is irreducible if it is not reducible.

Definition 1.2.3.3 (Primitivity)**.** *A nonnegative square matrix A is primitive if it is irreducible and has only one nonzero eigenvalue of maximum modulus.*

Stochasticity

A stochastic matrix describes the one-step transition probabilities of a Markov chain, i.e., each entry is a nonnegative real number between 0 and 1. A row-stochastic matrix is a nonnegative square matrix, with each row summing up to 1. A column-stochastic matrix is a nonnegative square matrix, with each column summing up to 1. A doubly-stochastic matrix is a nonnegative square matrix with both rows and columns summing up to 1.

Remark 1.2.3.1. *For an $n \times n$ doubly-stochastic matrix W, both the left and right eigenvectors corresponding to the eigenvalue 1 are the vector $\mathbf{1}_n$, i.e.,*

$$W\mathbf{1}_n = \mathbf{1}_n, \qquad \mathbf{1}_n^\top W = \mathbf{1}_n^\top.$$

For an $n \times n$ row-stochastic matrix A, on the other hand,

$$A\mathbf{1}_n = \mathbf{1}_n, \qquad \boldsymbol{\pi}_r^\top A = \boldsymbol{\pi}_r^\top,$$

where $\boldsymbol{\pi}_r \in \mathbb{R}^n$ is not necessarily equal to $\mathbf{1}_n$. Similarly, for an $n \times n$ column-stochastic matrix B,

$$B\boldsymbol{\pi}_c = \boldsymbol{\pi}_c, \qquad \mathbf{1}_n^\top B = \mathbf{1}_n^\top,$$

where $\boldsymbol{\pi}_c \in \mathbb{R}^n$ is not necessarily equal to $\mathbf{1}_n$.

Definition 1.2.3.4 (Stochatic Vector)**.** *A nonnegative vector $\mathbf{x} \in \mathbb{R}^n$ is stochastic if all the elements sum up to 1, i.e.,*

$$\mathbf{1}_n^\top \mathbf{x} = 1.$$

Definition 1.2.3.5 (Absolute Probability Sequence [6])**.** *For a sequence $\{R_k\}$ of row-stochastic matrices, an absolute probability sequence is a sequence $\{\boldsymbol{\pi}_k\}$*

of stochastic vectors such that

$$\boldsymbol{\pi}_k^\top = \boldsymbol{\pi}_{k+1}^\top R_k, \quad \forall\, k \geq 0.$$

Definition 1.2.3.6 (Ergodicity [7])**.** *An ergodic sequence of $n \times n$ row-stochastic matrices $\{R_k\}$ is such that for integers $s \geq 0$ and all $i, j = 1\,, \cdots, n$,*

$$\lim_{e \to \infty} [U_{(e,s)}]_{i,j} \to [\mathbf{d}_s]_j,$$

where $U_{(e,s)} = R_e \cdots R_s$ is the backward product of $\{R_k\}$ and $[\mathbf{d}_s]_j$ is a constant not depending on i.

1.2.4 Dissipativity Theory

Dissipativity theory gives a framework for the design and analysis of control systems using certain input-output properties related to the conservation, dissipation, and transport of energy. We refer to such input-output properties as dissipative properties, and systems with dissipative properties will be termed dissipative systems. More specifically, consider a general state space:

$$\begin{aligned} \dot{\mathbf{x}} &= f(\mathbf{x}, \mathbf{u}), \quad \mathbf{u} \in \mathbb{R}^m, \\ \mathbf{y} &= h(\mathbf{x}, \mathbf{u}), \quad \mathbf{y} \in \mathbb{R}^d, \end{aligned} \tag{1.1}$$

where $\mathbf{x} \in \mathbb{R}^p$ is the p-dimensional state vector and $(\mathbf{u}, \mathbf{y})$ is the input-output pair. We can provide a description of the system based on the concept of dissipativity, relating the internally stored energy of the system to a generalized energy supply rate function $s(\mathbf{u}(t), \mathbf{y}(t))$. The internally stored energy is measured by an energy storage function $S(\mathbf{x}(t))$. As a measure of energy, $S(\mathbf{x}) \geq 0, \forall\, \mathbf{x}$. There are many different notions of dissipativity introduced in various publications, see e.g., [4, Chapter 4] for a detailed discussion. In Chapter 2, we use the following notion of dissipativity:

Definition 1.2.4.1 (Dissipativity [8])**.** *A causal operator $\mathcal{T}$ with input $\mathbf{q}(t)$ and output $\mathbf{p}(t)$ is strictly (X, Y, Z)-dissipative, where $X = X^\top$, Y, and $Z = Z^\top$ are real matrices of appropriate dimensions with $\begin{bmatrix} X & Y \\ Y^\top & Z \end{bmatrix}$ full-rank, if there exists $\varepsilon > 0$ such that for all $\mathbf{q} \in \mathcal{L}_2^e$ and all $\tau \geq 0$,*

$$\int_0^\tau \begin{bmatrix} \mathbf{q}(t) \\ \mathbf{p}(t) \end{bmatrix}^\top \begin{bmatrix} X & Y \\ Y^\top & Z \end{bmatrix} \begin{bmatrix} \mathbf{q}(t) \\ \mathbf{p}(t) \end{bmatrix} dt \leq -\varepsilon \int_0^\tau \mathbf{q}(t)^\top \mathbf{q}(t)\, dt. \tag{1.2}$$

If the inequality in Eq. (1.2) is satisfied with $\varepsilon = 0$, the operator is said to be (X, Y, Z)-dissipative. If $\mathcal{T}$ is also stable and LTI, using Parseval's theorem [4, Theorem 2.5], we obtain the frequency domain equivalent of Eq. (1.2):

$$\begin{bmatrix} I \\ \mathcal{T}(j\omega) \end{bmatrix}^* \begin{bmatrix} X & Y \\ Y^\top & Z \end{bmatrix} \begin{bmatrix} I \\ \mathcal{T}(j\omega) \end{bmatrix} + \varepsilon I \preceq 0, \tag{1.3}$$

for some $\varepsilon > 0$ and almost every $\omega \geq 0$.

1.2.5 Fundamental Results on LMIs

We now revisit some well-established results that are essential to the analysis carried out in Chapter 2.

Lemma 1.2.5.1 (Bounded-Real Lemma, [9, Chapter 10]). *Given the CT-LTI system G:*

$$\dot{\mathbf{x}}(t) = A\mathbf{x}(t) + B\mathbf{u}(t),$$

$$\mathbf{y}(t) = C\mathbf{x}(t) + D\mathbf{u}(t),$$

we have $\|G\|_\infty < \gamma$ *if and only if there exists a real symmetric matrix* $P \succ 0$ *such that*

$$\begin{bmatrix} A^\top P + PA + C^\top C & PB + C^\top D \\ B^\top P + D^\top C & D^\top D - \gamma^2 I_n \end{bmatrix} \prec 0.$$

Lemma 1.2.5.2 (Elimination Procedure for Matrix Variables, [9, Chapter 2]). *Given matrices J, U, and V of appropriate dimensions, there exists a matrix Q satisfying*

$$J + UQV^\top + VQ^\top U^\top \succ 0,$$

if and only if

$$(i)\ \widetilde{U}^\top J \widetilde{U} \prec 0, \qquad and \qquad (ii)\ \widetilde{V}^\top J \widetilde{V} \prec 0,$$

hold, where $\widetilde{U}$ and $\widetilde{V}$ are orthogonal complements of U and V, respectively.

1.2.6 Properties of Functions

We now recap some standard definitions and properties of functions necessary to the last part of this thesis. The details can be found in any standard reference on convex optimization, see, e.g., [10].

Definition 1.2.6.1 (Convexity). *A function $f : \mathbb{R}^p \mapsto \mathbb{R}$ is convex if, for any points $\mathbf{x}$, $\mathbf{y} \in \mathbb{R}^p$, and $\theta \in [0, 1]$, it satisfies*

$$f(\theta\mathbf{x} + (1-\theta)\mathbf{y}) \leq \theta f(\mathbf{x}) + (1-\theta)f(\mathbf{y}).$$

Definition 1.2.6.2 (Smoothness). *A function $f : \mathbb{R}^p \mapsto \mathbb{R}$ is continuously differentiable if its derivative exists and is continuous. It is smooth if it has derivatives of all orders.*

Definition 1.2.6.3 (Strong Convexity). *A smooth convex function $f : \mathbb{R}^p \mapsto \mathbb{R}$ is further said to be strongly convex if there exists some positive μ such that for any point $\mathbf{x}$, $\mathbf{y}$, it satisfies*

$$\left(\boldsymbol{\nabla} f(\mathbf{x}) - \boldsymbol{\nabla} f(\mathbf{y})\right)^\top (\mathbf{x} - \mathbf{y}) \geq \mu\|\mathbf{x} - \mathbf{y}\|^2.$$

Definition 1.2.6.4 (Lipschitz Continuity). *A function $g : \mathbb{R}^p \mapsto \mathbb{R}^m$ is said to be Lipschitz-continuous if there exists a constant $\ell > 0$, such that*

$$\|g(\mathbf{x}) - g(\mathbf{y})\| \leq \ell\|\mathbf{x} - \mathbf{y}\|,$$

for all $\mathbf{x}$, $\mathbf{y} \in \mathbb{R}^p$.

Given the above definitions, we state a standard result in optimization theory regarding the optimality gap in the gradient descent method[1].

Lemma 1.2.6.1. *Let* $g : \mathbb{R}^p \mapsto \mathbb{R}$ *be* μ*-strongly-convex and have* ℓ*-Lipschitz gradient. Define* $\mathbf{x}^+ = \mathbf{x} - \zeta \nabla g(\mathbf{x})$*, where* $0 < \zeta < 2/\ell$*. Then the optimality gap in the domain space shrinks by at least a fixed ratio:*

$$\|\mathbf{x}^+ - \mathbf{x}^*\| \leq \chi \|\mathbf{x} - \mathbf{x}^*\|$$

where $\mathbf{x}^* = \arg\min_{\mathbf{x}} g(\mathbf{x})$ *and* $\chi = \max\{|1 - \zeta\mu|, |1 - \zeta\ell|\}$.

Proof. Given optimality condition, $\boldsymbol{\nabla} g(\mathbf{x}^*) = \mathbf{0}$ and we can treat the minimization problem $\min_{\mathbf{x}} g(\mathbf{x})$ as an equivalent nonlinear equation

$$\mathbf{x}_{k+1} = \Phi(\mathbf{x}_k), \quad k \geq 0, \tag{1.4}$$

where $\Phi : \mathbb{R}^p \mapsto \mathbb{R}^p$ and $\Phi(\mathbf{x}) = \mathbf{x} - \zeta \boldsymbol{\nabla} g(\mathbf{x})$. Note that $\mathbf{x}^*$ is a fixed point of Φ, i.e., $\Phi(\mathbf{x}^*) = \mathbf{x}^*$. Therefore, we can view the gradient descent method as a fixed-point iteration and based on the Contraction Mapping Theorem [11, Proposition A.26], $\mathbf{x}_{k+1}$ converges to the fixed point $\mathbf{x}^*$ if Φ is a contraction.

If we run the fixed-point method in Eq. (1.4) starting at $\mathbf{x}_0$, then we have:

$$\|\mathbf{x}_{k+1} - \mathbf{x}^*\| = \|\mathbf{x}_k - \zeta \boldsymbol{\nabla} g(\mathbf{x}_k) - \mathbf{x}^*\| = \|\Phi(\mathbf{x}_k) - \Phi(\mathbf{x}^*)\|.$$

[1]Refer to [11, Chapter 1] for a detailed introduction and analysis of gradient methods for unconstrained optimization.

Without loss of generality, assume g is twice continuously differentiable, then given the Lipschitz continuity of $\boldsymbol{\nabla} g$ and μ-strong-convexity of g, the eigenvalues of $\boldsymbol{\nabla}^2 g(\mathbf{x})$ are in the interval $[\mu,\, \ell]$ for all $\mathbf{x}$. We then have

$$\begin{aligned}
\|\Phi(\mathbf{y}) - \Phi(\mathbf{z})\| =& \big\|(\mathbf{y}-\mathbf{z}) - \zeta(\boldsymbol{\nabla} g(\mathbf{y}) - \boldsymbol{\nabla} g(\mathbf{z}))\big\| \\
=& \left\|(\mathbf{y}-\mathbf{z}) - \zeta \int_0^1 \boldsymbol{\nabla}^2 g\left(\mathbf{z} + t(\mathbf{y}-\mathbf{z})\right)(\mathbf{y}-\mathbf{z})\mathrm{d}t\right\| \\
=& \left\| \left(I - \zeta \int_0^1 \boldsymbol{\nabla}^2 g\left(\mathbf{z} + t(\mathbf{y}-\mathbf{z})\right)\mathrm{d}t\right)(\mathbf{y}-\mathbf{z})\right\| \\
\leq& \rho\left(I - \zeta \int_0^1 \boldsymbol{\nabla}^2 g\left(\mathbf{z} + t(\mathbf{y}-\mathbf{z})\right)\mathrm{d}t\right)\|\mathbf{y}-\mathbf{z}\|.
\end{aligned}$$

The eigenvalues of the matrix $I - \zeta \int_0^1 \boldsymbol{\nabla}^2 g\left(\mathbf{z} + t(\mathbf{y}-\mathbf{z})\right)\mathrm{d}t$ are in the range

$$[1-\zeta\ell,\, 1-\zeta\mu].$$

Therefore,

$$\rho\left(I - \zeta \int_0^1 \boldsymbol{\nabla}^2 g\left(\mathbf{z} + t(\mathbf{y}-\mathbf{z})\right)\mathrm{d}t\right) = \max\{|1-\zeta\mu|, |1-\zeta\ell|\}.$$

With $0 < \zeta < \frac{2}{\ell}$,

$$0 < \zeta\mu < \zeta\ell < 2 \iff -1 < 1-\zeta\ell < 1-\zeta\mu < 1.$$

Therefore, $\chi < 1$, we have a contraction, and the lemma follows.

□

1.2.7 Convergence Rate for Iterative Methods

Consider the sequence $\{\mathbf{x}_k\}$ and suppose it converges to the limit $\mathbf{x}^*$.

Definition 1.2.7.1 (Q-Linear Convergence). *The sequence* $\{\mathbf{x}_k\}$ *is said to converge Q-linearly (linearly for short) to* $\mathbf{x}^*$ *if there exists a number* $\tau \in (0, 1)$ *such that*

$$\lim_{k\to\infty} \frac{\|\mathbf{x}_{k+1} - \mathbf{x}^*\|}{\|\mathbf{x}_k - \mathbf{x}^*\|} = \tau.$$

The number τ is called the rate of convergence.

Definition 1.2.7.2 (R-Linear Convergence). *The sequence* $\{\mathbf{x}_k\}$ *is said to converge R-linearly to* $\mathbf{x}^*$ *if there exists a sequence* $\{\tau_k\}$ *converging Q-linearly to* 0 *such that*

$$\|\mathbf{x}_k - \mathbf{x}^*\| \leq \tau_k, \quad \forall\, k. \tag{1.5}$$

The R-linear rate extends the definition of linear convergence rate in that the overall convergence rate remains linear while the convergence "speed" at every iteration may vary.

Definition 1.2.7.3 (Sublinear Convergence). *We say that* $\{\mathbf{x}_k\}$ *converges sublinearly to* $\mathbf{x}^*$, *if there exists a number* $\tau_k \to 1$ *for* $k \to \infty$ *such that*

$$\lim_{k\to\infty} \frac{\|\mathbf{x}_{k+1} - \mathbf{x}^*\|}{\|\mathbf{x}_k - \mathbf{x}^*\|} = \tau_k.$$

Typical sublinear rates include $O(\frac{\ln k}{\sqrt{k}})$, $O(\frac{\ln k}{k})$.

1.3 Summary

In this chapter, we provide an outline on how we plan to take a control theoretic approach to obtain insights and tools for the analysis and control of networks in the presence of distributed information. We briefly introduce each of the problems addressed in this thesis and present the necessary notations and concepts.

1.3.1 Contributions

We now summarize the main contributions of this thesis.

1. An input-output approach for distributed estimation (Chapter 2): We take a novel input-output approach toward designing a networked Kalman-type distributed estimator for CT-LTI systems. Our design procedure consists of solving quasiconvex optimization problems involving LMIs. To the best of our knowledge, this work is the first input-output approach for distributed estimation of CT-LTI systems. Parts of the results of this chapter have been published in the proceedings of the 2018 IEEE European Control Conference [12].

2. An epidemiological perspective toward product adoption in heterogeneous networks (Chapter 3): Inspired by the theory of epidemic pro-

cesses, we introduce a new model of viral marketing in social networks and devise an optimal control problem to optimize product adoption in the target market. The results of this chapter have been published in the proceedings of the 52^{nd} IEEE Asilomar Conference on Signals, Systems, and Computers [13].

3. Computationally efficient distributed optimization over dynamic directed networks(Chapter 4): We develop an algorithm for distributed optimization over directed time-varying graphs where the goal is to optimize an objective function composed of a sum of private local functions. Unlike existing algorithms over dynamic directed graphs, our algorithm does not rely on eigenvector estimation to address the information asymmetry in the network. Instead, using a novel information mixing regime based on both row and column-stochastic weight matrices, our algorithm provides a computationally efficient approach to tackle the communication asymmetry without addressing further nonlinearity in the algorithm. This algorithm can be viewed as a general framework for distributed optimization over time-varying directed graphs covering many existing algorithms. In addition, our analysis approach is novel in that it uses the notion of absolute probability sequence and the concept of ergodicity to establish contractions and proves convergence using results

from matrix perturbation theory. The results of this chapter are to be presented in 2019 IEEE Data Science Workshop [14]. A journal version of the results and contributions of this chapter is currently under review for publication in IEEE Transactions on Automatic Control [15].

Chapter 2

Distributed Estimation: An Input-Output Approach

In this chapter, we investigate the distributed estimation of Continuous-Time, Linear Time-Invariant (CT-LTI) systems monitored by a network of agents communicating over an undirected graph. We assume that no agent may possess enough measurements in its neighborhood to estimate the entire state on its own. In this context, we propose a networked Kalman-type estimator that combines prediction and innovation with information fusion among agents and present an approach based on designing static estimator gains. We analyze the estimation error using the notion of dissipativity and the input-output approach[1], which enable us to formulate the stability and performance

[1]Refer to Section 1.2.4 for more details.

arguments as quasiconvex optimization problems [16, Chapter 3.4] involving Linear Matrix Inequalities (LMIs) [9]. We show that the resulting estimation error is stable provided the connectivity of the communication graph and a certain observability argument and further ensures a given level of performance regarding noise rejection. We finish the chapter with numerical simulations.

2.1 Introduction

Distributed estimation of physical and social phenomena has long been a topic of significant interest, see e.g., [17–21]. Some prime examples include tracking objects with multi-agent networks [22], estimating the state of a large-scale power system [23], and studying opinion formation or voting models in complex social networks [24]. Estimating the underlying dynamics in such systems is a challenging problem as measurements are typically distributed over a network of geographically-dispersed agents (sensors, robots, individuals). Distributed estimation, see e.g., relevant work in [25–27], thus enables estimating the dynamics without collecting measurements at a central location, a practically infeasible task, by exploiting local estimation and information fusion.

Relevant work on decentralized estimation of CT-LTI systems can be found in [28–31]. For instance, Ref. [28] considers decentralized state estimation of linear stochastic systems based on a combination of local Kalman filters and a dynamic consensus scheme among the agents. Ref. [29] proposes a theoretical framework for coupled distributed estimation and motion control of mobile sensor networks based on distributed Kalman filtering for collaborative target tracking. Ref. [30] extends adaptive diffusion models to continuous-time setups. Moreover, a recursive algorithm is presented in [31] for the distributed estimation of a moving target under switching interconnection topologies, where the stability of the algorithm is analyzed under mild observability and connectivity assumptions. Of significant relevance to this chapter is Ref. [8], which tackles the problem of control law design for interconnected systems, ensuring global stability and a certain pre-specified performance criterion using the notion of dissipativity, focusing on certain input-output properties of dynamical systems referred to as dissipative properties.

Given that no agent possesses enough measurements in its neighborhood to be able to estimate the entire state vector on its own, standard estimation techniques are not applicable. Our approach, employing a predictor plus innovation estimator, recovers the observability at each agent with the help of consensus on the neighboring predictions. To keep the estimator design simple and develop an estimator that requires minimal computation and coordination, we use a static gain that is the same for both consensus and innovation terms. In this context, we use the machinery developed in Ref. [8] and cast the distributed estimation problem in a similar decentralized control framework, where based on dissipativity characterization of the dynamical systems, we show that the gain design problem can be reduced to two quasiconvex optimization problems under LMI constraints. In particular, we apply the bounded-real lemma and matrix elimination procedure [9, Chapter 2] to obtain existence conditions and a design procedure for a static estimator gain, which guarantees stable error dynamics while also satisfying a given performance level in terms of an upper bound on the H_∞ norm[2] of the global error transfer function. Our design is based on the input-output approach, i.e., given a power spectral density (PSD) specification on the input, the H_∞ norm is closely related to the PSD of the output, see e.g., [32–34].

We now describe the rest of this chapter. Section 2.2 formulates the problem and presents fundamental results on dissipativity and the input-output approach. Sections 2.3 and 2.4 contain the estimation error analysis and present our main results on the design of a static estimator gain ensuring stability and performance specifications, respectively. Section 2.5 illustrates our results and Section 2.6 concludes the chapter.

[2] See Definition 1.2.1.2.

2.2 Problem Formulation

Consider the following CT-LTI dynamics:

$$\dot{\mathbf{x}}(t) = A\mathbf{x}(t), \tag{2.1}$$

where $t \geq 0$ is the continuous time variable, $\mathbf{x}(t) \in \mathbb{R}^p$ is the state vector at time t, and A is the system matrix. The system is assumed to be evolving in response to initial condition $\mathbf{x}(0)$ only.

The measurements for this system are distributed over a network of n potentially geographically dispersed agents, communicating according to an undirected graph $\mathcal{G}(\mathcal{V}, \mathcal{E})$[3]. Each agent i has the following observation model:

$$\mathbf{y}_i(t) = H_i\mathbf{x}(t) + \mathbf{r}_i(t), \tag{2.2}$$

where $\mathbf{y}_i(t) \in \mathbb{R}^{d_i}$ is the local measurement, H_i is the local observation matrix, and $\mathbf{r}_i(t)$ is the zero-mean additive noise whose PSD is bounded by 1. Letting $\mathcal{A}$ and D denote the corresponding adjacency and degree matrices, respectively, the normalized adjacency and Laplacian matrices are defined as $\overline{\mathcal{A}} = D^{-\frac{1}{2}}\mathcal{A}D^{-\frac{1}{2}}$ and $\overline{\mathcal{L}} = I_n - \overline{\mathcal{A}}$, respectively.

Given the dynamical system described by Eq. (2.1) and local observations in Eq. (2.2), the goal is to estimate the state $\mathbf{x}(t)$ of the system in a distributed manner. We assume the state to be globally observable as defined below.

[3]Refer to Section 1.2.2 for preliminaries on graph theory.

Definition 2.2.1 (Global Observability)**.** *The state is said to be globally observable when the matrix, $G = \sum_{i=1}^{N} H_i^\top H_i$, is invertible.*

Clearly, this concept of observability does not require observability at any agent or any neighborhood. As a result, due to a lack of (neighborhood) observability, no agent can implement the standard Kalman filtering equations to estimate the state vector, $\mathbf{x}(t)$, even if it collects all of the measurements in its neighborhood. The distributed estimation problem is thus to estimate the state of the system in this setting.

We propose a variant of the Networked Kalman-type Estimator (NKE), initially introduced in [35], which follows a prediction + innovation framework based on state and output exchange among agents with an additional consensus term from inter-agent interactions to address the distributed nature of the problem. Not only does this force agreement but it also diffuses information on the states for which there may be no measurement in the neighborhood:

$$\dot{\widehat{\mathbf{x}}}_i(t) = \underbrace{A\widehat{\mathbf{x}}_i(t)}_{\text{predictor}} + \underbrace{\sum_{j \in \mathcal{N}_i} K_{ij}\left(\widehat{\mathbf{x}}_j(t) - \widehat{\mathbf{x}}_i(t)\right)}_{\text{state exchange: consensus}} + \underbrace{\sum_{j \in \mathcal{N}_i} B_{ij} H_j^\top \Big(\mathbf{y}_j(t) - H_j \widehat{\mathbf{x}}_i(t)\Big)}_{\text{measurement exchange: innovation}}, \tag{2.3}$$

where $\widehat{\mathbf{x}}_i(t)$ is the local state estimate at agent i, $K_{ij} \in \mathbb{R}^{p \times p}$ are consensus gain matrices, and $B_{ij} \in \mathbb{R}^{p \times p}$ are innovation gain matrices between agents i and j. Towards a simplified estimator that relies on minimal coordination among the agents, we assume the gain matrices to be identical over the consensus and innovation terms and across each agent, i.e., $K_{ij} = \frac{K}{|\mathcal{N}_i|}$, $B_{ij} = K$, where $K \in \mathbb{R}^{p\times p}$; this also serves as a baseline with respect to the solutions obtained with higher degrees of freedom.

2.2.1 Error Dynamics

Defining the local estimation error as $\mathbf{e}_i(t) \triangleq \widehat{\mathbf{x}}_i(t) - \mathbf{x}(t)$, it is straightforward to show that

$$\begin{aligned}
\dot{\mathbf{e}}_i(t) &= \dot{\widehat{\mathbf{x}}}_i(t) - \dot{\mathbf{x}}(t) \\
&= A\mathbf{e}_i(t) + \frac{K}{|\mathcal{N}_i|}\sum_{j\in\mathcal{N}_i}[\mathbf{e}_j(t) - \mathbf{e}_i(t)] - K\left(\sum_{j\in\mathcal{N}_i} H_j^\top H_j\right)\mathbf{e}_i(t) \\
&+ \quad \underbrace{K\sum_{j\in\mathcal{N}_i} H_j^\top \mathbf{r}_j(t)}_{\text{external input due to noise}} \quad .
\end{aligned} \tag{2.4}$$

The matrix K can be thought of as a static estimator gain, designing which is the main goal of this chapter such that the estimation error dynamics are stable at each agent and further meet certain performance criteria with regard to noise rejection. The block diagram corresponding to the graphical representation of the local estimation error dynamics is depicted in Fig. 2.1.

The signals enclosed in the dashed octagon represent the estimation errors from the neighborhood $\mathcal{N}_i$ of agent i, constructing the auxiliary variable $\mathbf{e}_{\mathcal{N}_i}$ as labeled in Fig. 2.1. The aggregate auxiliary signal from the entire network, denoted as $\overline{\mathbf{e}}(t)$, reveals how the network topology affects the global estimation

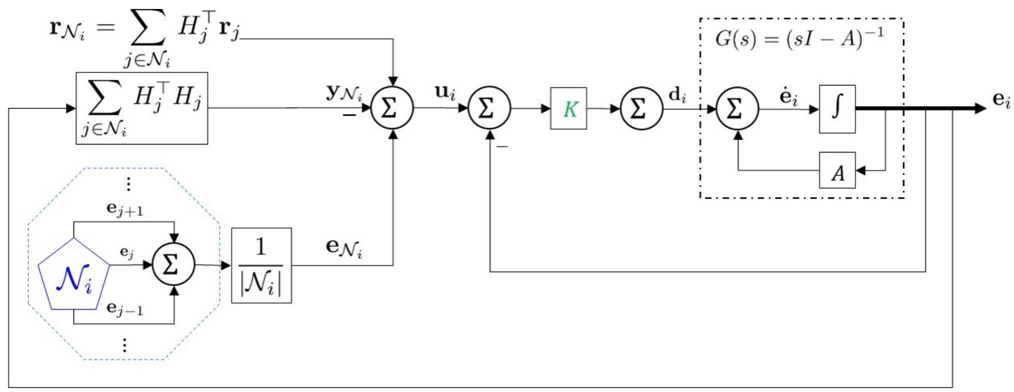

Figure 2.1: Local error dynamics.

error dynamics and is obtained from the global estimation error:

$$\bar{\mathbf{e}}(t) = \begin{bmatrix} \mathbf{e}_{\mathcal{N}_1}(t) \\ \vdots \\ \mathbf{e}_{\mathcal{N}_n}(t) \end{bmatrix} = (\overline{\mathcal{A}} \otimes I_p) \begin{bmatrix} \mathbf{e}_1(t) \\ \vdots \\ \mathbf{e}_n(t) \end{bmatrix} \triangleq (\overline{\mathcal{A}} \otimes I_p)\mathbf{e}(t).$$

Next we investigate the effect of agent measurements on the global estimation error dynamics:

$$\bar{\mathbf{y}}(t) = \begin{bmatrix} \mathbf{y}_{\mathcal{N}_1}(t) \\ \vdots \\ \mathbf{y}_{\mathcal{N}_n}(t) \end{bmatrix} = D_H \begin{bmatrix} \mathbf{e}_1(t) \\ \vdots \\ \mathbf{e}_n(t) \end{bmatrix},$$

where D_H is a block-diagonal matrix with $\sum_{j\in\mathcal{N}_i} H_j^\top H_j$ as its i^{th} block, and

$$\bar{\mathbf{r}}(t) = \begin{bmatrix} \mathbf{r}_{\mathcal{N}_1}(t) \\ \vdots \\ \mathbf{r}_{\mathcal{N}_n}(t) \end{bmatrix} = \begin{bmatrix} \sum_{j\in\mathcal{N}_1} H_j^\top r_j(t) \\ \vdots \\ \sum_{j\in\mathcal{N}_n} H_j^\top r_j(t) \end{bmatrix}, \tag{2.5}$$

which is the external input due to measurement noise.

The input-output relationship of the local error dynamics represented in Fig. 2.1 can be further simplified by taking Laplace transform and noting that

$$\mathbf{e}_i(s) = G(s)K\left(\mathbf{r}_{\mathcal{N}_i}(s) + \mathbf{e}_{\mathcal{N}_i}(s) - \mathbf{y}_{\mathcal{N}_i}(s) - \mathbf{e}_i(s)\right),$$

where $\mathbf{u}_i(s) \triangleq \mathbf{r}_{\mathcal{N}_i}(s) + \mathbf{e}_{\mathcal{N}_i}(s) - \mathbf{y}_{\mathcal{N}_i}(s)$, $G(s)$ is the transfer function from $\mathbf{d}_i$ (as labeled in Fig. 2.1) to $\mathbf{e}_i$, and

$$\mathbf{e}_i(s) = T_i(s)\mathbf{u}_i(s),$$

where $T_i(s) = (I+G(s)K)^{-1}G(s)K$ is the unity feedback system from $\mathbf{u}_i$ to $\mathbf{e}_i$, depicted in Fig. 2.2a. By rewriting $T_i(s)$ as $G(s)K(I+\ G(s)K)^{-1}$ based on the push-through rule from [36, Chapter 3], we can express $T_i(s)$ in terms of the lower LFT[4] of $\mathcal{P}(s)$ with respect to K:

$$\mathcal{F}_l(\mathcal{P}(s), K) = \mathcal{P}_{11}(s) + \mathcal{P}_{12}(s)K(I - \mathcal{P}_{22}(s)K)^{-1}\mathcal{P}_{21}(s),$$

as in Fig. 2.2b, where

$$\mathcal{P}(s) = \begin{bmatrix} \mathcal{P}_{11}(s) & \mathcal{P}_{12}(s) \\ \mathcal{P}_{21}(s) & \mathcal{P}_{22}(s) \end{bmatrix} = \begin{bmatrix} \mathbf{0} & G(s) \\ I & -G(s) \end{bmatrix}. \tag{2.6}$$

For the global error process, concatenating $\mathbf{u}_i(t)$ in a vector $\mathbf{u}(t)$ results in:

$$\mathbf{u}(t) = \overline{\mathbf{r}}(t) + \overline{\mathbf{e}}(t) - \overline{\mathbf{y}}(t) = \overline{\mathbf{r}}(t) + [(\overline{\mathcal{A}} \otimes I_p) - D_H]\mathbf{e}(t).$$

The resulting global error process with $\overline{\mathbf{r}}(t)$ as the input and $\mathbf{e}(t)$ as the output is represented in Fig. 2.3. This system can be interpreted as the lower LFT of n

[4] See Definition 1.2.1.1.

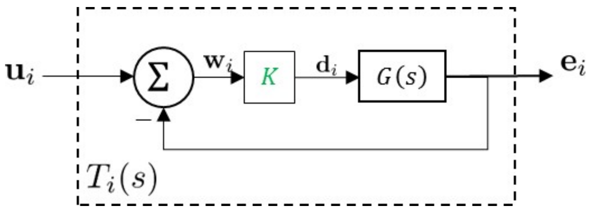

(a) Unity feedback.

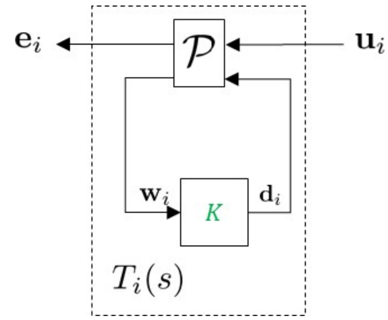

(b) Lower LFT.

Figure 2.2: Equivalent representations of $T_i(s)$.

identical subsystems $T_i(s) = T(s)$ with respect to F, mathematically denoted as $\mathcal{F}_l\left(I_n \otimes T(s), F\right)$, where

$$\begin{aligned} \mathbf{e}(s) &= \left(I_n \otimes T\left(s\right)\right)\mathbf{u}(s), \\ \begin{bmatrix} \mathbf{u} \\ \mathbf{e} \end{bmatrix} &= \underbrace{\begin{bmatrix} \underbrace{(\overline{\mathcal{A}} \otimes I_p) - D_H}_{\triangleq F_{11}} & I_{pn} \\ I_{pn} & \mathbf{0} \end{bmatrix}}_{F} \begin{bmatrix} \mathbf{e} \\ \bar{\mathbf{r}} \end{bmatrix}. \end{aligned} \tag{2.7}$$

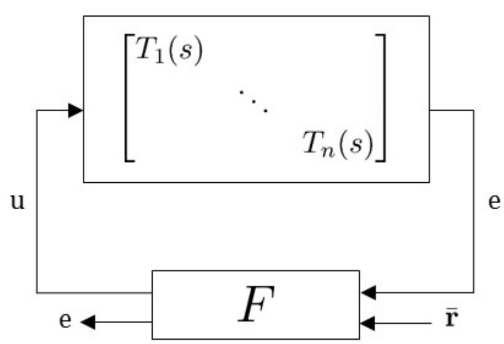

Figure 2.3: Global error dynamics.

In Eq. (2.7), the interconnection F is static; i.e., it is a gain matrix, which means that the equation holds in both time and frequency domains. Having laid the necessary foundation, we now describe the main problem addressed in this chapter.

Problem 2.1 (Distributed Estimation)**.** *Given the above formulation, find the estimator gain matrix K such that given the local dynamics $\mathcal{P}$ as defined in Eq.* (2.6) *and the interconnection matrix F in Eq.* (2.7)*, the global error process, depicted in Fig. 2.3, is stable and meets the performance specification*

$$\|\mathcal{F}_l\left(I_n \otimes T, F\right)\|_\infty < \eta, \tag{2.8}$$

for a given $\eta > 0$. This objective directly affects noise rejection properties of the global error by setting an upper bound η on the noise amplification from $\bar{\mathbf{r}}$ to $\mathbf{e}$, see Fig. 2.3.

To this aim, we will design procedures based on the dissipativity properties of the interconnection matrix F and the local system $T(s)$. We now recap the background material required for our analysis. We start with the following theorem, serving as the basis for our proposed solution to the problem investigated in this chapter. The analysis is carried out in Sections 2.3 and 2.4 for stability and performance, respectively.

Theorem 2.2.1.1 ([8, Theorem 1])**.** *Given $\eta > 0$, a stable interconnection F, a local plant $\mathcal{P}(s)$, and the real matrices $X = X^\top \prec 0$, Y, and $Z = Z^\top$ of appropriate dimensions, if there exist* *(i) a positive-definite matrix $S \in \mathbb{R}^{n\times n}$ such that F is*

$$\left(diag\left[S\otimes X, -\eta^2 I\right], diag\left[S\otimes Y, \mathbf{0}\right], diag\left[S\otimes Z, I\right]\right)\text{-}dissipative;$$

(ii) a local controller K such that $T(s) = \mathcal{F}_l(\mathcal{P}(s), K)$ is

$$strictly\ \left(-Z, -Y^\top, -X\right)\text{-}dissipative;$$

then the large-scale system $\mathcal{F}_l\left(I_n \otimes T(s), F\right)$, depicted in Fig. 2.3 is stable and $\|\mathcal{F}_l\left(I_n\otimes T, F\right)\|_\infty \leq \eta$.

Theorem 2.2.1.1 can be specialized to analyze the internal stability:

Corollary 2.2.1.1 ([8, Corollary 1])**.** *Given a stable interconnection F, a plant $\mathcal{P}(s)$, and real matrices $X = X^\top \prec 0$, Y, and $Z = Z^\top$ of appropriate dimensions, if there exist*

(i) a positive-definite matrix $S \in \mathbb{R}^{n\times n}$ such that $M = F_{11}$ in Eq. (2.7), is

$$\left(S\otimes X, S\otimes Y, S\otimes Z\right)\text{-}dissipative;$$

(ii) a local controller K such that $T(s) = \mathcal{F}_l(\mathcal{P}(s), K)$ is

$$strictly\ \{-Z, -Y^\top, -X\}\text{-}dissipative;$$

then the large-scale system depicted in Fig. 2.3 is stable.

In this chapter, we assume diagonal matrices of the form

$$X = xI_p, \quad Y = yI_p, \quad Z = zI_p, \tag{2.9}$$

for the choice of X, Y, and Z in Theorem 2.2.1.1 and Corollary 2.2.1.1 and find x, y, and z such that conditions (i) and (ii) are both satisfied.

2.3 Error Stability

Recall that our goal is to design the estimator gain matrix K such that the global error dynamics are internally stable and satisfy a given level of performance. In this section, we consider the stability of the error process, which ensures that the estimation error would vanish if no measurement noise is present across the network; the performance will be discussed in the next section. We only focus on the case where the system matrix A is unstable, i.e., there exists an eigenvalue of A with a positive real part, since otherwise, the error process is stable with $K = \mathbf{0}$. We now present our main result on the error stability.

Theorem 2.3.1 (Stability). *Given the dynamics in Eq.* (2.1) *with an unstable system matrix A, the global estimation error process $\mathcal{F}_l\left(I_n \otimes T(s), F\right)$, and $M = F_{11} = \overline{\mathcal{A}} \otimes I_p - D_H$, there exists an estimator gain matrix $K \in \mathbb{R}^{p \times p}$ ensuring internal stability if there exist a positive-definite matrix $S \in \mathbb{R}^{n \times n}$,* *and real values* $\chi > 0$ *and* c *such that*

$$M^\top \underbrace{(S \otimes I_p)}_{\triangleq\ \widetilde{S}} M \preceq \chi (cM - I_{pn})^\top \widetilde{S} (cM - I_{pn}), \tag{2.10}$$

$$\chi < \min\{\frac{1}{c^2}, \frac{1}{(c-1)^2}\}. \tag{2.11}$$

Proof. The proof is derived by directly applying Corollary 2.2.1.1. Choosing $x = -1$, $y = c$, and $z = \frac{1}{\chi} - c^2$ in Eq. (2.9), Eq. (2.10) is equivalent to condition (i) of Corollary 2.2.1.1. Moreover, the frequency domain equivalent of condition (ii) of Corollary 2.2.1.1 can be expressed as[5]

$$\begin{bmatrix} I \\ T(j\omega) \end{bmatrix}^* \begin{bmatrix} \left(c^2 - \frac{1}{\chi}\right) I & -cI \\ -cI & I \end{bmatrix} \begin{bmatrix} I \\ T(j\omega) \end{bmatrix} \prec 0,$$

which is equivalent to

$$T^*(j\omega)T(j\omega) - cT^*(j\omega) - cT(j\omega) + \left(c^2 - \frac{1}{\chi}\right) I \prec 0 \Leftrightarrow$$

$$\left(T(j\omega) - cI\right)^* \left(T(j\omega) - cI\right) - \frac{1}{\chi} I \prec 0. \tag{2.12}$$

In order to satisfy the hypotheses of Lemma 1.2.5.1 and to use it in our proof, we apply common loop transformations, i.e., linear multiplication and shift to the closed loop system $T(s)$ to obtain $\widehat{T}(s) = \sqrt{\chi}\,(T(s) - cI)$. As demonstrated in Fig. 2.4, $\widehat{T}(s)$ can be viewed as the transfer matrix from signal $\mathbf{u}_i$ to an auxiliary signal $\widehat{\mathbf{z}}_i$.

[5]Refer to Eq. (1.3) in Section 1.2.4.

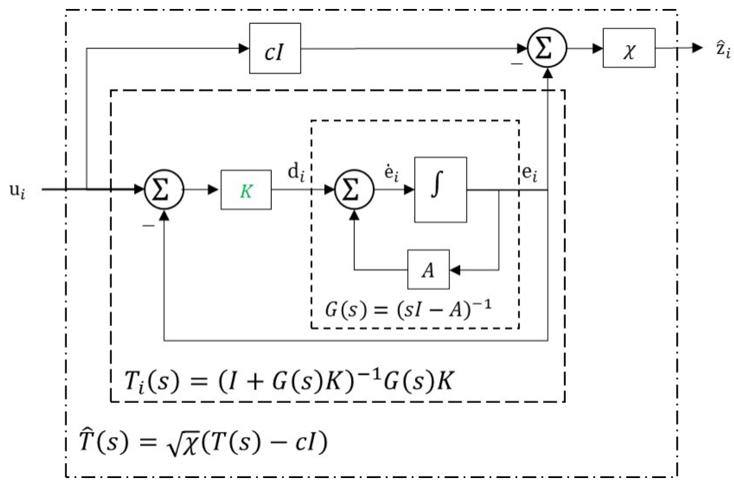

Figure 2.4: Modified system due to loop transformations.

Consequently, the state-space representation of $\widehat{T}(s)$ is:

$$\begin{aligned} \dot{\mathbf{e}}_i &= (A - K)\mathbf{e}_i + K\mathbf{u}_i \\ \widehat{\mathbf{z}}_i &= \sqrt{\chi}I\mathbf{e}_i - c\sqrt{\chi}I\mathbf{u}_i \end{aligned} \quad . \tag{2.13}$$

We now show that Eq. (2.12) is equivalent to $\|\widehat{T}\|_\infty < 1$:

$$\begin{aligned} &(T(j\omega) - cI)^* (T(j\omega) - cI) - \frac{1}{\chi}I \prec 0 \\ \Leftrightarrow\ & \lambda_{\max}\left((T(j\omega) - cI)^* (T(j\omega) - cI)\right) < \frac{1}{\chi} \Leftrightarrow\ \lambda_{\max}\left(\widehat{T}^*(j\omega)\widehat{T}(j\omega)\right) < 1 \\ \Leftrightarrow\ & \sup\{\ \|\widehat{T}(j\omega)\| \mid \omega \in \mathbb{R}\ \} < 1 \Leftrightarrow\ \|\widehat{T}\|_\infty < 1\ \therefore \end{aligned}$$

Given the state-space representation in Eq. (2.13), we can apply Bounded-Real Lemma[6] to $\widehat{T}(s)$ and with the change of variables $Q = PK$, $\|\widehat{T}\|_\infty < 1$ if

[6]Lemma 1.2.5.1.

and only if there exists a positive-definite matrix $P \in \mathbb{R}^{p\times p}$ such that

$$\begin{bmatrix} A^\top P + PA - (Q^\top + Q) + \chi I & Q - c\chi I \\ Q^\top - c\chi I & (c^2\chi - \gamma^2)I \end{bmatrix} \prec 0, \tag{2.14}$$

for $\gamma^2 = 1$. We proceed by proving that the feasibility of Eq. (2.14) is equivalent to Eq. (2.11). First note that Eq. (2.14) can be expressed in the following form:

$$\begin{aligned} &\underbrace{\begin{bmatrix} A^\top P + PA + \chi I & -c\chi I \\ -c\chi I & (c^2\chi - 1)I \end{bmatrix}}_{\triangleq\ \Omega} + \begin{bmatrix} -(Q^\top + Q) & Q \\ Q^\top & \mathbf{0} \end{bmatrix} \\ &= \Omega + \underbrace{\begin{bmatrix} I \\ \mathbf{0} \end{bmatrix}}_{U} Q \underbrace{\begin{bmatrix} -I & I \end{bmatrix}}_{V^\top} + \left(\begin{bmatrix} I \\ \mathbf{0} \end{bmatrix} Q \begin{bmatrix} -I & I \end{bmatrix} \right)^\top \\ &= \Omega + UQV^\top + VQ^\top U^\top \prec 0. \end{aligned} \tag{2.15}$$

Applying the Elimination Procedure[7], Eq. (2.15) is equivalent to:

$$\widetilde{U}^\top \Omega \widetilde{U} \prec 0, \tag{2.16a}$$

$$\widetilde{V}^\top \Omega \widetilde{V} \prec 0, \tag{2.16b}$$

where $\widetilde{U} = \begin{bmatrix} \mathbf{0} & I \end{bmatrix}^\top$ and $\widetilde{V} = \begin{bmatrix} I & I \end{bmatrix}^\top$. From Eq. (2.16a), we have

$$\begin{bmatrix} \mathbf{0} & I \end{bmatrix} \begin{bmatrix} A^\top P + PA + \chi I & -c\chi I \\ -c\chi I & (c^2\chi - 1)I \end{bmatrix} \begin{bmatrix} \mathbf{0} \\ I \end{bmatrix} \prec 0 \Leftrightarrow$$

[7] Lemma 1.2.5.2.

$$(c^2\chi - 1)I \prec 0 \Leftrightarrow c^2\chi < 1 \Leftrightarrow \chi < \frac{1}{c^2},$$

and Eq. (2.16b) results in

$$\begin{aligned}
&\begin{bmatrix} I & I \end{bmatrix} \begin{bmatrix} A^\top P + PA + \chi I & -c\chi I \\ -c\chi I & (c^2\chi - 1)I \end{bmatrix} \begin{bmatrix} I \\ I \end{bmatrix} \prec 0 \Leftrightarrow \\
&A^\top P + PA + \left[\chi(c-1)^2 - 1\right] I \prec 0 \Leftrightarrow \\
&1 - \chi(c-1)^2 > \lambda_{\max}\left(A^\top P + PA\right). \qquad (2.17)
\end{aligned}$$

It remains to show the equivalence between Eq. (2.17) and $\chi < \frac{1}{(c-1)^2}$ to complete the proof. If Eq. (2.17) holds for the unstable system matrix A (as assumed earlier), based on the Lyapunov stability criterion, see, e.g., [37], the matrix $A^\top P + PA$ is not negative-definite for all real symmetric matrices $P \succ 0$, which implies that the left hand side of Eq. (2.17) is positive, further implying $\chi < \frac{1}{(c-1)^2}$.

For the other direction, assuming $\chi < \frac{1}{(c-1)^2}$, we have $1 - \chi(c-1)^2 > 0$ and for an unstable matrix A, we can always find a sufficiently small $P_\epsilon \succ 0$ such that

$$1 - \chi(c-1)^2 > \lambda_{\max}\left(A^\top P_\epsilon + P_\epsilon A\right) \Leftrightarrow A^\top P_\epsilon + P_\epsilon A + \left[\chi(c-1)^2 - 1\right] I \prec 0;$$

for instance, $P_\epsilon = \epsilon I$, where $0 < \epsilon < \frac{1-\chi(c-1)^2}{2\max_i \Re\{\lambda_i(A)\}}$ is a candidate, where $\Re\{\cdot\}$ denotes the real part of the given complex argument.

Consequently, Eq. (2.14) is feasible if and only if the condition in Eq. (2.11) holds and the proof is complete.

□

Theorem 2.3.1 establishes the existence conditions for a stabilizing estimator gain matrix K. In the remainder of this section, we provide an algorithm to compute K based on this theorem and the resulting observations made in the following *Remarks*.

Remark 2.3.1. *For a single-input single-output (SISO) system T, Eq.* (2.12) *means that the Nyquist plot of the transfer function $T(s)$ lies inside the circle centered at $c + j0$ with radius $\frac{1}{\sqrt{\chi}}$. A similar interpretation applies to the multiple-input multiple-output (MIMO) case as well. To relax this constraint for a given center c, the radius has to be maximized, which is equivalent to minimizing χ.*

The key idea of the algorithm is based on the fact that minimizing χ, as mentioned in Remark 2.3.1, would strengthen the constraint in Eq. (2.10); therefore, Eqs. (2.10) and (2.12) cannot be simultaneously relaxed. As a result, the following optimization problem can be solved to satisfy the conditions of Theorem 2.3.1, leading to the computation of the estimator gain matrix K

ensuring global stability.

$$\begin{aligned} \underset{\chi,S}{\text{minimize}} \quad & \chi \\ \text{subject to} \quad & S \succ 0,\ \widetilde{S} = S \otimes I_n, \\ & M^\top \widetilde{S} M \preceq \chi \left(cM - I_{nN}\right)^\top \widetilde{S} \left(cM - I_{nN}\right), \end{aligned} \tag{2.18}$$

which is a generalized eigenvalue problem for a fixed value of c (see Remark. 2.3.2), with $S \in \mathbb{R}^{n\times n}$ and $\chi \in \mathbb{R}^+$ as the decision variables, [9].

Remark 2.3.2. *If the center c is selected as a decision variable, the optimization problem in Eq.* (2.18) *is no longer a generalized eigenvalue minimization problem; therefore, it has to be fixed in order to have a tractable optimization problem. The choice of c must be in a way that Eq.* (2.10) *is feasible. In what follows next, we derive a* ***necessary*** *condition on c based on the spectrum of M. First, note that Eq.* (2.10) *can be alternatively expressed as:*

$$\left(M + \frac{c\chi}{1-c^2\chi} I\right)^\top \widetilde{S} \underbrace{\left(M + \frac{c\chi}{1-c^2\chi} I\right)}_{\mathcal{M}} \preceq \underbrace{\frac{\chi}{\left(1-c^2\chi\right)^2}}_{\mu} \widetilde{S} \tag{2.19}$$

where $\mu > 0$ by definition. Decomposing $\widetilde{S} \succ 0$ as $\widetilde{S} = \widetilde{S}^{\frac{1}{2}} \widetilde{S}^{\frac{1}{2}}$, we obtain:

$$\mathcal{M}^\top \widetilde{S} \mathcal{M} \preceq \mu \widetilde{S} \Leftrightarrow \mathcal{M}^\top \widetilde{S}^{\frac{1}{2}} \widetilde{S}^{\frac{1}{2}} \mathcal{M}^\top \preceq \mu \widetilde{S}^{\frac{1}{2}} \widetilde{S}^{\frac{1}{2}}.$$

Multiplying by $\widetilde{S}^{\frac{-1}{2}}$ from right and left, on both sides, we have:

$$\left(\widetilde{S}^{\frac{1}{2}} \mathcal{M} \widetilde{S}^{\frac{-1}{2}}\right)^\top \left(\widetilde{S}^{\frac{1}{2}} \mathcal{M} \widetilde{S}^{\frac{-1}{2}}\right) \preceq \mu I \Leftrightarrow \sigma_{\max}\left(\widetilde{S}^{\frac{1}{2}} \mathcal{M} \widetilde{S}^{\frac{-1}{2}}\right) \leq \sqrt{\mu}, \tag{2.20}$$

where $\sigma_{\max}(\cdot)$ *denotes the maximum singular value of its argument. The Eqs.* (2.19) *and* (2.20) *are in general difficult to verify. From the submultiplicative property of the matrix 2-norm,*

$$\sigma_{\max}\left(\widetilde{S}^{\frac{1}{2}}\mathcal{M}\widetilde{S}^{\frac{-1}{2}}\right) \leq \sigma_{\max}\left(\widetilde{S}^{\frac{1}{2}}\right)\sigma_{\max}\left(\mathcal{M}\right)\sigma_{\max}\left(\widetilde{S}^{\frac{-1}{2}}\right) = cond\left(\widetilde{S}^{\frac{1}{2}}\right)\sigma_{\max}\left(\mathcal{M}\right),$$

where cond$(\cdot)$ *denotes the condition number of its argument and equality holds for the case of a diagonal matrix* $\widetilde{S} = \delta I$*. Therefore, imposing a diagonal structure* δI $(\delta > 0)$ *on* S *in* $\widetilde{S} = S \otimes I_n$*, allows us to simplify Eq.* (2.19)*, at the price of a more* ***restrictive*** *condition on c:*

$$\left(M + \frac{c\chi}{1-c^2\chi}I\right)^\top \left(M + \frac{c\chi}{1-c^2\chi}I\right) \preceq \mu I.$$

We can further simplify the above equation by exploiting the symmetry of M for an undirected network topology:

$$\left(\lambda_i(M) + \underbrace{\frac{c\chi}{1-c^2\chi}}_{=c\sqrt{\mu\chi}}\right)^2 \leq \mu, \quad \forall\ i \tag{2.21}$$

$$\Leftrightarrow \lambda_i^2(M) + 2c\sqrt{\mu\chi}\lambda_i(M) + c^2\mu\chi \leq \mu \Rightarrow \underbrace{\mu(1-c^2\chi)}_{\sqrt{\mu\chi}} - 2c\sqrt{\mu\chi}\lambda_i(M) > 0,$$

for all $\lambda_i(M) \neq 0$*. Dividing the last inequality by* $\sqrt{\mu\chi}$*, we obtain the following* ***necessary*** *condition on c:*

$$c\lambda_i(M) < \frac{1}{2}, \quad \textit{for } \lambda_i(M) \neq 0, \tag{2.22}$$

which is further expressed as:

$$\begin{cases} c < \frac{1}{2\max_i(\lambda_i(M))} & \text{if } \exists\ \lambda_i(M) > 0 \\ c > \frac{1}{2\min_i(\lambda_i(M))} & \text{if } \exists\ \lambda_i(M) < 0 \end{cases}. \tag{2.23}$$

Based on Eq. (2.23)*, we can make the following implications:*

(a) If $M \succeq 0$ with at least one positive eigenvalue, c is bounded from above by a positive real number:

$$c < \frac{1}{2\lambda_{\max}(M)}.$$

(b) If $M \preceq 0$ with at least one negative eigenvalue, c is bounded from below by a negative real number:

$$c > \frac{1}{2\lambda_{\min}(M)}.$$

(c) If M is indefinite, c is bounded with bounds of opposite signs:

$$\frac{1}{2\lambda_{\min}(M)} < c < \frac{1}{2\lambda_{\max}(M)}.$$

Remark 2.3.3. *Having formulated the optimization in Eq.* (2.18) *as a generalized eigenvalue problem (with $c = c^*$ selected according to the discussion in Remark 2.3.2), we cannot include Eq.* (2.11) *as an explicit constraint; consequently, we proceed in the following iterative manner: We use the objective value obtained from the optimization in Eq.* (2.18)*, i.e., χ^*, to verify whether the constraint in Eq.* (2.11) *is met, in which case the static estimator gain is computed as $K = (P^f)^{-1}Q^f$, where P^f and Q^f are solutions to the feasibility* *problem in Eq.* (2.14) *for* $\gamma = 1$, $c = c^*$, *and* $\chi = \chi^*$. *If not, we fix a new value* c^* *for* c *according to Eq.* (2.23) *and repeat the earlier steps. Given a sufficiently large number of feasible values for the parameter* c *– selected according to Eq.* (2.23) *– and gathered in the sample set* $\mathcal{C}$, *one approach is to do a linear search on* c *until the conditions of Theorem 2.3.1 are met or the sample set is exhausted, the latter implying that a static estimator gain* K, *ensuring stability of the global error, was not found.*

The above procedure to compute the static estimator gain matrix K is summarized in Algorithm 1.

Algorithm 1 Compute Static Estimator Gain K

given M, $\mathcal{C} = \{c$ is selected according to Eq. (2.23)$\}$,
repeat
  $c^* \leftarrow$ a value in $\mathcal{C}$
  $\chi^* \leftarrow$ solve the generalized eigenvalue problem in Eq. (2.18) for $c = c^*$
  if $\chi^* < \min\{\frac{1}{c^{*2}}, \frac{1}{(c^*-1)^2}\}$ **then**
    $P^{\mathrm{f}}, Q^{\mathrm{f}} \leftarrow$ solve the feasibility problem in Eq. (2.14) for $c = c^*$, $\chi = \chi^*$
    $K \leftarrow \left(P^{\mathrm{f}}\right)^{-1} Q^{\mathrm{f}}$
    return K
  end if
until $\mathcal{C}$ has been exhausted.
return Static estimator gain K not found

Remark 2.3.4. *In case of a stable system matrix* A, *the condition in Eq.* (2.11) *simplifies to* $\chi < \frac{1}{c^2}$, *since we can always find a real symmetric matrix* $P \succ 0$ *such that Eq.* (2.17) *is satisfied; i.e.,* $\lambda_{\max}\left(A^\top P + PA\right) < 1 - \chi(c-1)^2$.

2.3.1 Discussion on Network Connectivity and Observability

We now discuss the interplay between the stability of the global error dynamics and network connectivity and global observability from two different perspectives.

1) *Fixing* c: As mentioned in Remark 2.3.1 regarding Theorem 2.3.1, the algorithm to find controller gain matrix K relies on satisfying Eq. (2.10) while relaxing Eq. (2.11) as much as possible. As demonstrated in Fig. 2.5, the upper bound in Eq. (2.11) is largest for $c = \frac{1}{2}$. In order for Eq. (2.10) to be feasible with $c = \frac{1}{2}$, M must satisfy the following condition:

$$\text{for } \lambda_i(M) \neq 0 : \ \lambda_i(M) < 1 \Rightarrow \lambda_{\max}(M) < 1.$$

The reasoning follows directly from Eq. (2.22). As stated earlier,

$$M = F_{11} = (\overline{\mathcal{A}} \otimes I_p) - D_H = I_{pn} - \underbrace{\left(\overline{\mathcal{L}} \otimes I_p + D_H\right)}_{\mathcal{Q}=\mathcal{Q}^\top} \Rightarrow$$

$$\lambda_{\max}(M) = 1 + \lambda_{\max}(-\mathcal{Q}) = 1 - \lambda_{\min}(\mathcal{Q}) \Rightarrow \lambda_{\max}(M) < 1 \Leftrightarrow \lambda_{\min}(\mathcal{Q}) > 0;$$

the matrix $\mathcal{Q}$ was shown to be positive-definite in [35] for a globally observable and connected system.

In what follows next, we prove that global observability and connectivity are also necessary conditions for $\mathcal{Q} \succ 0 \Leftrightarrow \lambda_{\max}(M) < 1$, which is a **necessary**

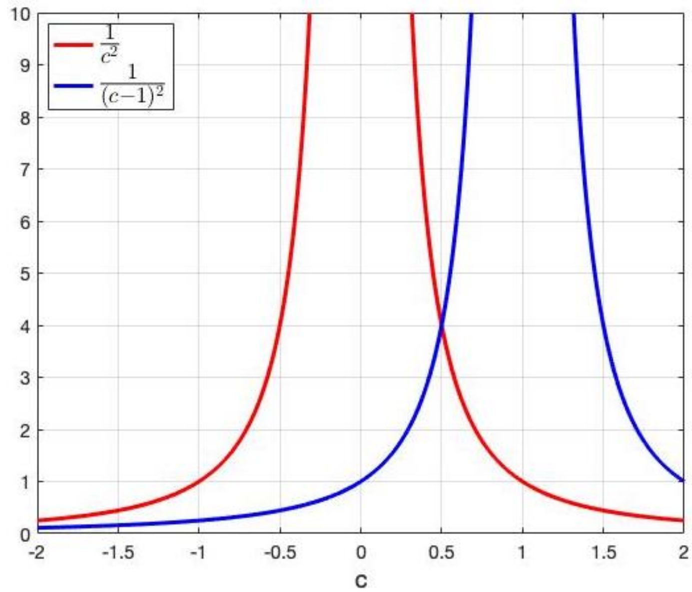

Figure 2.5: The bound in Eq. (2.11) plotted versus c.

condition for Eq. (2.10) to be feasible for $c = \frac{1}{2}$ and $S = \delta I$; in this case, the upper bound in Eq. (2.11) is at its largest!

Lemma 2.3.1.1. *For real symmetric matrices $X \succeq 0$ and $Y \succeq 0$ in $\mathbb{R}^{n\times n}$,*

$$\mathit{rank}(X+Y) \geq \max\left(\mathit{rank}(X), \mathit{rank}(Y)\right).$$

Proof. Let null$(\cdot)$ denote the null space. For any $\mathbf{v} \in \text{null}(X+Y)$:

$$\mathbf{v}^\top (X+Y)\mathbf{v} = 0 \Leftrightarrow \mathbf{v}^\top X \mathbf{v} = 0\ ,\ \mathbf{v}^\top Y \mathbf{v} = 0.$$

Consequently, $\mathbf{v} \in \text{null}(X)$ and $\mathbf{v} \in \text{null}(Y)$ equivalent to

$$\text{null}(X+Y) = \text{null}(X) \cap \text{null}(Y).$$

Therefore, denoting the dimension of a given vector space by dim$(\cdot)$:

$$\text{rank}(X+Y) = n - \dim\left(\text{null}(X+Y)\right) = n - \dim\left(\text{null}(X) \cap \text{null}(Y)\right)$$

$$\geq n - \dim\left(\text{null}(X)\right) = \text{rank}(X).$$

Similarly, $\text{rank}(X+Y) \geq \text{rank}(Y)$ and the lemma follows.

$\square$

Lemma 2.3.1.2. $\mathcal{Q} = \overline{\mathcal{L}} \otimes I_p + D_H \succ 0$ *implies network connectivity and global observability*[8].

Proof. By contradiction, assume that the state is not globally observable or the network is disconnected, which is true if global observability doesn't hold, i.e., if G, as defined in Definition 2.2.1, is not full-rank. Note that the network can be either connected or disconnected; we present our argument in both cases:

(i) The network is connected: In this case, $\overline{\mathcal{L}} \otimes I_p$ has p eigenpairs of form $(0\ ,\ \mathbf{1}_n \otimes \mathbf{v})$, where $\mathbf{v}$, is any nonzero vector in $\mathbb{R}^p$ – according to [2, Theorem 4.2.12].

Also, note that given the rank deficiency of G, any block in D_H is also rank deficient according to Lemma 2.3.1.1, i.e.,

$$\text{null}\left(\sum_{j\in\mathcal{N}_i} H_j^\top H_j\right) \neq \emptyset, \quad \forall\ i \in \mathcal{V}.$$

[8]See Definition 2.2.1.

Furthermore, $\text{null}(G) \subseteq \text{null}\left(\sum_{j\in\mathcal{N}_i} H_j^\top H_j\right)$, for all $i \in \mathcal{V}$, i.e.,

$$\text{null}(G) \subseteq \bigcap_{i=1}^{N} \text{null}\left(\sum_{j\in\mathcal{N}_i} H_j^\top H_j\right).$$

Now, pick an eigenvector $\mathbf{v}$ of I_p such that $\mathbf{v} \in \text{null}(G)$. Note that this is possible as G is rank deficient, i.e., $\text{null}(G) \neq \emptyset$. We have

$$\begin{aligned}
&(\mathbf{1}_n \otimes \mathbf{v})^\top \mathcal{Q} (\mathbf{1}_n \otimes \mathbf{v}) \\
=& (\mathbf{1}_n \otimes \mathbf{v})^\top \left(\overline{\mathcal{L}} \otimes I_n\right) (\mathbf{1}_n \otimes \mathbf{v}) + (\mathbf{1}_n \otimes \mathbf{v})^\top D_H (\mathbf{1}_n \otimes \mathbf{v}) \\
=& 0 + \sum_{i=1}^{N} \mathbf{v}^\top \left(\sum_{j\in\mathcal{N}_i} H_j^\top H_j\right) \mathbf{v} = 0,
\end{aligned}$$

which contradicts the fact that $\mathcal{Q} \succ 0$.

(ii) The netowrk is disconnected, i.e., the algebraic connectivity (second-smallest eigenvalue) of the normalized Laplacian $\overline{\mathcal{L}}$ is equal to zero; or equivalently, the algebraic multiplicity of the zero eigenvalue, C (the number of connected components), is greater than one. In this case, after suitably renumbering the vertices, we can write

$$\overline{\mathcal{L}} = \text{diag}\left[\overline{\mathcal{L}}^{(1)}, \ddots, \overline{\mathcal{L}}^{(C)}\right],$$

where $\overline{\mathcal{L}}^{(c)}$, $c = 1, \cdots, C$, is the normalized Laplacian of the c^{th} connected component, $\mathcal{G}_c$, consisting of n_c agents. Note that $\overline{\mathcal{L}}$ has at least C orthogonal eigenvectors corresponding to the zero eigenvalue:

$$\mathbf{v}^{(1)} = \begin{bmatrix} \mathbf{1}_{n_1} \\ \mathbf{0}_{n-n_1} \end{bmatrix}, \quad \cdots \quad, \mathbf{v}^{(C)} = \begin{bmatrix} \mathbf{0}_{n-n_C} \\ \mathbf{1}_{n_C} \end{bmatrix};$$

Rearranging the blocks in D_H accordingly and picking an eigenvector $\mathbf{v}$ of I_p in null(G) , we have

$$\begin{aligned}\left(\mathbf{v}^{(c)} \otimes \mathbf{v}\right)^\top \mathcal{Q}\left(\mathbf{v}^{(c)} \otimes \mathbf{v}\right) &= 0 + \left(\mathbf{v}^{(c)} \otimes \mathbf{v}\right)^\top D_H \left(\mathbf{v}^{(c)} \otimes \mathbf{v}\right) \\ &= \sum_{i \in \mathcal{G}_c} \mathbf{v}^\top \left(\sum_{j \in \mathcal{N}_i} H_j^\top H_j\right) \mathbf{v} = 0,\end{aligned}$$

where the last equality follows from the same line of reasoning as in case (i), contradicting the fact that $\mathcal{Q} \succ 0$.

$\square$

Remark 2.3.1.1. *Note that network disconnectivity on its own is not sufficient for $\mathcal{Q}$ to be rank deficient since in that case $\mathcal{Q} \succ 0$ if there exists a connected component in which global observability holds, i.e., if there exists $c \in \{1, \cdots, C\}$ such that $G_c = \sum_{i \in \mathcal{G}_c} H_i^\top H_i$ is full-rank!*

Remark 2.3.2 and the above discussion is summarized in the following:

Proposition 2.3.1.1. *Let $c = \frac{1}{2}$; there exists $\delta > 0$ such that Eq.* (2.10) *holds for $S = \delta I$* ***only if*** *the network is connected and the state is globally observable.*

Proof. The proof follows directly from the equivalence between $\mathcal{Q} \succ 0$ and network connectivity and global observability.

$\square$

2) *Spectrum of M*: From Eq. (2.21), we have the following bounds for the spectrum of M and $\mathcal{Q}$:

$$|\lambda_i(M) + c\sqrt{\mu\chi}| \leq \sqrt{\mu} \Leftrightarrow -\sqrt{\mu}(1 + c\sqrt{\chi}) \leq \lambda_i(M) \leq \sqrt{\mu}(1 - c\sqrt{\chi}).$$

Since $\lambda_i(\mathcal{Q}) = 1 - \lambda_i(M)$,

$$1 - \sqrt{\mu}(1 - c\sqrt{\chi}) \leq \lambda_i(\mathcal{Q}) \leq \underbrace{1 + \sqrt{\mu}(1 + c\sqrt{\chi})}_{\text{positive}}. \tag{2.24}$$

We now show that if the condition in Eq. (2.11) holds, the lower bound in Eq. (2.24) is poisitive which is equivalent to $\mathcal{Q} \succ 0$.

$$\begin{aligned} Eq.~(2.11) &\Leftrightarrow \max\{|c|, |c-1|\} < \frac{1}{\sqrt{\chi}} \\ \Rightarrow 1 - \sqrt{\mu}(1 - c\sqrt{\chi}) &= \frac{1 + \sqrt{\chi}(c-1)}{1 + c\sqrt{\chi}} > 0 \Leftrightarrow \mathcal{Q} \succ 0. \end{aligned}$$

Proposition 2.3.1.2. *There exists $\delta > 0$ such that Eq.* (2.10) *holds for $S = \delta I$ and $\chi < \min\{\frac{1}{c^2}, \frac{1}{(c-1)^2}\}$ (Eq.* (2.11)*)* ***only if*** *the network is connected and the state is globally observable.*

Proof. The proof follows directly from the equivalence between $\mathcal{Q} \succ 0$ and network connectivity and global observability.

$\square$

2.4 Performance

In this section, we compute an estimator gain matrix K satisfying the H_∞ performance objective specified in Eq. (2.8) in addition to stability; as mentioned earlier, this performance objective sets an upper bound η on the noise amplification gain from the external signal $\bar{\mathbf{r}}$ to the global estimation error $\mathbf{e}$ – depicted in Fig. 2.3 – directly affecting noise rejection properties of the global error process. We now present our main result on H_∞ performance characteristics of the global error process.

Theorem 2.4.1 (Performance)**.** *Given the global error process $\mathcal{F}_l\left(I_n \otimes T, F\right)$, there exists an estimator gain matrix K ensuring performance objective*

$$\|\mathcal{F}_l\left(I_n \otimes T, F\right)\|_\infty < \eta,$$

if there exist a positive-definite matrix $S \in \mathbb{R}^{n\times n}$, and real values $\chi > 0$ and c such that

$$\Phi^\top \left[\begin{array}{cc|cc} 0 & 0 & 0 & 0 \\ 0 & 0 & 0 & 0 \\ \hline 0 & 0 & \frac{1}{\chi}\underbrace{S \otimes I_p}_{\widetilde{S}} & 0 \\ 0 & 0 & 0 & I \end{array}\right] \Phi \preceq \chi \Phi^\top \left[\begin{array}{cc|cc} \frac{1}{\chi}\widetilde{S} & 0 & 0 & 0 \\ 0 & \frac{\eta^2}{\chi} I & 0 & 0 \\ \hline 0 & 0 & 0 & 0 \\ 0 & 0 & 0 & 0 \end{array}\right] \Phi, \tag{2.25}$$

where $\Phi = \left[\begin{array}{cc|cc} I & 0 & -cI & 0 \\ 0 & I & 0 & 0 \\ \hline 0 & 0 & I & 0 \\ 0 & 0 & 0 & I \end{array}\right] \begin{bmatrix} I \\ F \end{bmatrix}$, *and*

$$\chi < \min\{\frac{1}{c^2}, \frac{1}{(c-1)^2}\}. \tag{2.26}$$

Proof. The proof is based on Theorem 2.2.1.1 and is similar in part to the proof of Theorem 2.3.1. Choosing $x = -1$, $y = c$, and $z = \frac{1}{\chi} - c^2$ in Eq. (2.9), Eq. (2.25) is derived from condition (i) of Theorem 2.2.1.1 following some algebraic manipulations. Moreover, as proved in Theorem 2.3.1, the condition in Eq. (2.26) is equivalent to condition (ii) of Theorem 2.2.1.1 (or equivalently Eq. (2.12)); thus, there exists an estimator gain K ensuring the performance $\|\mathcal{F}_l\left(I_n \otimes T, F\right)\|_\infty < \eta$ if Eqs. (2.25) and (2.26) are satisfied.

□

Similar to the case of internal stability, we present a systematic procedure to compute an estimator gain matrix K satisfying the performance specification in Eq. (2.8) in addition to internal stability based on Theorem 2.4.1. An analogous observation to the one made in Remark 2.3.1, reveals that Eqs. (2.12) and (2.25) cannot be simultaneously relaxed, leading to the following optimization problem:

$$\begin{aligned}
\underset{\chi, S}{\text{minimize}} \quad & \chi \\
\text{subject to} \quad & S \succ 0,\ \widetilde{S} = S \otimes I_p, \\
& \Phi^\top \left[\begin{array}{cc:cc} 0 & 0 & 0 & 0 \\ 0 & 0 & 0 & 0 \\ \hdashline 0 & 0 & \frac{1}{\chi}\widetilde{S} & 0 \\ 0 & 0 & 0 & I \end{array}\right] \Phi \preceq \chi \Phi^\top \left[\begin{array}{cc:cc} \frac{1}{\chi}\widetilde{S} & 0 & 0 & 0 \\ 0 & \frac{\eta^2}{\chi} I & 0 & 0 \\ \hdashline 0 & 0 & 0 & 0 \\ 0 & 0 & 0 & 0 \end{array}\right],
\end{aligned} \tag{2.27}$$

with Φ as defined earlier.

To formulate the optimization in Eq. (2.27) as a generalized eigenvalue problem, we fix both c and χ by first solving the stability problem and using the resulting values for c, χ and $\|\mathcal{F}_l\,(I_n \otimes T, F)\,\|_\infty$ (as a baseline for η) and introduce the change of variables $\varsigma = \frac{1}{\chi}S$ and $\beta = \frac{\eta^2}{\chi}$. The resulting optimization problem, presented in Eq. (2.28), is a generalized eigenvalue problem with $\varsigma \in \mathbb{R}^{n\times n}$ and $\chi \in \mathbb{R}^+$ as the decision variables, [9].

$$\begin{aligned} \underset{\chi,\varsigma}{\text{minimize}} \quad & \chi \\ \text{subject to} \quad & \varsigma \succ 0,\ \widetilde{\varsigma} = \varsigma \otimes I_p, \\ & \Phi^\top \left[\begin{array}{cc:cc} 0 & 0 & 0 & 0 \\ 0 & 0 & 0 & 0 \\ \hdashline 0 & 0 & \widetilde{\varsigma} & 0 \\ 0 & 0 & 0 & I \end{array}\right] \Phi \preceq \chi \Phi^\top \left[\begin{array}{cc:cc} \widetilde{\varsigma} & 0 & 0 & 0 \\ 0 & \beta I & 0 & 0 \\ \hdashline 0 & 0 & 0 & 0 \\ 0 & 0 & 0 & 0 \end{array}\right] \Phi. \end{aligned} \tag{2.28}$$

In the optimization problem above, β acts as a tuning parameter; if the optimization problem has no solution, β should be increased to relax the last constraint of the problem. Also note that for a given value of β, minimizing χ results in the minimization of the upper bound on noise amplification gain η according to the relation $\eta^2 = \chi\beta$.

As demonstrated in [34], conditions (i) and (ii) of Corollary 2.2.1.1 are necessary conditions for conditions (i) and (ii) of Theorem 2.2.1.1; therefore, the necessity of network connectivity and global observability apply to the performance problem as well.

2.5 Simulations

In this section, we illustrate the concepts introduced in this paper and evaluate the effectiveness of the proposed static gain distributed estimator in terms of internal stability and H_∞ performance, experimentally. We consider a network of $n = 20$ agents communicating over a random undirected graph generated based on the Barabási–Albert model [38]; one instance of such formation is shown in Fig. 2.6a. The agents' goal is to estimate the state of an unstable $p = 3$-dimensional CT-LTI dynamical system evolving according to the model in Eq. (2.1) with a randomly chosen initial condition $\mathbf{x}(0)$ using Eq. (2.3), with the following structure for the system matrix A as in Eq. (2.29) where $\times$ is a uniform random variable in the interval $[0\ ,\ 2]$, ensuring unstable dynamics. The measurement model, H_i, at agent i is chosen from the set Ω^H in Eq. (2.29) according to the specific protocol determined by the chosen setup as explained below.

$$A = \begin{bmatrix} 1 & 0.5 & 0 \\ 0 & 1 & 0 \\ 0 & 0.5 & \times \end{bmatrix}, \quad \Omega^H = \left\{ \begin{bmatrix} 1 & 0 & 0 \end{bmatrix}, \begin{bmatrix} 0 & 1 & 0 \end{bmatrix}, \begin{bmatrix} 0 & 0 & 1 \end{bmatrix} \right\}. \qquad (2.29)$$

(1) Setup I: In the first setup, 3 non-neighboring agents i_1, i_2, and i_3 are selected at random such that each of these three agents measures one of the system states while the rest of the agents make no measurement;

i.e. $H_i = \begin{bmatrix} 0 & 0 & 0 \end{bmatrix}$ for $i \notin \{i_1,\ i_2,\ i_3\}$.

(2) Setup II: In this setup, an agent i is randomly picked and the measurement matrices in its neighborhood are picked such that the system is not observable in i's neighborhood. This is guaranteed by avoiding the simultaneous appearance of $\begin{bmatrix} 1 & 0 & 0 \end{bmatrix}$ and $\begin{bmatrix} 0 & 0 & 1 \end{bmatrix}$ in $\mathcal{N}_i$ as this would make the system observable in the neighborhood. For the agents not in $\mathcal{N}_i$, measurement matrices are chosen randomly from Ω^H.

(3) Setup III: In the third setup, the measurement model at each agent i is randomly chosen from Ω^H.

Note that with the choice of measurement matrices given in Ω^H, no agent is able to estimate the state based on its own observations alone. Furthermore, no agent is observable in its neighborhood in Setup I, while at least one agent is not observable in its neighborhood in Setup II.

In the remainder of this section, we demonstrate the stability and performance characteristics of the static gain estimator through a series of Monte Carlo simulations.

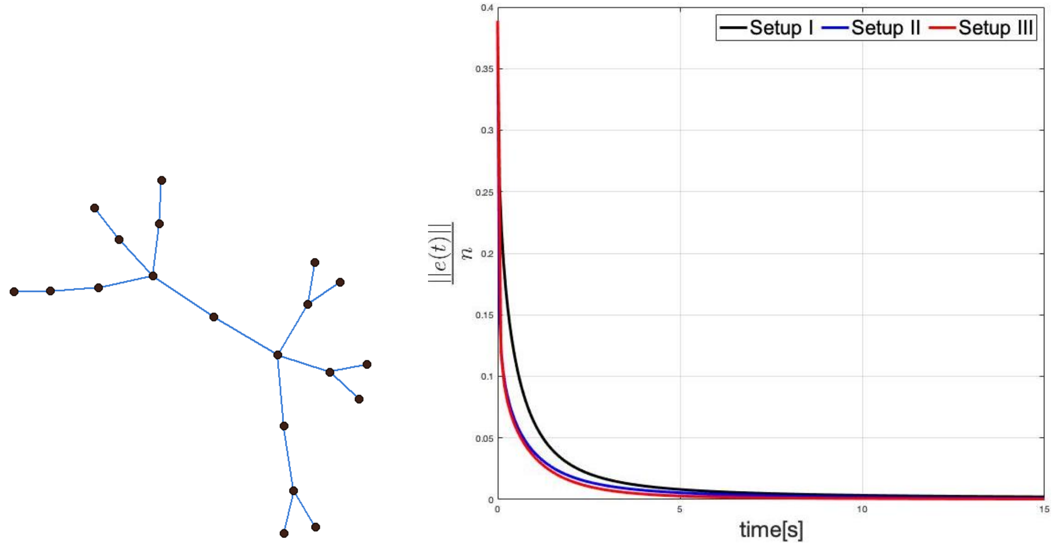

(a) Network of 20 agents.

(b) Averaged normalized error.

Figure 2.6: Network topology and global error signals.

2.5.1 Internal Stability

To illustrate the stability of the estimation error process, agents are assumed to have perfect (noise-free) observations; i.e., $\mathbf{r}_i(t) = 0$. Given zero initial estimate $\widehat{\mathbf{x}}_i(0)$, each agent makes an estimate of the system state using Eq. (2.3) for $t \in [0,\, 15]$ seconds. This procedure is repeated over 100 Monte Carlo simulations, each with randomly generated sets of system matrix A and observation matrices H_i (according to the setup-specific protocol).

Numerically consistent with the theory presented in previous sections, exploiting the information exchange among agents, the distributed estimator in Eq. (2.3) results in asymptotically stable error dynamics in all setups as illustrated in Fig. 2.7c, where the normalized 2-norm of the global errors, i.e., $\frac{\|\mathbf{e}(t)\|}{N}$

– averaged over 100 Monte Carlo simulations – has been plotted. The three setups are further shown over each trial in Fig. 2.7, where the normalized 2-norm of the global error is plotted for each setup. As expected, the setup with a more limited observation protocol has a longer settling time; i.e., the error takes the longest to vanish in setup I.

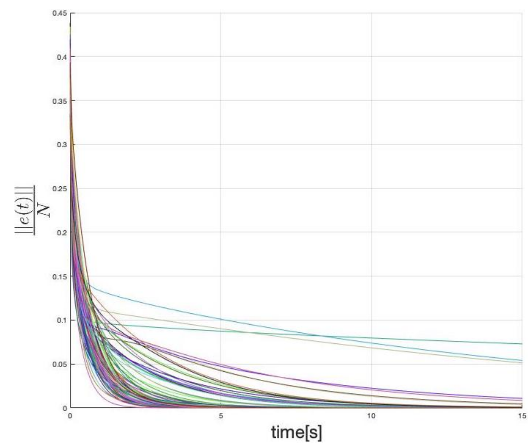

(a) Setup I.

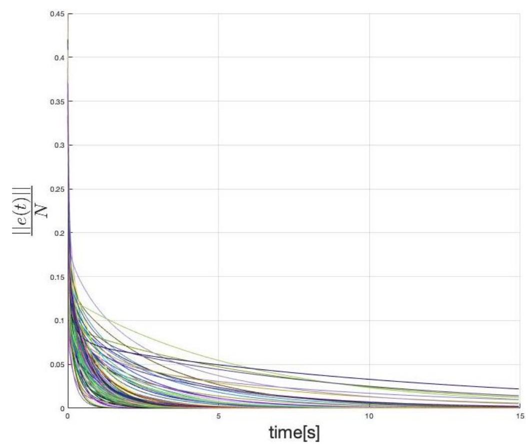

(b) Setup II.

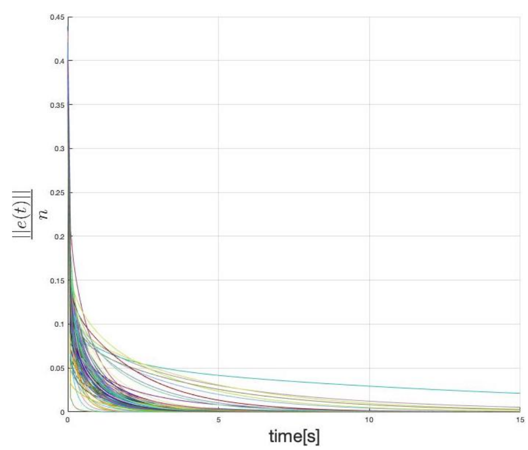

(c) Setup III.

Figure 2.7: Normalized errors.

2.5.2 Performance

In this subsection, the performance level η in Eq. (2.8) is set equal to 288, 36, and 24, for setups I, II and III, respectively – note that the stricter the observation regime, the higher the performance level η needs to be – and the performance characteristics of the global error process are demonstrated in presence of noise signal $\bar{\mathbf{r}}(t)$ defined in Eq. (2.5), for the case where agent observations are subject to Additive White Gaussian Noise (AWGN) with PSD equal to $\sigma^2 = 0.25$. For each of the observation setups explained, this procedure is repeated over 100 Monte Carlo simulations with a fixed set of system matrix A, communication graph $\mathcal{G}$, and setup-specific observation matrices H_i. The resulting normalized 2-norm of the global error signal is plotted in Fig. 2.8, averaged over 100 Monte Carlo simulations.

It's worth mentioning that setups II and III can achieve better (lower) performance levels given the less limited observation regime they follow. As we can see, the error process is stable. The H_∞-norm of the resulting global error process $\|\mathcal{F}_l\left(I_n \otimes T, F\right)\|_\infty$, is found to be 159.2574, 27.7207, and 16.5032 for setups I, II, and III, respectively, satisfying the performance specification in Eq.(2.8) for η as specified above.

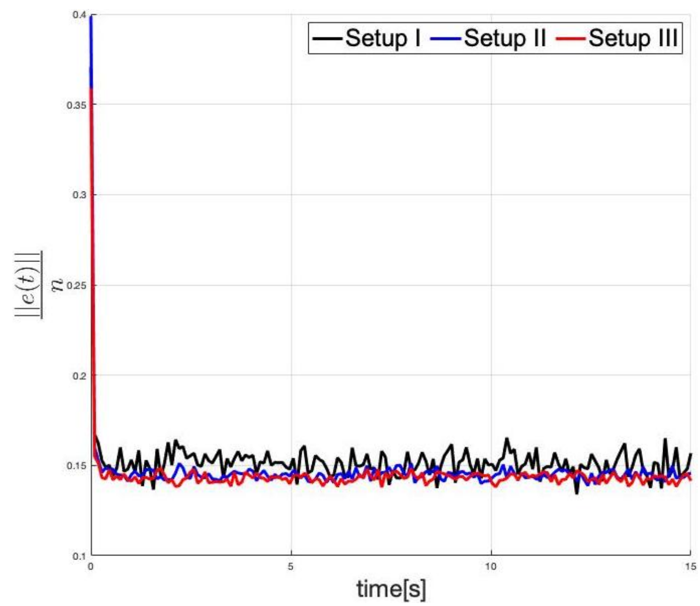

Figure 2.8: Two-norm of the normalized error.

2.6 Summary

In this chapter, we describe a static estimator gain design method to solve the distributed estimation problem for CT-LTI systems monitored by a network of agents. In this context, we express the problem of distributed estimation as corresponding optimization problems and apply techniques based on the input-output approach to perform stability and performance analyses. We derive existence conditions for a static estimator gain matrix resulting in stable error dynamics, i.e., estimation error vanishing over time in the absence of measurement noise; additionally, we derive existence conditions regarding static estimator gain design, guaranteeing desirable performance characteristics for the error process in terms of noise rejection.

Chapter 3

Optimal Control of Spreading Processes

In this chapter, we study a variant of the viral marketing phenomenon over heterogeneous networks. The marketing objective investigated in this framework is product adoption. In this context, we borrow concepts from the theory of epidemic processes to model the transitions of the members of the target market in between different stages of the adoption process; specifically, we introduce a 3-compartment model, i.e., the potential-adopting-dormant-potential (PADoP) model, which is the equivalent of the susceptible-infected-recovered-susceptible (SIRS) epidemic model. We then formulate the simultaneous optimization of the population of the adopting and dormant states under certain time and resource constraints as an optimal control problem and prove the existence of a solution. Furthermore, using the Pontryagin Maximum Principle and forward-backward sweep method (FBSM), we provide analytical and numerical solutions, respectively. Simulations illustrate the findings of the chapter.

3.1 Introduction

The last decade has witnessed a rapid development of online social networks (OSNs), such as Facebook, YouTube, Twitter, and Instagram, making the modern world more connected than ever [39]. This connectedness has manifested itself in the surprisingly fast and intense spread of news, information, rumors, and new products as well as epidemics and financial crises around the globe. These phenomena are not only based on the links that connect us and the ways in which each of our decisions can affect outcomes of everyone else's, but they also revolve around networks, incentives, and the aggregate behavior of groups of people [40].

Business strategists have noted an increasing tendency in the target market to search for and diffuse product information using OSNs. The information individuals receive and the opinions they form as a result are significantly influenced by other individuals within their social network; in a sense, a piece of information, awareness of brands, products, ideas, and political ideologies propagate through such a network much like infections in the human network, leading to the phenomenon of "information epidemics" and a class of marketing techniques referred to as Viral Marketing in which new products are advertised by certain influential users in the OSN in a cascading manner [41]. As a result, firms have become more interested in models of spreading processes in social networks in order to improve their marketing campaigns. In particular, many retailers are interested in exploiting information about the dynamics of the spread in order to maximize their product consumption and achieve the most profit in a competitive market [42]. It is also worth mentioning that in the past few years, there has been a large body of research on spreading processes, viewing the problem through the lens of various academic disciplines [43–46].

As explained above, the goal of the marketing campaign is to have as many individuals as possible adopt a certain product by the campaign deadline. Moreover, considering the advertisement cost and limited resources, there is a need to devise optimal campaigning strategies which can achieve this goal while respecting the constraints. To this aim, inspired by the theory of mathematical epidemiology, we model the adoption process of a product in a target market, e.g., the social network under study, with a microscopic (node-based) model equivalent to the SIRS epidemic model, namely the PADoP model. In this context, we deploy tools from graph theory to describe networks and to characterize the connections between individuals; we start with a Markovian description of the adoption process and move to a deterministic mean-field approximation, see e.g., [47] for a detailed analysis of the exact Markov chain model of the SIRS spreading process and the connection to its nonlinear "mean-field" approximation.

In this chapter, using the proposed model of product adoption, we cast the marketing problem as a constrained optimal control problem for which we prove the existence of the solution; i.e., we find control inputs to simultaneously increase the size of the adopting population and decrease the number of dormant individuals. Analytical and numerical solutions are obtained using the Pontryagin Maximum Principle and a version of forward-backward sweep algorithm, respectively. It is worth mentioning that optimal control of node-based information epidemics has received much less attention compared to the analysis of disease-free equilibria in epidemic models, see the survey [48] for a comprehensive overview of the development, analysis, and control of epidemic models. Stability and fixed-point analyses of the susceptible-infected-susceptible (SIS) epidemic model can be found in [49] and [50] while [51] and [52] present results on the optimal control of the node-based SIS model. Our work, while focusing on enhancing product adoption, extends the 2-compartment SIS model to 3 compartments allowing to study a broader range of products and campaigning strategies. Also note that the control problem we address, although based on the same epidemic model, is different in nature from the problem addressed in [53], where the focus is on regulating the probabilities of transitioning into the infected and recovered states to desired values.

The rest of this chapter is organized as follows. Section 3.2 formulates the problem and describes related concepts in epidemiology, networks, and graph theory. Sections 3.3 and 3.4 prove the existence of the solution and provide the algorithm to solve the problem, respectively. We illustrate our results in Section 3.5. Finally, Section 3.6 concludes the chapter.

3.2 Problem Formulation

Consider a marketing campaign during the time interval $[t_0,\, t_f]$ targeting a social network, mathematically modeled as a digraph $\mathcal{G}(\mathcal{V}, \mathcal{E})$, where $\mathcal{V}$ and $\mathcal{E}$ denote the set of individuals and links – social ties, not necessarily bidirectional – among them. Let $\mathcal{A}$ denote the corresponding weighted adjacency matrix where $[\mathcal{A}]_{i,j}$ quantifies the influence of node j on node i. We assume the market size $|\mathcal{V}|$ to be the constant n as the time-scale of marketing campaigns is usually much shorter than the period in which significant change in the size of the target market can occur, due to e.g., births and deaths.

3.2.1 Mathematical Modeling of Spreading Processes

We now explain the PADoP model for the product adoption process. In this model, at any time t, a node i of the target network is assumed to be in one of the 3 possible states, i.e., potential (P) are those individuals who might buy the campaign target product (referred to as the product in short from now on), adopting (A) are those who are actively paying for and consuming the product, and dormant (Do) individuals are those individuals who have no intent of buying the product (maybe because they have previously purchased the product or a similar rival product).

In this chapter, we study the word-of-mouth (WoM) advertisement technique [54]. Therefore, we assume that product adoption occurs only via interactions between individuals; i.e., a potential customer has no chance of actually adopting the product unless at least one of their neighbors is already an adopter. Under this assumption, the process of a potential customer adopting the product is influenced by two factors:

(i) The rate β at which an adopting individual spreads positive WoM regarding the product: modeled as a Poisson process; and,

(ii) the degree to which a potential individual i is affected by WoM from an adopting individual j in making decisions regarding product adoption: modeled by the network weighted adjacency matrix $\mathcal{A}$.

We also investigate the role of customer loyalty programs in retaining currently adopting customers, this directly influences the transition of individuals from the adopting state to the dormant state. Consequently, as shown in Fig. 3.1, an individual i can transition between different states with different rates. Assuming Markovian interacting agents, the transitions are modeled by independent Poisson processes with the following positive rates:

$$P \to A: \ \bar{\beta}_i, \qquad A \to Do: \ \delta_i, \qquad Do \to A: \ \gamma_i.$$

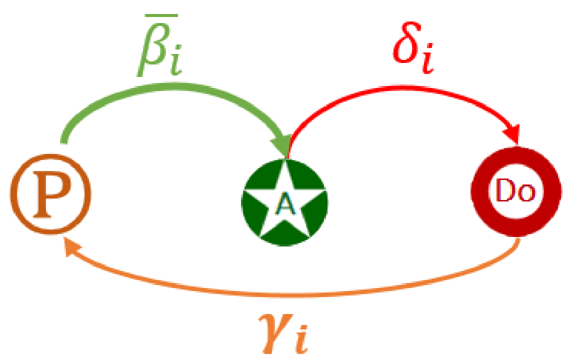

Figure 3.1: Node-based PADoP and the transition rates.

The effective transition rate $\bar{\beta}_i$ is derived from the mean-field approximation of the node-based PADoP model and denotes the eagerness of node i to adopt the product. For small Δt, the model works according to the following ordinary differential equations (ODEs):

$$q_i(t+\Delta t) = \Delta t \sum_{j \in \mathcal{N}_i} \beta_j q_j(t) \underbrace{(1 - q_i(t) - r_i(t))}_{p_i(t)} + (1 - \Delta t \delta_i) q_i(t) + o(\Delta t) \Rightarrow$$

$$\frac{\mathrm{d}}{\mathrm{dt}}q_i(t) = \lim_{\Delta t \to 0} \frac{q_i(t+\Delta t) - q_i(t)}{\Delta t} = (1 - q_i(t) - r_i(t)) \underbrace{\sum_{j=1}^{n} [\mathcal{A}]_{i,j}\beta_j q_j(t)}_{\bar{\beta}_i} - \delta_i q_i(t),$$

$$r_i(t+\Delta t) = \Delta t \delta_i q_i(t) - \gamma_i \Delta t r_i(t) + o(\Delta t) \Rightarrow$$

$$\frac{\mathrm{d}}{\mathrm{dt}}r_i(t) = \lim_{\Delta t \to 0} \frac{r_i(t+\Delta t) - r_i(t)}{\Delta t} = \delta_i q_i(t) - \gamma_i r_i(t),$$

where $0 \leq p_i(t)$, $q_i(t)$, $r_i(t) \leq 1$ are the instantaneous probabilities of node i being in potential, adopting, and dormant states at time t, respectively.

The network-wide equations are:

$$\dot{\mathbf{q}}(t) = \frac{\mathrm{d}}{\mathrm{dt}} \begin{bmatrix} q_1(t) \\ \vdots \\ q_n(t) \end{bmatrix} = (I - Q(t) - R(t))\, \mathcal{A} B \mathbf{q}(t) - D\mathbf{q}(t), \tag{3.1}$$

$$\dot{\mathbf{r}}(t) = \frac{\mathrm{d}}{\mathrm{dt}} \begin{bmatrix} r_1(t) \\ \vdots \\ r_n(t) \end{bmatrix} = D\mathbf{q}(t) - \Gamma \mathbf{r}(t), \tag{3.2}$$

where

$$\begin{aligned} Q(t) &= \mathrm{diag}[\mathbf{q}(t)], \qquad R(t) = \mathrm{diag}[\mathbf{r}(t)], \\ \boldsymbol{\beta} &= \begin{bmatrix} \beta_1 & \dots & \beta_n \end{bmatrix}^\top, \qquad B = \mathrm{diag}[\boldsymbol{\beta}], \\ \boldsymbol{\gamma} &= \begin{bmatrix} \gamma_1 & \dots & \gamma_n \end{bmatrix}^\top, \qquad \Gamma = \mathrm{diag}[\boldsymbol{\gamma}], \\ \boldsymbol{\delta} &= \begin{bmatrix} \delta_1 & \dots & \delta_n \end{bmatrix}^\top, \qquad D = \mathrm{diag}[\boldsymbol{\delta}]. \end{aligned}$$

Note that starting with initial conditions

$$0 \leq p_i(t_0),\, q_i(t_0),\, r_i(t_0) \leq 1, \qquad p_i(t_0) + q_i(t_0) + r_i(t_0) = 1,$$

for all $i \in \mathcal{V}$, the state occupancy probabilities are guaranteed to remain in the interval [0, 1] and sum up to 1 at any time, due to positively invariance property of the set $\Omega = \{(\mathbf{q}(t),\, \mathbf{r}(t)) |\, 0 \leq q_i(t),\, r_i(t) \leq 1,\, q_i(t) + r_i(t) \leq 1\}$; see [55] for an overview of positively invariant sets and their application to the analysis and synthesis of control systems.

3.2.2 Formulation of the Optimal Control Problem

The campaign implements two marketing strategies:

1. Referral reward programs where individuals are incentivized to spread positive WoM about the product at even higher rates: increasing β_i by $u_i(t)$ at some cost.

2. Customer loyalty programs aiming to decrease the rate at which individuals transition from adopting to dormant states: dynamically decreasing δ_i by $v_i(t)$ at some cost.

Defining $\mathbf{u}(t) = [u_1(t), \cdots, u_n(t)]^\top$, $U(t) = \mathrm{diag}[\mathbf{u}(t)]$, $\mathbf{v}(t) = [v_1(t), \cdots, v_n(t)]^\top$, and $V(t) = \mathrm{diag}[\mathbf{v}(t)]$, the network-wide controlled process is expressed as

$$\dot{\mathbf{q}}(t) = (I - Q(t) - R(t))\, \mathcal{A}\, (B + U(t))\, \mathbf{q}(t) - (D - V(t))\, \mathbf{q}(t), \tag{3.3}$$

$$\dot{\mathbf{r}}(t) = (D - V(t))\, \mathbf{q}(t) - \Gamma \mathbf{r}(t). \tag{3.4}$$

Defining $\mathbf{x}(t) = \begin{bmatrix} \mathbf{q}(t) \\ \mathbf{r}(t) \end{bmatrix}$ and $\mathbf{w}(t) = \begin{bmatrix} \mathbf{u}(t) : \\ \mathbf{v}(t) \end{bmatrix}$,

$$\dot{\mathbf{x}} = f(\mathbf{x}, \mathbf{w}) = \begin{bmatrix} (I - Q - R)\,\mathcal{A}\,(B + U)\,\mathbf{q} - (D - V)\,\mathbf{q} \\ (D - V)\,\mathbf{q} - \Gamma\mathbf{r} \end{bmatrix}. \tag{3.5}$$

Realistically, the control inputs $\mathbf{u}(t)$ and $\mathbf{v}(t)$ are constrained to be in the bounded sets $\mathbb{U}$ and $\mathbb{V}$, where

$$\mathbb{U} \triangleq \{\mathbf{u}(t) : u_i(t) \text{ is Lebesgue integrable, } 0 \leq u_i(t) \leq u_{\max}, \forall\ i \in \mathcal{V}\},$$

$$\mathbb{V} \triangleq \{\mathbf{v}(t) : v_i(t) \text{ is Lebesgue integrable, } 0 \leq v_i(t) \leq v_{\max}, \forall\ i \in \mathcal{V}\}.$$

The goal is to simultaneously maximize the probability of the individuals being in the adopting state and minimize the probability of the individuals being in the dormant state at the end of the campaign, i.e., $\mathbf{q}(t_f)$ and $\mathbf{r}(t_f)$, respectively, given the constraint sets on the control inputs, while spending the minimum campaign budget, i.e., we address the following problem in this chapter.

Problem 3.1. *Find the control functions* $\mathbf{u} : [t_0, t_f] \mapsto \mathbb{R}^n$ *and* $\mathbf{v} : [t_0, t_f] \mapsto \mathbb{R}^n$ *such that the performance index* J *is maximized and the system equations and input constraints are satisfied:*

$$\underset{\mathbf{u}(t)\in\mathbb{U},\,\mathbf{v}(t)\in\mathbb{V}}{\textit{minimize}}\ J = \underbrace{\begin{bmatrix}\mathbf{1}^\top & -\mathbf{1}^\top\end{bmatrix}\mathbf{x}(t_f)}_{\phi(t_f)} - \int_0^{t_f} \underbrace{\begin{bmatrix}\mathbf{u}(t)\\ \mathbf{v}(t)\end{bmatrix}^\top \begin{bmatrix}W_u & 0\\ 0 & W_v\end{bmatrix} \begin{bmatrix}\mathbf{u}(t)\\ \mathbf{v}(t)\end{bmatrix}}_{L(\mathbf{u}(t),\mathbf{v}(t))} dt,$$

$$\textit{subject to } (3.5), \quad \mathbf{x}(t)\in\Omega, \quad \mathbf{x}(t_0) = \mathbf{x}_0 = \begin{bmatrix}\mathbf{q}_0 & \mathbf{r}_0\end{bmatrix}^\top, \tag{3.6}$$

where $L(\mathbf{u}(t),\mathbf{v}(t))$ is the running cost of the marketing campaign with constant diagonal positive definite weighting matrices W_u and W_v associated with referral rewards (control input $\mathbf{u}$) and customer loyalty programs (control input $\mathbf{v}$), respectively. The quantity $\phi(t_f) = \sum_{i=1}^{n}(q_i(t_f) - r_i(t_f))$ abstracts the marketing objective and is the reward associated with campaign deadline t_f.

3.3 Existence of the Solution

In this section, we verify the existence of the solution to Problem 3.1 using fundamental results from [56]. Let $\mathcal{F}$ denote the class of all $(\mathbf{x}_0, \mathbf{w}(t))$ such that $\mathbf{u}(t)\in\mathbb{U}$, $\mathbf{v}(t)\in\mathbb{V}$, and the solution to the Cauchy problem in Eq. (3.5) satisfies the initial condition $\mathbf{x}(t_0) = \mathbf{x}_0 \in \Omega$.

Theorem 3.3.1 (Existence)**.** *There exist $(\mathbf{x}_0^*, \mathbf{w}^*(t))$ maximizing the performance index J on $\mathcal{F}$.*

Proof. The proof is based on verifying the assumptions and conditions of the Cesari Theorem [56, Chapter III] for Problem 3.1 which we have repeated here for convenience:

Assumption 3.3.1. *The function f in Eq.* (3.5) *is continuous and there exist positive constants C_1, C_2 such that for all $t \in \mathbb{R}$, $\mathbf{x}(t)$, $\dot{\mathbf{x}}(t) \in \mathbb{R}^{2n}$, and $\mathbf{w}(t) \in \mathbb{U} \times \mathbb{V}$,*

$$\|f\left(\mathbf{x}(t), \mathbf{w}(t)\right)\|_1 \leq C_1(1 + \|\mathbf{x}(t)\|_1 + \|\mathbf{w}(t)\|_1), \tag{3.7}$$

$$\|f\left(\mathbf{x}_1(t), \mathbf{w}(t)\right) - f(\mathbf{x}_2(t), \mathbf{w}(t))\|_1 \leq C_2\|\mathbf{x}_1(t) - \mathbf{x}_2(t)\|_1(1 + \|\mathbf{w}(t)\|_1). \tag{3.8}$$

From Eq. (3.5) f is continuous by definition; also since the the set $\mathbb{U} \times \mathbb{V}$ is bounded, the term $\|\mathbf{w}(t)\|_1$ can be omitted from the right-hand side of Eqs. (3.7) and (3.8), with C_1 and C_2 replaced by different constants. Taking this into consideration, for the assumption in Eq. (3.7), we have

$$\begin{aligned}
&\|f\left(\mathbf{x}(t), \mathbf{w}(t)\right)\|_1 = \sum_{i=1}^{n} |\dot{q}_i(t)| + |\dot{r}_i(t)| \\
&= \sum_{i=1}^{n} \left|(1 - q_i(t) - r_i(t)) \sum_{j=1}^{n} [\mathcal{A}]_{i,j}(\beta_j + u_j(t))q_j(t) - (\delta_i - v_i(t))q_i(t)\right| \\
&\quad + \sum_{i=1}^{n} |(\delta_i - v_i(t))q_i(t) - \gamma_i r_i(t)| \\
&\leq \sum_{i=1}^{n}\sum_{j=1}^{n} [\mathcal{A}]_{i,j}(\beta_j + u_j(t))q_j(t) + \sum_{i=1}^{n}(q_i(t) + r_i(t)) \sum_{j=1}^{N} [\mathcal{A}]_{i,j}(\beta_j + u_j(t))q_j(t) \\
&\quad + \sum_{i=1}^{n} 2\delta_i q_i(t) + \sum_{i=1}^{n} \gamma_i r_i(t)
\end{aligned}$$

$$
\begin{aligned}
\leq & [\mathcal{A}]_{\max}(\beta_{\max} + u_{\max})\|\mathbf{q}(t)\|_1 \sum_{i=1}^{n} (1 + q_i(t) + r_i(t)) \\
& + 2\delta_{\max}\|\mathbf{q}(t)\|_1 + \gamma_{\max}\|\mathbf{r}(t)\|_1 \\
\leq & [\mathcal{A}]_{\max}(\beta_{\max} + u_{\max})\|\mathbf{q}(t)\|_1 (n + \|\mathbf{x}(t)\|_1) + \max\{2\delta_{\max}, \gamma_{\max}\}\|\mathbf{x}(t)\|_1 \\
\leq & n[\mathcal{A}]_{\max}(\beta_{\max} + u_{\max}) (n + \|\mathbf{x}(t)\|_1) + \max\{2\delta_{\max}, \gamma_{\max}\}\|\mathbf{x}(t)\|_1 \\
= & n^2[\mathcal{A}]_{\max}(\beta_{\max} + u_{\max}) + \Big(n[\mathcal{A}]_{\max}(\beta_{\max} + u_{\max}) \\
& \qquad + \max\{2\delta_{\max}, \gamma_{\max}\}\Big)\|\mathbf{x}(t)\|_1 \\
\leq & n^2[\mathcal{A}]_{\max}(\beta_{\max} + u_{\max}) + \max\{2\delta_{\max}, \gamma_{\max}\} \\
& + \left(n^2[\mathcal{A}]_{\max}(\beta_{\max} + u_{\max}) + \max\{2\delta_{\max}, \gamma_{\max}\}\right) \|\mathbf{x}(t)\|_1 \\
\leq & \underbrace{\left(n^2[\mathcal{A}]_{\max}(\beta_{\max} + u_{\max}) + \max\{2\delta_{\max}, \gamma_{\max}\}\right)}_{C_1} (1 + \|\mathbf{x}(t)\|_1),
\end{aligned}
$$

where $[\mathcal{A}]_{\max}$ is the maximum element of the weighted adjacency matrix $\mathcal{A}$.

The assumption in Eq. (3.8), is equivalent to proving Lipschitz continuity[1] of the function f relative to $\mathbf{x}$. Using 1-norm as the metric on the domain and range of f, we have

$$
\begin{aligned}
&\|f(\mathbf{x}(t), \mathbf{w}(t)) - f(\widehat{\mathbf{x}}, \mathbf{w}(t))\|_1 = \sum_{i=1}^{n} \left|\dot{q}_i(t) - \dot{\widehat{q}}_i(t)\right| + \left|\dot{r}_i(t) - \dot{\widehat{r}}_i(t)\right| = \\
&\sum_{i=1}^{n} \Big|(\delta_i - v_i(t))(\widehat{q}_i - q_i) + (1 - q_i(t) - r_i(t)) \sum_{j=1}^{n} [\mathcal{A}]_{i,j}(\beta_j + u_j(t))q_j(t) \\
&\qquad - (1 - \widehat{q}_i(t) - \widehat{r}_i(t)) \sum_{j=1}^{n} [\mathcal{A}]_{i,j}(\beta_j + u_j(t))\widehat{q}_j(t)\Big|
\end{aligned}
$$

[1] See Definition 1.2.6.4.

$$
\begin{aligned}
&+\sum_{i=1}^{n} |(\delta_i - v_i(t))(q_i(t) - \widehat{q}_i(t)) + \gamma_i(\widehat{r}_i(t) - r_i(t))| = \\
&2\delta_{\max}\|\mathbf{q}(t) - \widehat{\mathbf{q}}(t)\|_1 + \gamma_{\max}\|\mathbf{r}(t) - \widehat{\mathbf{r}}(t)\|_1 \\
&+\sum_{i=1}^{n}\Big|\sum_{j=1}^{n}[\mathcal{A}]_{i,j}(\beta_j + u_j(t))(q_j(t) - \widehat{q}_j(t)) \\
&\qquad + (\widehat{q}_i(t) + \widehat{r}_i(t))\sum_{j=1}^{n}[\mathcal{A}]_{i,j}(\beta_j + u_j(t))\widehat{q}_j(t) \\
&\qquad - (q_i(t) + r_i(t))\sum_{j=1}^{n}[\mathcal{A}]_{i,j}(\beta_j + u_j(t))q_j(t)\Big| \leq \\
&\max\{2\delta_{\max}, \gamma_{\max}\}\|\mathbf{x}(t) - \widehat{\mathbf{x}}(t)\|_1 + \sum_{i=1}^{n}[\mathcal{A}]_{\max}(\beta_{\max} + u_{\max})\|\mathbf{q}(t) - \widehat{\mathbf{q}}(t)\|_1 \\
&+\sum_{i=1}^{n}|\sum_{j=1}^{n}[\mathcal{A}]_{i,j}(\beta_j + u_j(t))(\widehat{q}_j(t)\widehat{q}_i(t) - q_j(t)q_i(t))| \\
&+\sum_{i=1}^{n}|\sum_{j=1}^{n}[\mathcal{A}]_{i,j}(\beta_j + u_j(t))(\widehat{q}_j(t)\widehat{r}_i(t) - q_j(t)r_i(t))| \leq \\
&\max\{2\delta_{\max}, \gamma_{\max}\}\|\mathbf{x}(t) - \widehat{\mathbf{x}}(t)\|_1 + n[\mathcal{A}]_{\max}(\beta_{\max} + u_{\max})\|\mathbf{q}(t) - \widehat{\mathbf{q}}(t)\|_1 \\
&+[\mathcal{A}]_{\max}(\beta_{\max} + u_{\max})\Big(\\
&\qquad \sum_{i=1}^{n}\sum_{j=1}^{n}(\widehat{q}_j(t)\widehat{q}_i(t) - \widehat{q}_j(t)q_i(t) + \widehat{q}_j(t)q_i(t) - q_j(t)q_i(t))\Big) \\
&+[\mathcal{A}]_{\max}(\beta_{\max} + u_{\max})\Big(\\
&\qquad \sum_{i=1}^{n}\sum_{j=1}^{n}(\widehat{q}_j(t)\widehat{r}_i(t) - \widehat{q}_j(t)r_i(t) + \widehat{q}_j(t)r_i(t) - q_j(t)r_i(t))\Big) \leq \\
&\max\{2\delta_{\max}, \gamma_{\max}\}\|\mathbf{x}(t) - \widehat{\mathbf{x}}(t)\|_1 + n[\mathcal{A}]_{\max}(\beta_{\max} + u_{\max})\|\mathbf{q}(t) - \widehat{\mathbf{q}}(t)\|_1 \\
&+n[\mathcal{A}]_{\max}(\beta_{\max} + u_{\max})\left(3\|\mathbf{q}(t) - \widehat{\mathbf{q}}(t)\|_1 + \|\mathbf{r}(t) - \widehat{\mathbf{r}}(t)\|_1\right) \\
&= \left(\max\{2\delta_{\max}, \gamma_{\max}\} + n[\mathcal{A}]_{\max}(\beta_{\max} + u_{\max})\right)\|\mathbf{x}(t) - \widehat{\mathbf{x}}(t)\|_1
\end{aligned}
$$

$$+ 3n\mathcal{A}_{\max}(\beta_{\max} + u_{\max})\|\mathbf{q}(t) - \widehat{\mathbf{q}}(t)\|_1$$

$$\leq \underbrace{(\max\{2\delta_{\max}, \gamma_{\max}\} + 4n[\mathcal{A}]_{\max}(\beta_{\max} + u_{\max}))}_{C_2} \|\mathbf{x}(t) - \widehat{\mathbf{x}}(t)\|_1;$$

Having shown that f is Lipschitz continuous relative to $\mathbf{x}$, there exists a unique solution to the Cauchy problem in Eq. (3.5) over $[t_0, t_f]$ for any initial condition $\mathbf{x}_0 \in \Omega$ according to the Global Existence and Uniqueness Theorem [37, Chapter 3]. Furthermore, the set of admissible inputs $\mathbb{U} \times \mathbb{V}$ is non-empty by definition; therefore, $\mathcal{F}$ is non-empty.

By structure, the set $\mathbb{U} \times \mathbb{V}$ is also closed and convex and the function f is linear in $\mathbf{w}$. The running cost function L is convex quadratic on $\mathbb{U} \times \mathbb{V}$ given positive definite weighting matrices W_u and W_v; in fact,

$$L(\underbrace{\mathbf{u}(t), \mathbf{v}(t)}_{\mathbf{w}(t)}) \geq \lambda_{\min}(\mathrm{diag}[W_u, W_v])\|\mathbf{w}(t)\|^2.$$

Finally, the set $\Omega \subset \mathbb{R}^{2n}$ is closed and bounded and therefore compact and the function ϕ is continuous on Ω. With all the assumptions and conditions of the Cesari Theorem satisfied, we conclude the existence of an optimal solution for Problem 3.1 on $\mathcal{F}$.

□

3.4 Solution to the Optimal Control Problem

Having guaranteed the existence of a solution, we now solve the optimal control problem formulated in Problem 3.1.

3.4.1 Analytical - Pontryagin Maximum Principle

The analytical solution is based on the necessary conditions provided in Pontryagin Maximum Principle [56, Chapter II]. The first step is to obtain the Hamiltonian H:

$$
\begin{aligned}
H\left(\mathbf{x}(t), \mathbf{w}(t), \boldsymbol{\lambda}(t)\right) &= -L\left(\mathbf{w}(t)\right) + \boldsymbol{\lambda}(t)^\top f\left(\mathbf{x}(t), \mathbf{w}(t)\right) \\
&= -\mathbf{u}(t)^\top W_u \mathbf{u}(t) - \mathbf{v}(t)^\top W_v \mathbf{v}(t) + \boldsymbol{\lambda}(t)^\top f\left(\mathbf{x}(t), \mathbf{w}(t)\right),
\end{aligned}
$$

where $\boldsymbol{\lambda}(t) = \begin{bmatrix} \boldsymbol{\lambda}_q^\top(t) & \boldsymbol{\lambda}_r^\top(t) \end{bmatrix}^\top \in \mathbb{R}^{2n}$ denotes the co-state vector, interpreted as the Lagrange multiplier associated with the state equation in Eq. (3.5). According to the Maximum Principle, the solutions to Problem 3.1 also solve the following set of differential equations:

- State equation:

$$
\dot{\mathbf{x}}(t) = \nabla_\lambda H = f\left(\mathbf{x}(t), \mathbf{w}(t)\right), \; \mathbf{x}(t_0) = \mathbf{x}_0.
$$

- Co-state equation:

$$
\dot{\boldsymbol{\lambda}}(t) = -\nabla_{\mathbf{x}} H = -\nabla_{\mathbf{x}}\left(\boldsymbol{\lambda}^\top(t) f\left(\mathbf{x}(t), \mathbf{w}(t)\right)\right),
$$

$$\boldsymbol{\lambda}(t_f) = (\nabla_{\mathbf{x}}\phi)\big|_{\mathbf{x}(t_f)} = \begin{bmatrix} \mathbf{1} \\ -\mathbf{1} \end{bmatrix};$$

therefore,

$$\begin{aligned}\dot{\boldsymbol{\lambda}}_q(t) &= \Lambda_q(t)\mathcal{A}\left(B + U(t)\right)\mathbf{q}(t) \\ &\quad - \left(B + U(t)\right)\mathcal{A}^\top\left(I - R(t) - Q(t)\right)\boldsymbol{\lambda}_q(t) \\ &\quad + \left(D - V(t)\right)\left(\boldsymbol{\lambda}_q(t) - \boldsymbol{\lambda}_r(t)\right), \\ \dot{\lambda}_r(t) &= \Lambda_q(t)\mathcal{A}\left(B + U(t)\right)\mathbf{q}(t) + \Gamma\boldsymbol{\lambda}_r(t),\end{aligned} \tag{3.9}$$

where $\Lambda_q(t) = \operatorname{diag}[\boldsymbol{\lambda}_q(t)]$.

- Optimality (stationarity) condition:

$$0 = \nabla_{\mathbf{w}}H = \nabla_{\mathbf{w}}L\left(\mathbf{w}(t)\right) + \nabla_{\mathbf{w}}\left(\boldsymbol{\lambda}^\top(t)f\left(\mathbf{x}(t), \mathbf{w}(t)\right)\right) \Rightarrow$$

$$0 = -2\begin{bmatrix} W_u & \\ & W_v \end{bmatrix}\begin{bmatrix} \mathbf{u}(t) \\ \mathbf{v}(t) \end{bmatrix} + \begin{bmatrix} Q(t)\mathcal{A}^\top\big(I - R(t) - Q(t)\big)\boldsymbol{\lambda}_q(t) \\ Q(t)\left(\boldsymbol{\lambda}_q(t) - \boldsymbol{\lambda}_r(t)\right) \end{bmatrix}.$$

The optimal controls are then computed as

$$\begin{aligned}\mathbf{u}^*(t) &= \frac{1}{2}W_u^{-1}Q^*(t)\mathcal{A}^\top\big(I - R^*(t) - Q^*(t)\big)\boldsymbol{\lambda}_q^*(t), \qquad && \mathbf{u}^*(t) \in \mathbb{U}, \\ \mathbf{v}^*(t) &= \frac{1}{2}W_v^{-1}Q^*(t)\left(\boldsymbol{\lambda}_q^*(t) - \boldsymbol{\lambda}_r^*(t)\right), && \mathbf{v}^*(t) \in \mathbb{V}.\end{aligned} \tag{3.10}$$

Remark 3.4.1.1. *The Pontryagin Maximum Principle delivers necessary conditions for optimality. As far as global maximality is concerned, the optimality condition stated above hints at a sufficient condition, i.e.,*

$$\begin{bmatrix} \mathbf{u}^*(t) \\ \mathbf{v}^*(t) \end{bmatrix} = \arg\max_{\mathbf{u}(t),\mathbf{v}(t)} H\left(\mathbf{x}(t), \begin{bmatrix} \mathbf{u}(t) \\ \mathbf{v}(t) \end{bmatrix}, \boldsymbol{\lambda}(t)\right).$$

Sufficient conditions for the above are, for example, the concavity of the Hamiltonian H in the control inputs $\mathbf{u}(t)$ and $\mathbf{v}(t)$ which is the case here.

The expression in Eq. (3.10), i.e., the characterization of the optimal control inputs $\mathbf{u}^*(t)$ and $\mathbf{v}^*(t)$, cannot be directly evaluated given that $\mathbf{q}^*(t)$, $\mathbf{r}^*(t)$, $\boldsymbol{\lambda}_q^*(t)$, and $\boldsymbol{\lambda}_r^*(t)$ are unknown beforehand. Substituting Eq. (3.10) in the state and co-state Eqs. (3.5) and (3.9) and using the state initial condition $\mathbf{x}(t_0)$ and co-state final condition $\boldsymbol{\lambda}(t_f)$, we get a system of ODEs which can be solved numerically using standard techniques. We next discuss one such method.

3.4.2 Numerical - FBSM

To solve for the optimal control inputs in Eq. (3.10), we use FBSM explained in [57] and [58]. This method is a discrete-time algorithm with sufficiently small sampling period T_s.

At each iteration k of Algorithm 2, we use an explicit method, i.e., forward Euler [59], to numerically solve Eq. (3.5):

$$\mathbf{x}^{(k)}(t_0) = \mathbf{x}_0, \qquad \mathbf{x}^{(k)}(t_{j+1}) = \mathbf{x}^{(k)}(t_j) + T_s f\left(\mathbf{x}^{(k)}(t_j), \begin{bmatrix} \mathbf{u}^{(k)}(t_j) \\ \mathbf{v}^{(k)}(t_j) \end{bmatrix}\right).$$

For Eq. (3.9), which is backward in time, using forward Euler would result

Algorithm 2 The Forward Backward Sweep Method (FBSM)

given set of admissible inputs $\mathbb{U} \times \mathbb{V}$, tolerance $\epsilon > 0$, and sampling period T_s:

· gather equidistant time steps in vector $\mathbf{t} = t_0 : T_s : t_f$ – indexed by j,

· make an initial guess for the control inputs over $\mathbf{t}$:

$$\begin{bmatrix} \mathbf{U}^{(0)}(\mathbf{t}) \\ \mathbf{V}^{(0)}(\mathbf{t}) \end{bmatrix} = \begin{bmatrix} \mathbf{u}^{(0)}(t_0), \mathbf{u}^{(0)}(t_0+T_s), \cdots, \mathbf{u}^{(0)}(t_f) \\ \mathbf{v}^{(0)}(t_0), \mathbf{v}^{(0)}(t_0+T_s), \cdots, \mathbf{v}^{(0)}(t_f) \end{bmatrix}, \quad \begin{bmatrix} \mathbf{u}^{(0)}(t_0+jT_s) \\ \mathbf{v}^{(0)}(t_0+jT_s) \end{bmatrix} \in \mathbb{U} \times \mathbb{V}.$$

$k \leftarrow 0$

repeat

· Forward in time: compute $\mathbf{x}^{(k)}(\mathbf{t})$, the solution to Eq. (3.5) corresponding to the series of inputs $\mathbf{U}^{(k)}(\mathbf{t})$ and $\mathbf{V}^{(k)}(\mathbf{t})$ and initial condition $\mathbf{x_0}$.

· Backward in time: compute $\boldsymbol{\lambda}^{(k)}(\mathbf{t})$, the solution to Eq. (3.9) corresponding to the series of inputs $\mathbf{U}^{(k)}(\mathbf{t})$ and $\mathbf{V}^{(k)}(\mathbf{t})$, the state $\mathbf{x}^{(k)}(\mathbf{t})$, and terminal condition $\boldsymbol{\lambda}(t_f)$.

· Compute $\mathbf{U}^{(k+1)}(\mathbf{t})$ and $\mathbf{V}^{(k+1)}(\mathbf{t})$ according to Eq. (3.10) using $\mathbf{x}^{(k)}(\mathbf{t})$ and $\boldsymbol{\lambda}^{(k)}(\mathbf{t})$ obtained from previous steps.

until $\| \begin{bmatrix} \mathbf{U}^{(k+1)}(\mathbf{t}) \\ \mathbf{V}^{(k+1)}(\mathbf{t}) \end{bmatrix} - \begin{bmatrix} \mathbf{U}^{(k)}(\mathbf{t}) \\ \mathbf{V}^{(k)}(\mathbf{t}) \end{bmatrix} \| < \epsilon.$

in an implicit method as follows:

$$\boldsymbol{\lambda}^{(k)}(t_f) = \begin{bmatrix} \mathbf{1} \\ \\ -\mathbf{1} \end{bmatrix}, \qquad \boldsymbol{\lambda}^{(k)}(t_{j-1}) = \boldsymbol{\lambda}^{(k)}(t_j) - T_s \dot{\boldsymbol{\lambda}}^{(k)}(t_{j-1}).$$

The resulting system of linear equations solving for $\boldsymbol{\lambda}^{(k)}(t_{j-1})$ given $\boldsymbol{\lambda}^{(k)}(t_j)$ has the following matrix form:

$$\left(I_{2n} + T_s \underbrace{\begin{bmatrix} M_{11} & M_{12} \\ \\ M_{21} & M_{22} \end{bmatrix}}_{M} \right) \begin{bmatrix} \boldsymbol{\lambda}_q^{(k)}(t_{j-1}) \\ \\ \boldsymbol{\lambda}_r^{(k)}(t_{j-1}) \end{bmatrix} = \begin{bmatrix} \boldsymbol{\lambda}_q^{(k)}(t_j) \\ \\ \boldsymbol{\lambda}_r^{(k)}(t_j) \end{bmatrix}.$$

The block-diagonal matrix M has the following blocks:

$$
\begin{aligned}
M_{11} =& \left(D - V^{(k)}(t_{j-1})\right) + \operatorname{diag}\left[\mathcal{A}\left(B + U^{(k)}(t_{j-1})\right)\mathbf{q}^{(k)}(t_{j-1})\right] \\
& - \left(B + U^{(k)}(t_{j-1})\right)\mathcal{A}^\top \left(I - R^{(k)}(t_{j-1}) - Q^{(k)}(t_{j-1})\right), \\
M_{21} =& \operatorname{diag}\left[\mathcal{A}\left(B + U^{(k)}(t_{j-1})\right)\mathbf{q}^{(k)}(t_{j-1})\right], \\
M_{12} =& -\left(D - V^{(k)}(t_{j-1})\right), \quad M_{22} = \Gamma,
\end{aligned}
$$

where $U^{(k)} = \operatorname{diag}\left[\mathbf{u}^{(k)}\right]$ and $V^{(k)} = \operatorname{diag}\left[\mathbf{v}^{(k)}\right]$. Thus,

$$
\boldsymbol{\lambda}^{(k)}(t_f) = \begin{bmatrix} \mathbf{1} \\ \\ -\mathbf{1} \end{bmatrix}, \quad \boldsymbol{\lambda}^{(k)}(t_{j-1}) = (I_{2N} + T_s M)^{-1}\boldsymbol{\lambda}^{(k)}(t_j).
$$

3.5 Simulations

In this section, we illustrate the concepts introduced in this chapter. We consider a random undirected social network with $n = 50$ nodes generated using the Erdős-Rényi model $\mathcal{G}(N, p_e)$ [60] where each edge is included in the graph with probability p_e independent from every other edge. Choosing $p_e = \frac{2}{n-1}$ ensures the existence of a large connected component in the network. A realization of this random graph is shown in Fig. 3.2a. The transition rates β_i, δ_i, and γ_i are randomly selected from the intervals (0.5, 0.7), (0.4, 0.6), and (0.3, 0.5), respectively. The initial probabilities of an individual i being in the adopting and dormant compartments, $q_i(0)$ and $r_i(0)$, are randomly chosen in the interval $(0, 0.01)$, which represents the low probability of individuals actively adopting or having previously adopted the product in the beginning of the marketing campaign. The weighting matrices W_u and W_v in the campaign running cost L, are chosen such that for customer i, $W_{u_{ii}} = 2 + 0.02d_i$, and $W_{v_{ii}} = 1 + 0.01d_i$, where d_i is the number of neighbors i has; i.e., the weight for each individual is composed of a constant cost associated with a specific marketing strategy and an individual-specific component directly related to the number of connections an individual has, e.g., celebrities tend to require considerable incentives to adopt a new product and usually expect a flawless customer experience. The difference between the two strategies' constant costs reflects that fact that attracting new customers is usually costlier than maintaining the current clientele. The campaign time t_f and inputs bounds $u_{\max}$ and $v_{\max}$ are set to 12, 0.3, and 0.4, respectively.

The effectiveness of the proposed marketing strategies on optimizing the marketing objective, i.e., $\phi(t)$, is illustrated in Fig. 3.2b where we have averaged $\phi(t)$ over 100 Monte Carlo simulations. Comparing the end reward $\phi(t_f)$ in the presence and lack thereof control inputs, i.e., marketing strategies, the optimal control regime proves to have been effective.

In Fig. 3.2c, we have plotted the components of $\phi(t)$ separately; the final sum $\mathbf{1}^\top \mathbf{q}(t_f)$ is an approximation of the expected size of the adopting population while $\mathbf{1}^\top \mathbf{r}(t_f)$ approximates the expected number of individuals in the dormant state.

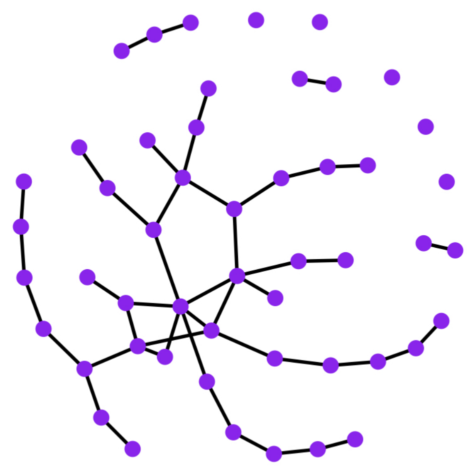

(a) Erdős-Rényi network.

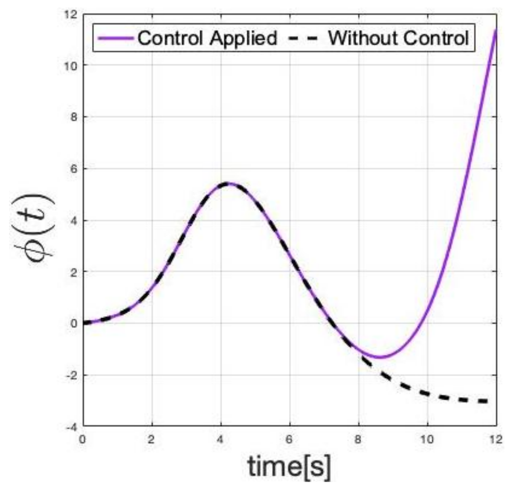

(b) $\phi(t)$ with and without control.

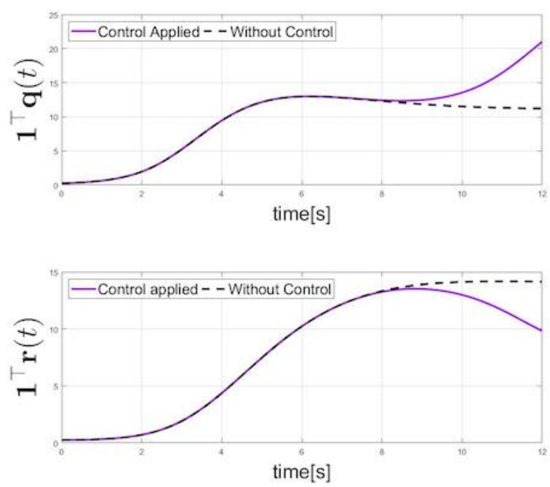

(c) Components of $\phi(t) = \mathbf{1}^\top (\mathbf{q}(t) - \mathbf{r}(t))$.

Figure 3.2: Network topology, $\phi(t)$, and its components.

3.6 Conclusions

In this chapter, we study the optimal control of marketing campaigns on heterogeneous networks. We propose a model of product adoption equivalent to the node-based SIRS epidemic model. In this context, the performance criterion is formulated based on optimizing the expected number of individuals adopting the product while taking resource limitations into account. We prove the existence of a solution according to Cesari theorem and solve the optimal control problem analytically using the Pontryagin Maximum Principle. Additionally, a numerical method is proposed to compute the performance and control inputs.

Chapter 4

Distributed Optimization Over Dynamic Directed Graphs

In this chapter, we provide a distributed optimization algorithm, termed as TV-$\mathcal{AB}$, that minimizes a sum of convex functions over time-varying digraphs. Contrary to the existing work, the algorithm we propose does not require eigenvector estimation to estimate the (non-$\mathbf{1}$) Perron eigenvector of a stochastic matrix. Instead, the proposed approach relies on a novel information mixing approach that exploits both row and column-stochastic weights to achieve agreement towards the optimal solution when the underlying graph is directed. We show that TV-$\mathcal{AB}$ converges linearly to the optimal solution when the global objective is smooth and strongly-convex, and the underlying time-varying graphs exhibit bounded connectivity, i.e., a union of every $\mathcal{C}$

consecutive graphs is strongly-connected. We derive the convergence results based on the stability analysis of a linear system of inequalities along with a matrix perturbation argument. Simulations confirm the theoretical results of this chapter.

4.1 Introduction

Emerging technologies such as artificial intelligence (AI), the blockchain, and virtual and augmented reality, enabled by the advent of 5G, are making their way into the mainstream. Many potential applications of these technologies rely heavily on training machine learning models based on the data collected by a large number of devices. For example, as a concrete application of AI, self-driving cars rely on computer vision in order to accurately navigate and plan their route. Such tasks can be framed as classification, regression, or risk minimization, with a simple sum of cost optimization at the core. Such problems arise for example in sensor networks [61], large-scale machine learning [62], distributed estimation [63], and localization [64]. However, the volume and velocity of data along with privacy concerns limit data sharing. It is therefore imperative to develop solutions to the underlying optimization problems that are local and distributed [65–67]. Furthermore, the algorithms must accommodate mobile and autonomous agents characterized by time-varying and non-deterministic information exchange.

Recently, there has been a large body of work on distributed optimization, where the goal is to minimize the following sum of costs:

$$\min_{\mathbf{x}} \frac{1}{n} \textstyle\sum_{i=1}^{n} f_i(\mathbf{x}),$$

such that each objective function, $f_i : \mathbb{R}^p \mapsto \mathbb{R}$, is private to agent i. In order to solve this problem, the agents exchange information with nearby nodes over a sparse communication graph. When the graphs are static and undirected, early work on first-order methods include [68–70] with the convergence rate[1] of $O(\frac{\ln k}{\sqrt{k}})$ for arbitrary convex functions and $O(\frac{\ln k}{k})$ for strongly-convex functions, where k denotes the number of iterations. The sublinear convergence is due to the use of diminishing stepsizes. The rate improves to linear with a constant stepsize though at the expense of a sub-optimal solution [71]. Methods based on the Lagrangian dual [72, 73] converge faster but suffer from a high computational burden as they require solving a subproblem at each iteration.

Optimization over digraphs is developed in [74–76], where push-sum [77, 78] is used to achieve consensus among the agents. The convergence rate, with diminishing stepsizes, is $O(\frac{\ln k}{\sqrt{k}})$ for arbitrary convex functions and $O(\frac{\ln k}{k})$ for strongly-convex functions. In contrast, Refs. [79, 80] use an alternate approach called surplus consensus [81] to achieve consensus but with the same

[1] Refer to Section 1.2.7 for details on the convergence of iterative algorithms.

convergence rates as [74–76]. The main reason for slow convergence is that a local gradient is used at each agent, which requires diminishing stepsizes to ensure optimality. To overcome this challenge, Refs. [82–84] replace the local gradient with an estimate of the global gradient, with the help of dynamic consensus [85] over undirected graphs, and show linear convergence to the optimal solution. This gradient estimation approach was combined with push-sum type methods in [84, 86–88] to achieve linear convergence to the optimal solution over digraphs. Related work along these lines also include [89] over undirected graphs and [90] over digraphs that are related to [84, 86]. An alternate approach that builds on [79, 80] and does not use push-sum has been developed in [91], where a row and a column-stochastic matrix are used simultaneously to achieve linear convergence to the optimal solution over digraphs. Accelerated methods can be found in [92–94], while non-convex problems are considered in [95].

In this chapter, our focus is on time-varying digraphs. Early work on time-varying communication among the agents can be found in [69, 96], where the exchange is undirected and in [97], where the exchange is directed. These methods are built on local gradients at each agent and are thus sublinearly convergent. Recent work includes [98], where the authors establish a geometrically converging distributed optimization algorithm over digraphs under uncoordinated yet bounded stepsizes, and [99], where agents communicate over graphs subject to random link failures. Further work on random graphs can be found in [100], where the problem of constrained convex optimization is investigated for non-differentiable costs under Markovian communication model. For random networks modeled by a sequence of independent, identically distributed (IID) random matrices drawn from the set of symmetric, stochastic matrices with positive diagonals, [101] proposes two accelerated distributed Nesterov-like gradient methods featuring resiliency to link failures, reduced computational load, and improved convergence rates compared to other gradient methods. Ref. [102] establishes a convergence rate of $O(\frac{1}{k})$ for distributed stochastic gradient methods over temporally IID random undirected graphs for strongly-convex costs when local gradients are subject to noise that is IID in time and has a finite second moment. Furthermore, asynchronous multi-agent optimization is considered in [103], where the authors adopt the curvature estimation technique of the Broyden-Fletcher-Goldfarb-Shanno quasi-Newton optimization method [104–106] for use in asynchronous distributed settings over undirected graphs [107]. An asynchronous implementation of subgradient-push [76] algorithm is also recently developed in [108].

In this chapter, we use gradient estimation as was used in [82–84, 86] and extend the $\mathcal{AB}$ algorithm introduced in [91] to time-varying digraphs. Of relevance in this context is Ref. [84], which uses gradient estimation and push-sum consensus [77, 78] to implement distributed optimization over time-varying graphs. However, the push-sum based methods [84, 86–88] involve estimating the (non-$\mathbf{1}$) Perron eigenvector of a stochastic matrix and an appropriate scaling with the estimated eigenvector components. The eigenvector estimation adds conservatism to the overall algorithm as its convergence may dominate the overall rate. In contrast, the $\mathcal{AB}$ algorithm [91] does not require such eigenvector estimation and employs both row and column-stochastic weights in a novel way. The time-varying algorithm proposed in this chapter, termed as TV-$\mathcal{AB}$, thus is applicable to time-varying digraphs without the need of eigenvector estimation resulting from push-sum.

The TV-$\mathcal{AB}$ algorithm we introduce involves a unique and rather counter-intuitive way of mixing information among the agents. As the graph at each iteration may not be strongly-connected, the mechanics of TV-$\mathcal{AB}$ can be explained over a single directed edge, $i \longrightarrow j$. First, we note that TV-$\mathcal{AB}$ involves two updates: one with a row-stochastic weight matrix, $\mathcal{A}$, and the other with a column-stochastic weight matrix, $\mathcal{B}$. The update involving $\mathcal{A}$ is standard where the receiving agent j implements a sum-preserving update to its past and the incoming information from agent i, while agent i assigns a weight of 1 to its past since it does not receive any information. However, the update with the column-stochastic weights, $\mathcal{B}$, requires the transmitting agent i to implement a strictly stable update (by assigning a weight less than 1 to its past) and the receiving agent to implement an unstable update (by assigning weights that sum to a number greater than 1 to its past and the incoming information from agent i) in order to maintain column-stochasticity of $\mathcal{B}$. In other words, the updates involving $\mathcal{B}$ are not sum-preserving, unlike the traditional information fusion.

We show that TV-$\mathcal{AB}$ converges linearly to the optimal solution when each local objective is smooth and the global objective is strongly-convex. The graph at each iteration can be generated randomly in an arbitrary fashion as long as the union of every $\mathcal{C}$ consecutive graphs is strongly-connected. This notion is known as bounded connectivity and is standard in the consensus and optimization literature on time-varying graphs, see e.g., [76, 84]. The bounded connectivity notion enables us to obtain more concrete convergence results as without this assumption, the analysis is restricted to the expected behavior of the optimization algorithm, see e.g., [96, 99, 101]. We show linear convergence with the help of a linear system of inequalities along with a matrix perturbation argument.

We now describe the rest of the chapter. Section 4.2 formulates the problem and introduces the assumptions necessary to algorithm development. Section 4.2.1 develops and interprets the TV-$\mathcal{AB}$ algorithm. Details on the convergence analysis are presented in Section 4.3 while Section 4.4 states the main result. Finally, Section 4.5 provides numerical experiments and Section 4.6 contains the concluding remarks.

4.2 Problem Formulation and Algorithm

In this section, we formulate the distributed optimization problem, state the assumptions, and introduce the TV-$\mathcal{AB}$ algorithm. To this aim, we assume that the set of agents, $\mathcal{V} = \{1, 2, \cdots, n\}$, communicate according to a time-varying digraph, $\mathcal{G}_k(\mathcal{V}, \mathcal{E}_k)$, where k is the discrete-time index and $\mathcal{E}_k$ is the set of directed communication links at time k. The goal of the agents is to collaboratively solve the following problem:

$$\text{Problem 1:} \qquad \min_{\mathbf{x}} f(\mathbf{x}) = \frac{1}{n} \textstyle\sum_{i=1}^{n} f_i(\mathbf{x}), \tag{4.1}$$

where each local objective function, $f_i : \mathbb{R}^p \mapsto \mathbb{R}$, is held privately at agent i. We next formalize the set of assumptions that are standard in the distributed optimization literature[2].

Assumption 4.2.1 (Strong-convexity)**.** *The global objective function f is μ-strongly-convex.*

For Assumption 4.2.1 to hold it suffices that each f_i is convex and at least one of them is strongly-convex. Under this assumption, Problem 1 has a unique optimal solution, denoted by $\mathbf{x}^*$.

Assumption 4.2.2 (Smoothness)**.** *Each f_i is ℓ_i-smooth, i.e., it is differentiable and has a Lipschitz-continuous gradient.*

[2]Refer to Section 1.2.6 on properties of functions.

Assumption 4.2.2 implies that $f = 1/n\sum_i f_i$ is $\bar{\ell}$-smooth, where $\bar{\ell} = 1/n\sum_{i=1}^n \ell_i$. Furthermore, collecting the local variables in column vectors

$$\mathbf{x} = \begin{bmatrix} \mathbf{x}^1 \\ \vdots \\ \mathbf{x}^n \end{bmatrix}, \quad \mathbf{f}(\mathbf{x}) = \begin{bmatrix} f_1(\mathbf{x}^1) \\ \vdots \\ f_n(\mathbf{x}^n) \end{bmatrix}, \quad \boldsymbol{\nabla}\mathbf{f}(\mathbf{x}) = \begin{bmatrix} \boldsymbol{\nabla} f_1(\mathbf{x}^1) \\ \vdots \\ \boldsymbol{\nabla} f_n(\mathbf{x}^n) \end{bmatrix},$$

we note that $\mathbf{f}$ is L-smooth, where $L = \max_i\{\ell_i\}$.

Assumption 4.2.3 ($\mathcal{C}$-bounded strong-connectivity)**.** *For the sequence of time-varying digraphs $\{\mathcal{G}_k(\mathcal{V}, \mathcal{E}_k \subseteq \mathcal{V}\times\mathcal{V})\}$, there exists some positive integer $\mathcal{C}$ such that the aggregate digraph $\mathcal{G}_k^{\mathcal{C}}(\mathcal{V}, \cup_{l=k}^{k+\mathcal{C}-1}\mathcal{E}_l)$ is strongly-connected $\forall\, k \geq 0$.*

Assumption 4.2.4 (Weights)**.** *For the sequence $\{\mathcal{G}_k(\mathcal{V}, \mathcal{E}_k)\}$ of time-varying digraphs and the sequences, $\{A_k\}$ and $\{B_k\}$, of $n \times n$ matrices compliant with $\mathcal{G}_k$, i.e., $(j,i) \in \mathcal{E}_k \Leftrightarrow [A_k]_{i,j}, [B_k]_{i,j} \neq 0$, the following hold.*

(i) Stochasticity: $\{A_k\}$ and $\{B_k\}$ are row and column-stochastic, respectively.

(ii) Aperiodicity: $\mathcal{G}_k$ has self-loops; i.e., $[A_k]_{i,i} > 0$ and $[B_k]_{i,i} > 0, \forall\, i \in \mathcal{V}$ and $\forall\, k \geq 0$.

(iii) Uniform positivity: There are scalars $0 < \alpha, \beta < 1$ such that $[A_k]_{i,j} \geq \alpha$ and $[B_k]_{i,j} \geq \beta$, $\forall\,(j,i) \in \mathcal{E}_k$, $k \geq 0$.

The strong-connectivity bound $\mathcal{C}$ and the uniform positivity bounds α and β introduced in Assumptions 4.2.3 and 4.2.4 are not required to be known at any of the agents. They are only used in the analysis of the algorithm.

4.2.1 Algorithm Development

We now describe the TV-$\mathcal{AB}$ algorithm to solve Problem 1. At each time k, agent $i \in \mathcal{V}$ maintains two variables, $\mathbf{x}_k^i$ and $\mathbf{y}_k^i$, both in $\mathbb{R}^p$, initialized with arbitrary $\mathbf{x}_0^i$ and $\mathbf{y}_0^i = \boldsymbol{\nabla} f_i(\mathbf{x}_0^i)$. The $\mathbf{x}_k^i$-update at each agent is essentially gradient descent, albeit after mixing incoming information, and where the descent direction is given by an estimate of the global gradient, $\mathbf{y}_k^i$, instead of the local gradient, $\boldsymbol{\nabla} f_i(\mathbf{x}_k^i)$. The $\mathbf{y}_k^i$-update at each agent tracks the global gradient and is based on column-stochastic weights.

We first use a simple framework to explain the algorithm where only one edge $i \longrightarrow j$ is active at time k. The $\mathbf{x}_k$-update follows the standard sum-preserving notion where weights assigned to the past information are non-negative and sum to 1:

$$\begin{aligned}
\mathbf{x}_{k+1}^i =& \mathbf{x}_k^i - \eta \mathbf{y}_k^i, \qquad \forall\, i \neq j, \\
\mathbf{x}_{k+1}^j =& [A_k]_{j,i} \mathbf{x}_k^i + [A_k]_{j,j} \mathbf{x}_k^j - \eta \mathbf{y}_k^j,
\end{aligned}$$

where η is a constant stepsize. The weight matrix, A_k, behind this update is row-stochastic: Each diagonal element, $[A_k]_{i,i} = 1, \forall\, i \neq j$, while the j^{th} row has only two positive elements such that $[A_k]_{j,i} + [A_k]_{j,j} = 1$.

Defining the auxiliary variable $\mathbf{z}_k^i$ as the successive difference of the gradients, $\nabla f_i(\mathbf{x}_{k+1}^i) - \nabla f_i(\mathbf{x}_k^i)$, the $\mathbf{y}_k$-update is given by

$$\begin{aligned}
\mathbf{y}_{k+1}^m =& [B_k]_{m,m}\mathbf{y}_k^m + \mathbf{z}_k^m, \qquad m \neq i, \quad m \neq j,\\
\mathbf{y}_{k+1}^i =& [B_k]_{i,i}\mathbf{y}_k^i + \mathbf{z}_k^i,\\
\mathbf{y}_{k+1}^j =& [B_k]_{j,i}\mathbf{y}_k^i + [B_k]_{j,j}\mathbf{y}_k^j + \mathbf{z}_k^j.
\end{aligned}$$

Note that every column of B_k, except for the i^{th}, has only one non-zero element as no agent other than i is transmitting. Hence, for B_k to be column-stochastic, $[B_k]_{j,j} = 1, \forall j \neq i$. For the transmitting agent, we have $[B_k]_{i,i} + [B_k]_{j,i} = 1$. In contrast to the traditional row or doubly-stochastic updates, the $\mathbf{y}_{k+1}^i$-update is locally stable as $[B_k]_{i,i} < 1$, while the $\mathbf{y}_{k+1}^j$-update is locally unstable as $[B_k]_{j,i} + [B_k]_{j,j} > 1$.

4.2.2 The TV-$\mathcal{AB}$ Algorithm

The simple scenario discussed above can be generalized to arbitrary graphs, resulting into the following algorithm:

$$\mathbf{x}_{k+1}^i = \sum_{j=1}^{n} [A_k]_{i,j}\mathbf{x}_k^j - \eta\mathbf{y}_k^i, \tag{4.2a}$$

$$\mathbf{y}_{k+1}^i = \sum_{j=1}^{n} [B_k]_{i,j}\mathbf{y}_k^j + \mathbf{z}_k^i, \tag{4.2b}$$

where the weights $[A_k]_{i,j}$ and $[B_k]_{i,j}$ satisfy Assumption 4.2.4. Letting $\mathcal{A}_k \triangleq A_k \otimes I_p$ and $\mathcal{B}_k \triangleq B_k \otimes I_p$, we present Eqs. (4.2) in a vector-matrix form, where the local variables $\mathbf{x}_k^i$'s, $\mathbf{y}_k^i$'s, and $\mathbf{z}_k^i$'s and gradients $\boldsymbol{\nabla} f_i(\mathbf{x}_k^i)$'s are stored in the column vectors $\mathbf{x}_k$, $\mathbf{y}_k$, $\mathbf{z}_k$, and $\boldsymbol{\nabla}\mathbf{f}(\mathbf{x}_k)$, respectively:

$$\mathbf{x}_{k+1} = \mathcal{A}_k \mathbf{x}_k - \eta \mathbf{y}_k, \tag{4.3a}$$

$$\mathbf{y}_{k+1} = \mathcal{B}_k \mathbf{y}_k + \mathbf{z}_k, \tag{4.3b}$$

where $\mathbf{z}_k = \boldsymbol{\nabla}\mathbf{f}(\mathbf{x}_{k+1}) - \boldsymbol{\nabla}\mathbf{f}(\mathbf{x}_k)$. The weight matrices, $\mathcal{A}_k$ and $\mathcal{B}_k$, are row- and column-stochastic, respectively. However, since each $\mathcal{G}_k$ is not necessarily strongly-connected, the weights $\mathcal{A}_k$ and $\mathcal{B}_k$ are not necessarily primitive or irreducible; thus, the standard Perron-Frobenius arguments [3, Theorem 8.8.4] are not applicable here. To overcome this issue, we use the notions of absolute probability sequences and ergodicity[3] to establish multi-step contractions as described next.

Lemma 4.2.2.1 ([109, Lemma 5.2.1])**.** *Under Assumptions 4.2.3 and 4.2.4, the row-stochastic matrix sequence* $\{D_s = \Pi_{l=s\mathcal{C}}^{s\mathcal{C}+\mathcal{C}-1} A_l\}$*, obtained from the backward product of* $\{A_k\}$ *and compliant with* $\mathcal{G}_{s\mathcal{C}}^{\mathcal{C}}(\mathcal{V}, \cup_{l=s\mathcal{C}}^{s\mathcal{C}+\mathcal{C}-1}\mathcal{E}_l)$*, for all* $s \geq 0$*, is ergodic, i.e.,*

$$\lim_{t\to\infty} D_t \cdots D_{s+1} D_s = \mathbf{1}\boldsymbol{\mu}_s^\top,$$

[3]Refer to Section 1.2.3.

where $\{\boldsymbol{\mu}_s\}$ is the unique absolute probability sequence for $\{D_s\}$ (see, e.g., [6], [110, Lemma 1]) and is uniformly bounded away from zero, i.e., there exists $0 < \delta < 1$ such that $[\boldsymbol{\mu}_s]_i \geq \delta$, $\forall\, i \in \mathcal{V}$ and $\forall\, s \geq 0$. Furthermore, the convergence rate is geometric, i.e., $\forall\, t \geq s \geq 0$:

$$\|D_t \cdots D_{s+1} D_s - \mathbf{1}\boldsymbol{\mu}_s^\top\| \leq \mathcal{M} q^{t-s},$$

where the constants $\mathcal{M} > 0$ and $q \in (0,\, 1)$ depend only on n and α introduced in Assumption 4.2.4.

The next corollary extends the result above, deriving the absolute probability sequence for the sequence $\{A_k\}$ in terms of $\{\boldsymbol{\mu}_k\}$ in Lemma 4.2.2.1.

Corollary 4.2.2.1. *Under the assumptions of Lemma 4.2.2.1, the sequence $\{\boldsymbol{\phi}_k\}$ is an absolute probability sequence for the matrix sequence $\{A_k\}$, where*

$$\begin{aligned} \boldsymbol{\phi}_k^\top =& \boldsymbol{\mu}_s^\top, \quad k = s\mathcal{C}, \\ \boldsymbol{\phi}_k^\top =& \boldsymbol{\mu}_{s+1}^\top A_{(s+1)\mathcal{C}-1} \cdots A_k, \quad s\mathcal{C} < k < (s+1)\mathcal{C}, \end{aligned} \tag{4.4}$$

for $s = 0,\, 1,\, 2,\, \cdots$.

Proof. Since the products $A_{(s+1)\mathcal{C}-1} \cdots A_k$ are row-stochastic and $\{\boldsymbol{\mu}_s\}$ is an absolute probability sequence from Lemma 4.2.2.1, each $\boldsymbol{\mu}_s$ is a stochastic vector by definition and so is the vector $\boldsymbol{\phi}_k$ in Eq. (4.4). In fact,

$$\boldsymbol{\phi}_k^\top = \boldsymbol{\mu}_{s+1}^\top A_{(s+1)\mathcal{C}-1} \cdots A_k = \boldsymbol{\mu}_{s+1}^\top A_{(s+1)\mathcal{C}-1} \cdots A_{k+1} A_k = \boldsymbol{\phi}_{k+1}^\top A_k,$$

for $s\mathcal{C} < k < (s+1)\mathcal{C}$ while for $k = s\mathcal{C}$, we have

$$\boldsymbol{\phi}_k^\top = \boldsymbol{\mu}_s^\top = \boldsymbol{\mu}_{s+1}^\top D_s = \boldsymbol{\phi}_{k+1}^\top A_{s\mathcal{C}} = \boldsymbol{\phi}_{k+1}^\top A_k;$$

i.e., the sequence $\{\boldsymbol{\phi}_k\}$ is an absolute probability sequence for $\{A_k\}$.

$\square$

The next lemma establishes multi-step contraction of a backward product of a series of row-stochastic matrices $\{A_k\}$. This result is fundamental to the convergence analysis of TV-$\mathcal{AB}$.

Lemma 4.2.1 ($\overline{\mathcal{C}}_\mathcal{A}$-step contraction for $\{\mathcal{A}_k\}$ [84, Lemma 5.3])**.** *Let Assumptions 4.2.3 and 4.2.4 hold. Recall that $\mathcal{A}_k = A_k \otimes I_p$ and define an integer $\overline{\mathcal{C}}_\mathcal{A} \geq \mathcal{C}$ such that*

$$\gamma_\mathcal{A} \triangleq Q_\mathcal{A}(1-\alpha^{n\mathcal{C}})^{\frac{\overline{\mathcal{C}}_\mathcal{A}-1}{n\mathcal{C}}} < 1, \quad Q_\mathcal{A} = 2n\frac{1+\alpha^{-n\mathcal{C}}}{1-\alpha^{n\mathcal{C}}}. \tag{4.5}$$

Then for any $k \geq \overline{\mathcal{C}}_\mathcal{A} - 1$ and any vector $\mathbf{b} \in \mathbb{R}^{np}$, if

$$\mathbf{a} = \mathcal{A}_{(k,k-(\overline{\mathcal{C}}_\mathcal{A}-1))}\mathbf{b},$$

where $\mathcal{A}_{(k,k-(\overline{\mathcal{C}}_\mathcal{A}-1))} \triangleq \mathcal{A}_k \cdots \mathcal{A}_{k-(\overline{\mathcal{C}}_\mathcal{A}-1)}$, we have

$$\left\| \left((I_n - \mathbf{1}_n\boldsymbol{\phi}_{k+1}^\top) \otimes I_p\right)\mathbf{a} \right\|_2 \leq \gamma_\mathcal{A} \left\| \left((I_n - \mathbf{1}_n\boldsymbol{\phi}_{k-(\overline{\mathcal{C}}_\mathcal{A}-1)}^\top) \otimes I_p\right)\mathbf{b} \right\|_2,$$

where $\{\boldsymbol{\phi}_k\}$ is the absolute probability sequence of $\{A_k\}$, defined in Eq. (4.4).

The next corollary establishes the multi-step contraction for the sequence $\{R_k = V_{k+1}^{-1} B_k V_k\}$, where $V_k = \mathrm{diag}[\mathbf{v}_k]$ and $\{\mathbf{v}_k\}$ evolves as

$$\mathbf{v}_{k+1} = B_k \mathbf{v}_k, \quad \mathbf{v}_0 = \mathbf{1}_n. \tag{4.6}$$

Corollary 4.2.2.2 ($\overline{\mathcal{C}}_{\mathcal{B}}$-step contraction for $\{\mathcal{R}_k\}$). *Let Assumptions 4.2.3 and 4.2.4 hold. Define $\mathcal{R}_k = R_k \otimes I_p$ and $\overline{\mathcal{C}}_{\mathcal{B}} \geq \mathcal{C}$ such that*

$$\gamma_{\mathcal{B}} \triangleq Q_{\mathcal{B}}(1 - \tau^{n\mathcal{C}})^{\frac{\overline{\mathcal{C}}_{\mathcal{B}}-1}{n\mathcal{C}}} < 1, \quad Q_{\mathcal{B}} = 2n\frac{1 + \tau^{-n\mathcal{C}}}{1 - \tau^{n\mathcal{C}}}, \tag{4.7}$$

where $\tau = \frac{\beta}{n^{n\mathcal{C}+1}}$; then for any $k \geq \overline{\mathcal{C}}_{\mathcal{B}} - 1$ and any vector $\mathbf{b} \in \mathbb{R}^{np}$, if

$$\mathbf{a} = \mathcal{R}_{(k,k-(\overline{\mathcal{C}}_{\mathcal{B}}-1))}\mathbf{b},$$

where $\mathcal{R}_{(k,k-(\overline{\mathcal{C}}_{\mathcal{B}}-1))} = \mathcal{R}_k \cdots \mathcal{R}_{k-(\overline{\mathcal{C}}_{\mathcal{B}}-1)}$, we have

$$\big\|\big((I_n - \mathbf{1}_n\mathbf{v}_{k+1}^\top) \otimes I_p\big)\mathbf{a}\big\|_2 \leq \gamma_{\mathcal{B}}\big\|\big((I_{np} - \mathbf{1}_n\mathbf{v}_{k-(\overline{\mathcal{C}}_{\mathcal{B}}-1)}^\top) \otimes I_p\big)\mathbf{b}\big\|_2.$$

Proof. It can be verified that

$$\begin{aligned}&((I_n - \mathbf{1}_n\mathbf{v}_{k+1}^\top) \otimes I_p)\mathcal{R}_{(k,k-(\overline{\mathcal{C}}_{\mathcal{B}}-1))}\\ =&((R_{(k,k-(\overline{\mathcal{C}}_{\mathcal{B}}-1))} - \mathbf{1}_n\mathbf{v}_{k-(\overline{\mathcal{C}}_{\mathcal{B}}-1)}^\top)(I_n - \mathbf{1}_n\mathbf{v}_{k-(\overline{\mathcal{C}}_{\mathcal{B}}-1)}^\top)) \otimes I_p.\end{aligned}$$

Therefore,

$$\begin{aligned}&\big\|\big((I_n - \mathbf{1}_n\mathbf{v}_{k+1}^\top) \otimes I_p\big)\mathbf{a}\big\|_2\\ \leq&\big\|R_{(k,k-(\overline{\mathcal{C}}_{\mathcal{B}}-1))} - \mathbf{1}_n\mathbf{v}_{k-(\overline{\mathcal{C}}_{\mathcal{B}}-1)}^\top\big\|_2\big\|((I_n - \mathbf{1}_n\mathbf{v}_{k-(\overline{\mathcal{C}}_{\mathcal{B}}-1)}^\top) \otimes I_p)\mathbf{b}\big\|_2,\end{aligned}$$

where the inequality follows from the compatibility of vector 2-norm with matrix spectral norm. We now find an upper bound for the first term on the right hand side of the above equation. First note that $[R_k]_{i,j} = [B_k]_{ij}[\mathbf{v}_k]_j/[\mathbf{v}_{k+1}]_i$. From [76, Corollary 2(b)], we have that $[\mathbf{v}_k]_j \geq 1/n^{n\mathcal{C}}, \forall\, k \geq 0$. Since $1/[\mathbf{v}_k]_j \geq 1/n$ and for any $(j,i) \in \mathcal{E}_k$, $[B_k]_{i,j} \geq \beta$ by Assumption 4.2.4, we have $[R_k]_{i,j} \geq \tau \triangleq \beta/n^{n\mathcal{C}+1}$, for any $(j,i) \in \mathcal{E}_k$. Therefore, noting that for an $n \times n$ matrix, X, $\|X\|_2 \leq n\|X\|_{\max}$, we have

$$\left\|R_{(k,k-(\overline{\mathcal{C}}_{\mathcal{B}}-1))} - \mathbf{1}_n\mathbf{v}_{k-(\overline{\mathcal{C}}_{\mathcal{B}}-1)}^\top\right\|_2 \leq n\left\|R_{(k,k-(\overline{\mathcal{C}}_{B}-1))} - \mathbf{1}_n\mathbf{v}_{k-(\overline{\mathcal{C}}_{B}-1)}^\top\right\|_{\max} \leq \gamma_{\mathcal{B}},$$

where $\gamma_{\mathcal{B}} \triangleq 2n\frac{1+\tau^{-n\mathcal{C}}}{1-\tau^{n\mathcal{C}}}(1-\tau^{n\mathcal{C}})^{\frac{\overline{\mathcal{C}}_{\mathcal{B}}-1}{n\mathcal{C}}}$ and the last inequality follows from [69, Lemma 4(c)].

$\square$

4.3 Convergence Analysis

To proceed with the analysis, we perform the state transformation

$$\mathbf{s}_k = (V_k^{-1} \otimes I_p)\mathbf{y}_k$$

on $\mathbf{y}_k$, where $V_k = \mathrm{diag}[\mathbf{v}_k]$ and $\mathbf{v}_k$ follows Eq. (4.6). The TV-$\mathcal{AB}$ algorithm is thus equivalently written as

$$\mathbf{x}_{k+1} = \mathcal{A}_k\mathbf{x}_k - \eta(V_k \otimes I_p)\mathbf{s}_k, \tag{4.8a}$$

$$\mathbf{s}_{k+1} = \mathcal{R}_k \mathbf{s}_k + (V_{k+1}^{-1} \otimes I_p)(\boldsymbol{\nabla}\mathbf{f}(\mathbf{x}_{k+1}) - \boldsymbol{\nabla}\mathbf{f}(\mathbf{x}_k)), \tag{4.8b}$$

It can be verified that $\{R_k\}$ is a sequence of row-stochastic matrices for which the absolute probability sequence[4] is $\{\mathbf{v}_k\}$.

We now proceed with the convergence analysis of the equivalent algorithm in Eqs. (4.6)-(4.8b). Our approach rests on a the following quantities:

(i) $\overline{\mathbf{x}}_k^{\mathrm{w}} = (\boldsymbol{\phi}_k^\top \otimes I_p)\mathbf{x}_k$, which is the average of $\mathbf{x}_k^i$'s weighted by the absolute probability sequence, $\{\boldsymbol{\phi}_k\}$, of $\{A_k\}$, see Corollary 4.2.2.1;

(ii) $\widetilde{\mathbf{x}}_k^{\mathrm{w}} = \mathbf{x}_k - \mathbf{1}_n \otimes \overline{\mathbf{x}}_k^{\mathrm{w}}$, which can be regarded as the weighted consensus error in the network;

(iii) $\mathbf{r}_k = \mathbf{1}_n \otimes (\overline{\mathbf{x}}_k^{\mathrm{w}} - \mathbf{x}^*)$, which is the optimality gap associated with the weighted average;

(iv) $\widetilde{\mathbf{s}}_k^{\mathrm{w}} = \mathbf{s}_k - (\mathbf{1}_n \mathbf{v}_k^\top \otimes I_p)\mathbf{s}_k$, which is an error term corresponding to the update in Eq. (4.8b).

With the help of these quantities, we define the vector

$$\mathbf{t}_k = \begin{bmatrix} \|\widetilde{\mathbf{x}}_k^{\mathrm{w}}\|_2 \\ \|\mathbf{r}_k\|_2 \\ \|\widetilde{\mathbf{s}}_k^{\mathrm{w}}\|_2 \end{bmatrix}, \tag{4.9}$$

[4] See Definition 1.2.3.5.

and show that it goes to zero as $k \to \infty$. Clearly, if $\mathbf{t}_k \to \mathbf{0}$, then $\mathbf{x}_k$ converges to $\mathbf{1}_n \otimes \mathbf{x}^*$, and rate of convergence of TV-$\mathcal{AB}$ is upper bounded by the rate at which $\mathbf{t}_k \to \mathbf{0}$. To establish that $\mathbf{t}_k \to \mathbf{0}$, we derive a linear system of inequalities that expresses the evolution of $\mathbf{t}_k$ in the following form:

$$\begin{bmatrix} \mathbf{t}_{k+1} \\ \vdots \\ \mathbf{t}_{k-(\overline{\mathcal{C}}-2)} \end{bmatrix} \leq M(\eta) \begin{bmatrix} \mathbf{t}_{k} \\ \vdots \\ \mathbf{t}_{k-(\overline{\mathcal{C}}-1)} \end{bmatrix}, \tag{4.10}$$

where the elements of $M(\eta)$ are the coefficients of the linear system. Clearly, if $\rho(M(\eta)) < 1$, then $\mathbf{x}_k$ converges to $\mathbf{1}_n \otimes \mathbf{x}^*$ at least at the rate of $\mathcal{O}(\rho(M(\eta))^k)$.

Fig. 4.1 provides a roadmap to establish Eq. (4.10). The next four lemmas establish the corresponding inequalities. The system of Eq. (4.10) is then analyzed in the next subsection.

Remark 4.3.1. *The constant $\overline{\mathcal{C}} = \max\{\overline{\mathcal{C}}_{\mathcal{A}}, \overline{\mathcal{C}}_{\mathcal{B}}\}$ used in the rest of the chapter, ensures concurrent multi-step contractions for both variables $\widetilde{\mathbf{x}}_k^w$ and $\widetilde{\mathbf{s}}_k^w$; see Lemma 4.2.1 and Corollary 4.2.2.2 for more details.*

Lemma 4.3.1. *The following inequality holds $\forall\, k \geq 0$:*

$$\|\mathbf{y}_k\|_2 \leq nL\|\widetilde{\mathbf{x}}_k^w\|_2 + nL\|\mathbf{r}_k\|_2 + \|\widetilde{\mathbf{s}}_k^w\|_2.$$

Proof. Recall that $\mathbf{s}_k = \widetilde{\mathbf{s}}_k^{\mathrm{w}} + (\mathbf{1}_n \mathbf{v}_k^\top \otimes I_p)\mathbf{s}_k$ and it can be verified that

$$(\mathbf{1}_n \mathbf{v}_k^\top \otimes I_p)\mathbf{s}_k = (\mathbf{1}_n \mathbf{1}_n^\top \otimes I_p)\boldsymbol{\nabla}\mathbf{f}(\mathbf{x}_k). \tag{4.11}$$

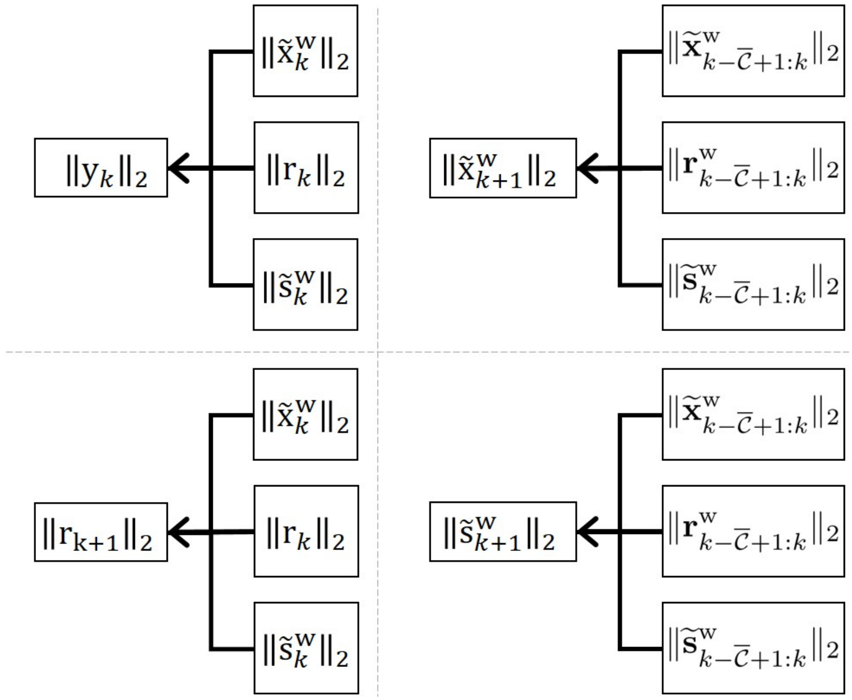

Figure 4.1: Roadmap of deriving the linear system of inequalities.

Exploiting the optimality condition $\sum_{i=1}^n \boldsymbol{\nabla} f_i(\mathbf{x}^*) = \mathbf{0}_p$, we can express $\mathbf{s}_k$ as

$$\mathbf{s}_k = \widetilde{\mathbf{s}}_k^{\mathrm{w}} + (\mathbf{1}_n \mathbf{1}_n^\top \otimes I_p)(\boldsymbol{\nabla}\mathbf{f}(\mathbf{x}_k) - \boldsymbol{\nabla}\mathbf{f}(\mathbf{1}_n \otimes \mathbf{x}^*)).$$

Therefore, from the triangle inequality we have

$$\begin{aligned}
\|\mathbf{s}_k\|_2 &\leq \|\widetilde{\mathbf{s}}_k^{\mathrm{w}}\|_2 + \sqrt{n}\textstyle\sum_{i=1}^n \|\boldsymbol{\nabla}\mathbf{f}_i(\mathbf{x}_k^i) - \boldsymbol{\nabla}\mathbf{f}_i(\mathbf{x}^*)\|_2, \\
&\leq \|\widetilde{\mathbf{s}}_k^{\mathrm{w}}\|_2 + \sqrt{n}L\textstyle\sum_{i=1}^n \|\mathbf{x}_k^i - \mathbf{x}^*\|_2, \\
&\leq \|\widetilde{\mathbf{s}}_k^{\mathrm{w}}\|_2 + nL\big\|\mathbf{x}_k + (\mathbf{1}_n\phi_k^\top \otimes I_p)(\mathbf{x}_k - \mathbf{x}_k) - \mathbf{1}_n \otimes \mathbf{x}^*\big\|_2, \\
&\leq \|\widetilde{\mathbf{s}}_k^{\mathrm{w}}\|_2 + nL\|\widetilde{\mathbf{x}}_k^{\mathrm{w}}\|_2 + nL\|\mathbf{r}_k\|_2.
\end{aligned}$$

where the second inequality uses Lipschitz continuity and the third inequality is a consequence of Cauchy-Schwarz. Noting that $\mathbf{y}_k = (V_k \otimes I_p)\mathbf{s}_k$, we have

$\|\mathbf{y}_k\|_2 \leq \|(V_k \otimes I_p)\|_2 \|\mathbf{s}_k\|_2$ from the compatibility of vector 2-norm with matrix spectral norm. Next, since $\|(V_k \otimes I_p)\|_2 = \|V_k\|_2 = \max_i [\mathbf{v}_k]_i < 1$, we have

$$\|\mathbf{y}_k\|_2 \leq \|\mathbf{s}_k\|_2 \leq nL\|\widetilde{\mathbf{x}}_k^{\mathrm{w}}\|_2 + nL\|\mathbf{r}_k\|_2 + \|\widetilde{\mathbf{s}}_k^{\mathrm{w}}\|_2,$$

and the lemma follows.

□

Lemma 4.3.2. *The following inequality holds $\forall\, k \geq \overline{\mathcal{C}} - 1$:*

$$\begin{aligned}\|\widetilde{\mathbf{x}}_{k+1}^w\|_2 \leq & \big(\gamma_{\mathcal{A}} + \eta Q_{\mathcal{A}} nL\big)\|\widetilde{\mathbf{x}}_{k-(\overline{\mathcal{C}}-1)}^w\|_2 + \eta Q_{\mathcal{A}} nL \sum_{l=0}^{\overline{\mathcal{C}}-2} \|\widetilde{\mathbf{x}}_{k-l}^w\|_2 \\ & + \eta Q_{\mathcal{A}} nL\Big(\|\mathbf{r}_{k-(\overline{\mathcal{C}}-1)}\|_2 + \sum_{l=0}^{\overline{\mathcal{C}}-2} \|\mathbf{r}_{k-l}\|_2\Big) \\ & + \eta Q_{\mathcal{A}}\Big(\|\widetilde{\mathbf{s}}_{k-(\overline{\mathcal{C}}-1)}^w\|_2 + \sum_{l=0}^{\overline{\mathcal{C}}-2} \|\widetilde{\mathbf{s}}_{k-l}^w\|_2\Big),\end{aligned}$$

where $\gamma_{\mathcal{A}}$ and $Q_{\mathcal{A}}$ are the constants defined in Lemma 4.2.1.

Proof. From Eq. (4.3a), we have

$$\mathbf{x}_{k+1} = \mathcal{A}_{(k,k-(\overline{\mathcal{C}}-1))}\mathbf{x}_{k-(\overline{\mathcal{C}}-1)} - \eta\left(\mathbf{y}_k + \sum_{l=1}^{\overline{\mathcal{C}}-1} \mathcal{A}_{k,k-(l-1)}\mathbf{y}_{k-l}\right),$$

which leads to

$$\begin{aligned}\|\widetilde{\mathbf{x}}_{k+1}^{\mathrm{w}}\|_2 = & \Big\|\big((I_n - \mathbf{1}_n\boldsymbol{\phi}_{k+1}^\top) \otimes I_p\big)\mathbf{x}_{k+1}\Big\|_2 \\ \leq & \Big\|\big((I_n - \mathbf{1}_n\boldsymbol{\phi}_{k+1}^\top) \otimes I_p\big)\mathcal{A}_{(k,k-(\overline{\mathcal{C}}-1))}\mathbf{x}_{k-(\overline{\mathcal{C}}-1)}\Big\|_2 \\ & + \eta\Bigg(\Big\|\big((I - \mathbf{1}_n\boldsymbol{\phi}_{k+1}^\top) \otimes I_p\big)\mathbf{y}_k\Big\|_2\end{aligned}$$

$$+\sum_{l=1}^{\overline{\mathcal{C}}-1}\big\|\big((I-\mathbf{1}_n\boldsymbol{\phi}_{k+1}^\top)\otimes I_p\big)\mathcal{A}_{k,k-(l-1)}\mathbf{y}_{k-l}\big\|_2\Bigg).$$

Consequently, $\forall\, k\geq\overline{\mathcal{C}}-1$,

$$\|\widetilde{\mathbf{x}}_{k+1}^{\mathrm{w}}\|_2 \leq\gamma_{\mathcal{A}}\|\widetilde{\mathbf{x}}_{k-(\overline{\mathcal{C}}-1)}^{\mathrm{w}}\|_2+\eta Q_{\mathcal{A}}\textstyle\sum_{l=0}^{\overline{\mathcal{C}}-1}\|\mathbf{y}_{k-l}\|_2,$$

where the second term follows from [69, Lemma 4(c)]. From Lemma 4.3.1,

$$\begin{aligned}\|\widetilde{\mathbf{x}}_{k+1}^{\mathrm{w}}\|_2 \leq&(\gamma_{\mathcal{A}}+\eta Q_{\mathcal{A}}nL)\|\widetilde{\mathbf{x}}_{k-(\overline{\mathcal{C}}-1)}^{\mathrm{w}}\|_2+\eta Q_{\mathcal{A}}nL\textstyle\sum_{l=0}^{\overline{\mathcal{C}}-2}\|\widetilde{\mathbf{x}}_{k-l}^{\mathrm{w}}\|_2,\\ &+\eta Q_{\mathcal{A}}nL\|\mathbf{r}_{k-(\overline{\mathcal{C}}-1)}\|_2+\eta Q_{\mathcal{A}}nL\textstyle\sum_{l=0}^{\overline{\mathcal{C}}-2}\|\mathbf{r}_{k-l}\|_2,\\ &+\eta Q_{\mathcal{A}}\|\widetilde{\mathbf{s}}_{k-(\overline{\mathcal{C}}-1)}^{\mathrm{w}}\|_2+\eta Q_{\mathcal{A}}\textstyle\sum_{l=0}^{\overline{\mathcal{C}}-2}\|\widetilde{\mathbf{s}}_{k-l}^{\mathrm{w}}\|_2,\end{aligned}$$

where $\gamma_{\mathcal{A}}$ and $Q_{\mathcal{A}}$ are the constants defined in Lemma 4.2.1.

□

Lemma 4.3.3. *The following inequality holds $\forall\, k\geq 0$:*

$$\|\mathbf{r}_{k+1}\|_2 \leq\eta nL\|\widetilde{\mathbf{x}}_k^{w}\|_2+\left(1-\eta\frac{\mu}{\eta^{n\mathcal{C}-1}}\right)\|\mathbf{r}_k\|_2+\eta\sqrt{n}\|\widetilde{\mathbf{s}}_k^{w}\|_2.$$

Proof. Note that $\mathbf{y}_k-(\mathbf{v}_k\mathbf{1}_n^\top\otimes I_p)\mathbf{y}_k=(V_k\otimes I_p)\widetilde{\mathbf{s}}_k^{\mathrm{w}}$, we have

$$\begin{aligned}\|\mathbf{r}_{k+1}\|_2 =&\big\|(\mathbf{1}_n\boldsymbol{\phi}_{k+1}^\top\otimes I_p)\mathbf{x}_{k+1}-\mathbf{1}_n\otimes\mathbf{x}^*\big\|_2\\ =&\big\|(\mathbf{1}_n\boldsymbol{\phi}_{k+1}^\top\otimes I_p)\big(\mathcal{A}_k\mathbf{x}_k-\eta\mathbf{y}_k+(\mathbf{v}_k\mathbf{1}_n^\top\otimes I_p)\mathbf{y}_k(-\eta+\eta)\big)-\mathbf{1}_n\otimes\mathbf{x}^*\big\|_2\\ \leq&\eta\big\|(\mathbf{1}_n\boldsymbol{\phi}_{k+1}^\top\otimes I_p)\big(\mathbf{y}_k-(\mathbf{v}_k\mathbf{1}_n^\top\otimes I_p)\mathbf{y}_k\big)\big\|_2\\ &+\big\|(\mathbf{1}_n\boldsymbol{\phi}_k^\top\otimes I_p)\mathbf{x}_k-\mathbf{1}_n\otimes\mathbf{x}^*-\eta\theta_k(\mathbf{1}_n\mathbf{1}_n^\top\otimes I_p)\mathbf{y}_k\big\|_2\end{aligned}$$

$$\leq \eta\sqrt{n}\|\widetilde{\mathbf{s}}_k^{\mathrm{w}}\|_2 + \left\|(\mathbf{1}_n\boldsymbol{\phi}_k^\top \otimes I_p)\mathbf{x}_k - \mathbf{1}_n \otimes \mathbf{x}^* - \eta\theta_k(\mathbf{1}_n\mathbf{1}_n^\top \otimes I_p)\boldsymbol{\nabla}\mathbf{f}(\mathbf{x}_k)\right\|_2, \tag{4.12}$$

where $\theta_k = \boldsymbol{\phi}_{k+1}^\top \mathbf{v}_k$. From [84, Section 5], we note that $\theta_k \geq 1/n^{n\mathcal{C}}$, while from Cauchy-Schwarz, $\theta_k \leq 1$, $\forall k$.

The substitution of $(\mathbf{1}_n\mathbf{1}_n^\top \otimes I_p)\mathbf{y}_k$ by $(\mathbf{1}_n\mathbf{1}_n^\top \otimes I_p)\boldsymbol{\nabla}\mathbf{f}(\mathbf{x}_k)$ follows a similar reasoning as in Eq. (4.11). Furthermore, the second term on the right hand side of the above inequality can be expressed as follows:

$$\begin{aligned}
&\Big\|\mathbf{1}_n \otimes \overline{\mathbf{x}}_k^{\mathrm{w}} - \eta\theta_k(\mathbf{1}_n\mathbf{1}_n^\top \otimes I_p)\boldsymbol{\nabla}\mathbf{f}(\mathbf{1}_n \otimes \overline{\mathbf{x}}_k^{\mathrm{w}}) - \mathbf{1}_n \otimes \mathbf{x}^* \\
&\quad + \eta\theta_k(\mathbf{1}_n\mathbf{1}_n^\top \otimes I_p)(\boldsymbol{\nabla}\mathbf{f}(\mathbf{1}_n \otimes \overline{\mathbf{x}}_k^{\mathrm{w}}) - \boldsymbol{\nabla}\mathbf{f}(\mathbf{x}_k))\Big\|_2 \\
\leq &\Big\|\mathbf{1}_n \otimes (\overline{\mathbf{x}}_k^{\mathrm{w}} - n\eta\theta_k\boldsymbol{\nabla} f(\overline{\mathbf{x}}_k^{\mathrm{w}}) - \mathbf{x}^*)\Big\|_2 \\
&\quad + \eta\theta_k\Big\|\mathbf{1}_n \otimes \big(\textstyle\sum_{i=1}^n(\boldsymbol{\nabla} f_i(\overline{\mathbf{x}}_k^{\mathrm{w}}) - \boldsymbol{\nabla} f_i(\mathbf{x}_k^i))\big)\Big\|_2 \\
\leq &\sqrt{n}\|\overline{\mathbf{x}}_k^{\mathrm{w}} - n\eta\theta_k\boldsymbol{\nabla} f(\overline{\mathbf{x}}_k^{\mathrm{w}}) - \mathbf{x}^*\|_2 + \eta nL\|\mathbf{1}_n \otimes \overline{\mathbf{x}}_k^{\mathrm{w}} - \mathbf{x}_k\|_2,
\end{aligned}$$

where the second term is due to Assumption 4.2.2. From Lemma 1.2.6.1, if $0 < \eta < \frac{2}{nL} < \frac{2}{nL\theta_k}$, we can bound the first term on the right hand side:

$$\sqrt{n}\|\overline{\mathbf{x}}_k^{\mathrm{w}} - n\eta\theta_k\boldsymbol{\nabla} f(\overline{\mathbf{x}}_k^{\mathrm{w}}) - \mathbf{x}^*\|_2 \leq \sqrt{n}\chi_k\|\overline{\mathbf{x}}_k^{\mathrm{w}} - \mathbf{x}^*\|_2 = \chi_k\|\mathbf{r}_k\|_2,$$

where

$$\begin{aligned}
\chi_k =& \max\{|1 - n\eta\theta_k\mu|, |1 - n\eta\theta_k L|\} \\
=& 1 - n\eta\theta_k\mu \leq 1 - \eta\frac{\mu}{n^{n\mathcal{C}-1}}
\end{aligned}$$

for $\eta < \frac{1}{nL} < \frac{1}{nL\theta_k}$. Going back to Eq. (4.12),

$$\begin{aligned}\|\mathbf{r}_{k+1}\|_2 \leq &\eta\sqrt{n}\|\widetilde{\mathbf{s}}^{\mathrm{w}}_k\|_2 + \chi_k\|\mathbf{r}_k\|_2 + \eta nL\|\widetilde{\mathbf{x}}^{\mathrm{w}}_k\|_2 \\ \leq &\eta nL\|\widetilde{\mathbf{x}}^{\mathrm{w}}_k\|_2 + \big(1 - \eta\frac{\mu}{n^{n\mathcal{C}-1}}\big)\|\mathbf{r}_k\|_2 + \eta\sqrt{n}\|\widetilde{\mathbf{s}}^{\mathrm{w}}_k\|_2,\end{aligned}$$

and the lemma follows.

□

Lemma 4.3.4. *The following inequality holds $\forall\, k \geq \overline{\mathcal{C}} - 1$:*

$$\begin{aligned}\|\widetilde{\mathbf{s}}^{w}_{k+1}\|_2 \leq &m\sqrt{n}(2+\eta L)\Big(\|\widetilde{\mathbf{x}}^{w}_{k-(\overline{\mathcal{C}}-1)}\|_2 + \sum_{l=0}^{\overline{\mathcal{C}}-2}\|\widetilde{\mathbf{x}}^{w}_{k-l}\|_2\Big) \\ &+ \eta mnL\Big(\|\mathbf{r}_{k-(\overline{\mathcal{C}}-1)}\|_2 + \sum_{l=0}^{\overline{\mathcal{C}}-2}\|\mathbf{r}_{k-l}\|_2\Big) \\ &+ (\eta m + \gamma_{\mathcal{B}})\|\widetilde{\mathbf{s}}^{w}_{k-(\overline{\mathcal{C}}-1)}\|_2 + \eta m\sum_{l=0}^{\overline{\mathcal{C}}-2}\|\widetilde{\mathbf{s}}^{w}_{k-l}\|_2,\end{aligned}$$

where $m = n^{n\mathcal{C}}Q_{\mathcal{B}}L$, and $\gamma_{\mathcal{B}}$ and $Q_{\mathcal{B}}$ are the constants defined in Corollary 4.2.2.2.

Proof. From Eq. (4.8b), we have

$$\mathbf{s}_{k+1} = \mathcal{R}_{(k,k-(\overline{\mathcal{C}}-1))}\mathbf{s}_{k-(\overline{\mathcal{C}}-1)} + (V_{k+1}^{-1}\otimes I_p)\mathbf{z}_k + \sum_{l=1}^{\overline{\mathcal{C}}-1}\mathcal{R}_{(k,k-(l-1))}(V_{k-(l-1)}^{-1}\otimes I_p)\mathbf{z}_{k-l}.$$

Applying triangle inequality, we get

$$\begin{aligned}\|\widetilde{\mathbf{s}}^{\mathrm{w}}_{k+1}\|_2 = &\|((I_n - \mathbf{1}_n\mathbf{v}_{k+1}^\top)\otimes I_p)\mathbf{s}_{k+1}\|_2 \\ \leq &\|((I_n - \mathbf{1}_n\mathbf{v}_{k+1}^\top)\otimes I_p)\mathcal{R}_{(k,k-(\overline{\mathcal{C}}-1))}\mathbf{s}_{k-(\overline{\mathcal{C}}-1)}\|_2 \\ &+ \|((I_n - \mathbf{1}_n\mathbf{v}_{k+1}^\top)\otimes I_p)(V_{k+1}^{-1}\otimes I_p)\mathbf{z}_k\|_2\end{aligned}$$

$$+\sum_{l=0}^{\overline{\mathcal{C}}-2}\|((I_n-\mathbf{1}_n\mathbf{v}_{k+1}^\top)\otimes I_p)\mathcal{R}_{(k,k-l)}(V_{k-l}^{-1}\otimes I_p)\mathbf{z}_{k-(l+1)}\|_2,$$

Therefore, $\forall\, k\geq\overline{\mathcal{C}}-1$,

$$\|\widetilde{\mathbf{s}}_{k+1}^{\mathrm{w}}\|_2\leq\gamma_{\mathcal{B}}\|((I-\mathbf{1}\mathbf{v}_{k-(\overline{\mathcal{C}}-1)}^\top)\otimes I_p)\mathbf{s}_{k-(\overline{\mathcal{C}}-1)}\|_2+Q_{\mathcal{B}}\textstyle\sum_{l=-1}^{\overline{\mathcal{C}}-2}\|(V_{k-l}^{-1}\otimes I_p)\mathbf{z}_{k-(l+1)}\|_2,$$

where the second term follows fromf [69, Lemma 4(c)]. With the help of [76, Corollary 2(b)] and Corollary 4.2.2.2, we have

$$\|\widetilde{\mathbf{s}}_{k+1}^{\mathrm{w}}\|_2\leq\gamma_{\mathcal{B}}\|\widetilde{\mathbf{s}}_{k-(\overline{\mathcal{C}}-1)}^{\mathrm{w}}\|_2+n^{n\mathcal{C}}Q_{\mathcal{B}}\textstyle\sum_{l=0}^{\overline{\mathcal{C}}-1}\|\mathbf{z}_{k-l}\|_2.$$

From Assumption 4.2.2, the summation in the second term can be bounded as follows:

$$\textstyle\sum_{l=0}^{\overline{\mathcal{C}}-1}\|\mathbf{z}_{k-l}\|_2\leq L\sum_{l=0}^{\overline{\mathcal{C}}-1}\|\mathbf{x}_{k-(l-1)}-\mathbf{x}_{k-l}\|_2.$$

Furthermore,

$$\begin{aligned}\|\mathbf{x}_{k-(l-1)}-\mathbf{x}_{k-l}\|_2=&\Big\|(\mathcal{A}_{k-l}-I_{np})\big(\mathbf{x}_{k-l}-(\mathbf{1}_n\boldsymbol{\phi}_{k-l}^\top\otimes I_p)\mathbf{x}_{k-l}\big)-\eta\mathbf{y}_{k-l}\Big\|_2\\ \leq&\|\mathcal{A}_{k-l}-I_{np}\|_2\|\widetilde{\mathbf{x}}_{k-l}^{\mathrm{w}}\|_2+\eta\|\mathbf{y}_{k-l}\|_2\end{aligned}$$

Summing over l leads to

$$\begin{aligned}&\sum_{l=0}^{\overline{\mathcal{C}}-1}\|\mathbf{x}_{k-(l-1)}-\mathbf{x}_{k-l}\|_2\\ \leq&2\sqrt{n}\|\widetilde{\mathbf{x}}_{k-(\overline{\mathcal{C}}-1)}^{\mathrm{w}}\|_2+\eta\|\mathbf{y}_{k-(\overline{\mathcal{C}}-1)}\|_2+\sum_{l=0}^{\overline{\mathcal{C}}-2}\Big(2\sqrt{n}\|\widetilde{\mathbf{x}}_{k-l}^{\mathrm{w}}\|_2+\eta\|\mathbf{y}_{k-l}\|_2\Big).\end{aligned}$$

From Lemma 4.3.1, we have $\forall\, k \geq \overline{\mathcal{C}} - 1$:

$$\begin{aligned}\|\widetilde{\mathbf{s}}^{\mathrm{w}}_{k+1}\|_2 \leq & m(2\sqrt{n} + \eta L n)\left(\|\widetilde{\mathbf{x}}^{\mathrm{w}}_{k-(\overline{\mathcal{C}}-1)}\|_2 + \textstyle\sum_{l=0}^{\overline{\mathcal{C}}-2} \|\widetilde{\mathbf{x}}^{\mathrm{w}}_{k-l}\|_2\right) \\ & + \eta n m L \left(\|\mathbf{r}_{k-(\overline{\mathcal{C}}-1)}\|_2 + \textstyle\sum_{l=0}^{\overline{\mathcal{C}}-2} \|\mathbf{r}_{k-l}\|_2\right) \\ & + (\eta m + \gamma_{\mathcal{B}})\|\widetilde{\mathbf{s}}^{\mathrm{w}}_{k-(\overline{\mathcal{C}}-1)}\|_2 + \eta m \textstyle\sum_{l=0}^{\overline{\mathcal{C}}-2} \|\widetilde{\mathbf{s}}^{\mathrm{w}}_{k-l}\|_2,\end{aligned}$$

and the lemma follows.

$\square$

4.3.1 The Resulting Linear System of Inequalities

Summarizing the results of Lemmas 4.3.2-4.3.4, for $0 < \eta < \frac{1}{nL}$, Eq. (4.10) can be expanded as follows:

$$\begin{aligned}\mathbf{t}_{k+1} \leq & \underbrace{\begin{bmatrix} \eta Q_{\mathcal{A}} n L & \eta Q_{\mathcal{A}} n L & \eta Q_{\mathcal{A}} \\ \eta n L & 1 - \eta \frac{\mu}{n^{n\mathcal{C}-1}} & \eta\sqrt{n} \\ m\sqrt{n}(2+\eta L) & \eta m n L & \eta m \end{bmatrix}}_{M_1} \mathbf{t}_k \\ & + \underbrace{\begin{bmatrix} \eta Q_{\mathcal{A}} n L & \eta Q_{\mathcal{A}} n L & \eta Q_{\mathcal{A}} \\ 0 & 0 & 0 \\ m\sqrt{n}(2+\eta L) & \eta m n L & \eta m \end{bmatrix}}_{M_2} (\mathbf{t}_{k-1} + \ldots + \mathbf{t}_{k-(\overline{\mathcal{C}}-2)})\end{aligned}$$

$$+\underbrace{\begin{bmatrix} \gamma_{\mathcal{A}}+\eta Q_{\mathcal{A}}nL & \eta Q_{\mathcal{A}}nL & \eta Q_{\mathcal{A}} \\ 0 & 0 & 0 \\ m\sqrt{n}(2+\eta L) & \eta mnL & \gamma_{\mathcal{B}}+\eta m \end{bmatrix}}_{M_{\overline{C}}}\mathbf{t}_{k-(\overline{\mathcal{C}}-1)},$$

which is equivalent to

$$\begin{bmatrix} \mathbf{t}_{k+1} \\ \mathbf{t}_{k} \\ \mathbf{t}_{k-1} \\ \vdots \\ \mathbf{t}_{k-(\overline{\mathcal{C}}-2)} \end{bmatrix} \leq \begin{bmatrix} M_1 & M_2 & \cdots & M_2 & M_{\overline{\mathcal{C}}} \\ I & & & & \\ & I & & & \\ & & \ddots & & \\ & & & I & \end{bmatrix} \begin{bmatrix} \mathbf{t}_{k} \\ \mathbf{t}_{k-1} \\ \vdots \\ \mathbf{t}_{k-(\overline{\mathcal{C}}-2)} \\ \mathbf{t}_{k-(\overline{\mathcal{C}}-1)} \end{bmatrix}. \tag{4.13}$$

The system matrix, $M(\eta)$, in the above can be partitioned as

$$\underbrace{\begin{bmatrix} M_1^0 & \cdots & M_2^0 & M_{\overline{\mathcal{C}}}^0 \\ I & & & \\ & \ddots & & \\ & & I & \end{bmatrix}}_{M^0} + \eta \underbrace{\begin{bmatrix} M_1^E & \cdots & M_2^E & M_{\overline{\mathcal{C}}}^E \\ \mathbf{0} & & & \\ & \ddots & & \\ & & \mathbf{0} & \end{bmatrix}}_{M^E}, \tag{4.14}$$

where

$$M_1^0 = \begin{bmatrix} 0 & 0 & 0 \\ 0 & 1 & 0 \\ 2m\sqrt{n} & 0 & 0 \end{bmatrix}, \quad M_1^E = \begin{bmatrix} Q_{\mathcal{A}}nL & Q_{\mathcal{A}}nL & Q_{\mathcal{A}} \\ nL & -\frac{\mu}{n^{n\mathcal{C}-1}} & \sqrt{n} \\ m\sqrt{n}L & mnL & m \end{bmatrix},$$

$$M_2^0 = \begin{bmatrix} 0 & 0 & 0 \\ 0 & 0 & 0 \\ 2m\sqrt{n} & 0 & 0 \end{bmatrix}, \; M_2^E = \begin{bmatrix} Q_{\mathcal{A}}nL & Q_{\mathcal{A}}nL & Q_{\mathcal{A}} \\ 0 & 0 & 0 \\ m\sqrt{n}L & mnL & m \end{bmatrix},$$

$$M_{\overline{C}}^0 = \begin{bmatrix} \gamma_{\mathcal{A}} & 0 & 0 \\ 0 & 0 & 0 \\ 2m\sqrt{n} & 0 & \gamma_{\mathcal{B}} \end{bmatrix}, \; M_{\overline{C}}^E = \begin{bmatrix} Q_{\mathcal{A}}nL & Q_{\mathcal{A}}nL & Q_{\mathcal{A}} \\ 0 & 0 & 0 \\ m\sqrt{n}L & mnL & m \end{bmatrix}.$$

Recall that our goal is to establish the geometric decay of $\mathbf{t}_k$ in Eq. (4.9). To this purpose, it is sufficient to show $\rho(M(\eta)) < 1$. As a first step, we finish this section with a lemma on the spectral radius of the matrix M^0 in Eq. (4.14) and its corresponding eigenvector.

Lemma 4.3.1.1. *The spectral radius of the matrix M^0 is 1 and $\lambda = 1$ is a simple eigenvalue of M^0. In addition, the right and left eigenvectors, $M_0\mathbf{u} = \mathbf{u}$, $\mathbf{w}^\top M_0 = \mathbf{w}^\top$, are given by*

$$\mathbf{u} = \mathbf{1}_{\overline{\mathcal{C}}} \otimes \begin{bmatrix} 0 & 1 & 0 \end{bmatrix}^\top, \qquad \mathbf{w} = \begin{bmatrix} 0 & 1 & 0 & \cdots & 0 \end{bmatrix}^\top.$$

Proof. Based on the successive application of Schur's determinant identity [3, 111], the characteristic polynomial of M^0 is given by

$$(-1)^{\overline{\mathcal{C}}}(\lambda - 1)(\gamma_{\mathcal{A}} - \lambda^{\overline{\mathcal{C}}})(\gamma_{\mathcal{B}} - \lambda^{\overline{\mathcal{C}}})\lambda^{(\overline{\mathcal{C}}-1)}.$$

Given that $\gamma_{\mathcal{A}}, \gamma_{\mathcal{B}} \in (0,\, 1)$, the spectral radius of M^0 is 1 and the corresponding eigenvalue, $\lambda = 1$, is simple. We now proceed to find the corresponding right and left eigenvectors, $\mathbf{u}$ and $\mathbf{w}$, respectively.

By decomposing $\mathbf{u}$ and $\mathbf{w}$ as follows,

$$\mathbf{u} = \begin{bmatrix} \mathbf{u}^1 \\ \vdots \\ \mathbf{u}^{\overline{\mathcal{C}}} \end{bmatrix}, \qquad \mathbf{w} = \begin{bmatrix} \mathbf{w}^1 \\ \vdots \\ \mathbf{w}^{\overline{\mathcal{C}}} \end{bmatrix},$$

where each $\mathbf{u}^i, \mathbf{w}^i$ is in $\mathbb{R}^3$, from $M^0\mathbf{u} = \mathbf{u}$, we get

$$\gamma_A[\mathbf{u}^{\overline{\mathcal{C}}}]_1 = [\mathbf{u}^1]_1, \qquad\qquad \mathbf{u}^i = \mathbf{u}^{i+1}, \quad 1 \leq i \leq \overline{\mathcal{C}} - 1,$$

resulting in $[\mathbf{u}^i]_1 = 0$, $\forall\, i$. Furthermore,

$$\gamma_B[\mathbf{u}^{\overline{\mathcal{C}}}]_3 + 2m\sqrt{n}\sum_{i=1}^{\overline{\mathcal{C}}}[\mathbf{u}^i]_1 = [\mathbf{u}^1]_3.$$

Therefore, $\gamma_B[\mathbf{u}^{\overline{\mathcal{C}}}]_3 = [\mathbf{u}^1]_3$ which implies $[\mathbf{u}^i]_3 = 0$, $\forall\, i$. The entries $[\mathbf{u}^i]_2$ are free variables and we set them equal to 1, $\forall\, i$. Consequently, $\mathbf{u}^i = \underline{\mathbf{u}} = \begin{bmatrix} 0 & 1 & 0 \end{bmatrix}^\top$ and $\mathbf{u} = \mathbf{1}_{\overline{\mathcal{C}}} \otimes \underline{\mathbf{u}}$.

Similarly, from $\mathbf{w}^\top M^0 = \mathbf{w}^\top$, we have

$$\begin{aligned} 2m\sqrt{n}[\mathbf{w}^1]_3 + [\mathbf{w}^{i+1}]_1 &= [\mathbf{w}^i]_1, \qquad\qquad i = 1, \ldots, \overline{\mathcal{C}} - 1, \\ 2m\sqrt{n}[\mathbf{w}^1]_3 + \gamma_A[\mathbf{w}^1]_1 &= [\mathbf{w}^{\overline{\mathcal{C}}}]_1. \end{aligned}$$

Summing over all i, we obtain

$$2\overline{\mathcal{C}}m\sqrt{n}[\mathbf{w}^1]_3 + \gamma_A[\mathbf{w}^1]_1 = [\mathbf{w}^1]_1. \tag{4.15}$$

Furthermore,

$$[\mathbf{w}^1]_2 + [\mathbf{w}^2]_2 = [\mathbf{w}^1]_2,$$

$$[\mathbf{w}^3]_2 = [\mathbf{w}^2]_2,$$

$$\vdots$$

$$[\mathbf{w}^{\overline{\mathcal{C}}}]_2 = [\mathbf{w}^{\overline{\mathcal{C}}-1}]_2,$$

$$[\mathbf{w}^{\overline{\mathcal{C}}}]_2 = 0,$$

resulting in $[\mathbf{w}^i]_2 = 0, \forall\, 2 \leq i \leq \overline{\mathcal{C}}$. Note that $[\mathbf{w}^1]_2$ is a free variable and we can set it equal to 1. Additionally,

$$[\mathbf{w}^2]_3 = [\mathbf{w}^1]_3,$$

$$[\mathbf{w}^3]_3 = [\mathbf{w}^2]_3,$$

$$\vdots$$

$$[\mathbf{w}^{\overline{\mathcal{C}}}]_3 = [\mathbf{w}^{\overline{\mathcal{C}}-1}]_3,$$

$$\gamma_B[\mathbf{w}^1]_3 = [\mathbf{w}^{\overline{\mathcal{C}}}]_3,$$

resulting in $[\mathbf{w}^i]_3 = 0$, which from Eq. (4.15) implies $[\mathbf{w}^i]_1 = 0$, for all i. Consequently,

$$\mathbf{w}^\top = \begin{bmatrix} 0 & [\mathbf{w}^1]_2 = 1 & 0 & 0 & \cdots & 0 \end{bmatrix}.$$

□

4.4 Linear Convergence

We now state the main convergence result for TV-$\mathcal{AB}$.

Theorem 4.4.1. *The spectral radius of $M(\eta)$ is strictly less than 1 provided η is sufficiently small. Therefore $\|\mathbf{x}_k - \mathbf{1}_n \otimes \mathbf{x}^*\|_2$ converges to zero (at least) at the rate of $O\big(\rho(M(\eta))^k\big)$.*

Proof. From Lemma 4.3.1.1, let $q(\eta)$ be the simple eigenvalue of $M(\eta)$, as a function of η, for which $q(0) = 1$. Recall that $M(\eta)$ can be partitioned as $M^0 + \eta M^E$ from Eq. (4.14). Borrowing a result from matrix perturbation theory [3, Theorem 6.3.12], we have

$$\left.\frac{\mathrm{d}q(\eta)}{\mathrm{d}\eta}\right|_{\eta=0} = \frac{\mathbf{w}^\top M^E \mathbf{u}}{\mathbf{w}^\top \mathbf{u}},$$

where $\mathbf{u}$ and $\mathbf{w}$ are right and left eigenvectors corresponding to the simple eigenvalue, $q(0)$. From Lemma 4.3.1.1, it can be verified that $\mathbf{w}^\top \mathbf{u} = 1$ and $\mathbf{w}^\top M^E \mathbf{u} = -\mu / n^{n\mathcal{C}-1} < 0$, which implies that $\frac{\mathrm{d}}{\mathrm{d}\eta} q(\eta)$ is negative at $\eta = 0$. Since the eigenvalues are a continuous function of the elements of a matrix, we have that $q(\eta)$ decreases for a sufficiently small η (slightly increasing from zero) and the theorem follows. □

4.5 Numerical Experiments

This section illustrates the application and performance of the TV-$\mathcal{AB}$ algorithm in a variety of numerical experiments. In the rest of this section, we adopt a simple uniform weighting strategy to construct the row and column-stochastic weights $[A_k]_{i,j}$ and $[B_k]_{i,j}$:

$$[A_k]_{i,j} = \begin{cases} 1/d^i_{k,\text{in}}, & (j,i) \in \mathcal{E}_k, \\ 0, & (j,i) \notin \mathcal{E}_k, \end{cases} \tag{4.16}$$

where $d^i_{k,\text{in}}$ is the in-degree of agent i at time k; and

$$[B_k]_{i,j} = \begin{cases} 1/d^j_{k,\text{out}}, & (j,i) \in \mathcal{E}_k, \\ 0, & (j,i) \notin \mathcal{E}_k, \end{cases} \tag{4.17}$$

where $d^j_{k,\text{out}}$ is the out-degree of agent j at time k.

4.5.1 Distributed Training for Binary Classification

In this experiment, we consider $n = 20$ agents communicating over a 15-bounded strongly-connected network. In this scenario, the agents communicate over a strongly-connected random graph every 15^{th} iteration and rely solely on local iterations for the rest of the time. The agents aim to collaboratively learn the parameters $(\mathbf{w}^*, b^*)$ for a regularized logistic regression model[5] to classify digits $\{3, 8\}$ from a downsampled subset of the MNIST database [113], given in [114]. Examples of the handwritten digits in the training observations are shown in Fig. 4.2 for both classes. For each digit we use a total of 700 samples from the database, where 540 samples are used for

[5]See, e.g., [112, Chapter 4].

training and the remaining 160 for testing. The training set is further partitioned equally and randomly among agents such that an agent i has access to $m = N/n$ training examples: $(\mathbf{c}^{i(j)}, y^{i(j)})$, for $j = 1, 2, \cdots, m$, where $\mathbf{c}^{i(j)}$ is the 16×16-dimensional feature vector of the j^{th} training sample at the i^{th} agent and $y^{i(j)} \in \{-1, 1\}$ is the corresponding binary label for digits 3 and 8, respectively. The agents solve the following distributed optimization problem:

$$\min_{\mathbf{w},b} F(\mathbf{w}, b) = \sum_{i=1}^{n} f_i(\mathbf{w}, b),$$

where the private loss function f_i at agent i is the empirical negative log-likelihood plus a regularization term:

$$f_i(\mathbf{w}, b) = \sum_{j=1}^{m} \ln\left[1 + e^{-y^{i(j)}\left(\mathbf{w}^\top \mathbf{c}^{i(j)} + b\right)}\right] + \frac{\lambda}{2}\left(\|\mathbf{w}\|_2^2 + b^2\right).$$

Figure 4.2: Samples of 16×16 grayscale images of handwritten 3's and 8's, enlarged for clarity.

The regularization parameter λ penalizes large model parameters and guarantees the strong-convexity of the loss functions f_i. The decision variable $\mathbf{w}$ represents the coefficient(s) of the logistic regression algorithm and b is the bias term. It is straightforward to verify that the local loss functions f_i satisfy both

Assumptions 4.2.1 and 4.2.2. Fig. 4.3 compares the performance of TV-$\mathcal{AB}$ with Push-DIGing [84] with the average residual $1/n \sum_{i=1}^{n} \|\mathbf{x}_k^i - \mathbf{x}^*\|_2$ as the evaluation metric. In this experiment, $\mathbf{x}^*$ is the solution obtained from centralized gradient descent (CGD) and the stepsizes have been hand-optimized to give faster convergence and more accurate solution for all algorithms. This numerical experiment confirms that TV-$\mathcal{AB}$ converges linearly. Furthermore, it is observed to be faster than Push-DIGing given no eigenvalue estimation iteration involved.

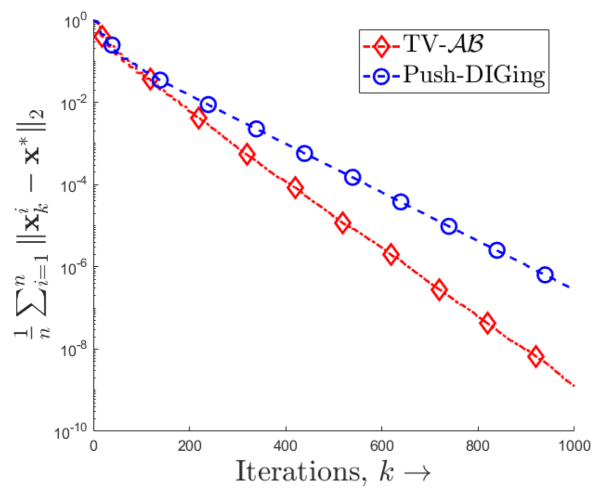

Figure 4.3: Performance comparison based on the average residual.

In Figs. 4.4, we look at the accuracy attained on the 160 samples we set aside for testing. Fig. 4.4a compares the algorithms based on average accuracy, while Fig. 4.4b focuses on TV-$\mathcal{AB}$ where the shaded region shows the maximum and minimum accuracy at different nodes in the same experiment.

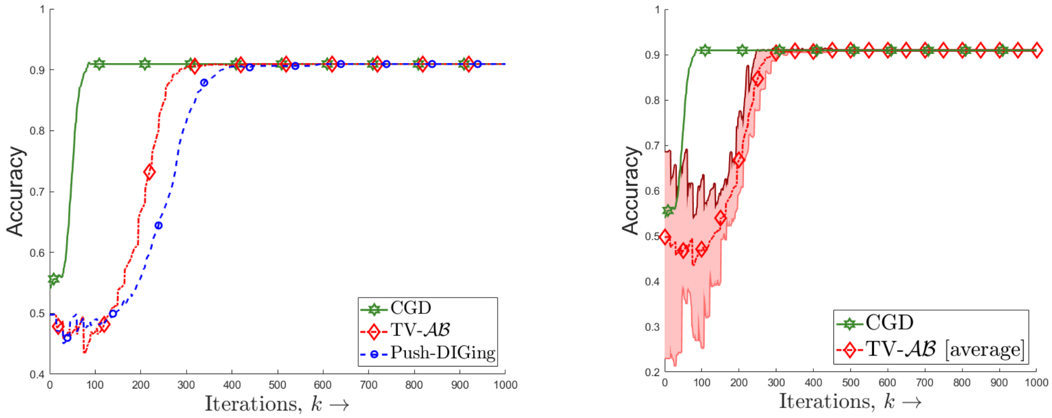

(a) Comparing with the state-of-the-art. (b) Closer look at TV-$\mathcal{AB}$.

Figure 4.4: Performance comparison based on accuracy on the test set.

4.5.2 Distributed Least Squares on Random Directed Graphs

In this example, we consider a network of $n = 12$ agents. In perfect communication conditions, the agents' communication topology is based on the strongly-connected digraph $\mathcal{G}^*$ shown in Fig. 4.5. However, we assume the network is subject to random link failures such that at every iteration, the agents communicate according to the digraph generated through randomly uniformly sampling the edges from $\mathcal{G}^*$ with 90 percent. The agents aim to collaboratively find the solution $\mathbf{x}^*$ of the following least-squares problem:

$$f(\mathbf{x}) = \sum_{i=1}^{n} f_i(\mathbf{x}) = \frac{1}{2} \sum_{i=1}^{n} \|H_i\mathbf{x} - \mathbf{b}_i\|_2^2,$$

where the vectors and matrices are of appropriate dimensions. We choose each H_i such that it is rank-deficient but $\sum_i H_i^\top H_i$ is invertible. In other words, no agent can find $\mathbf{x}^*$ on its own and must cooperate.

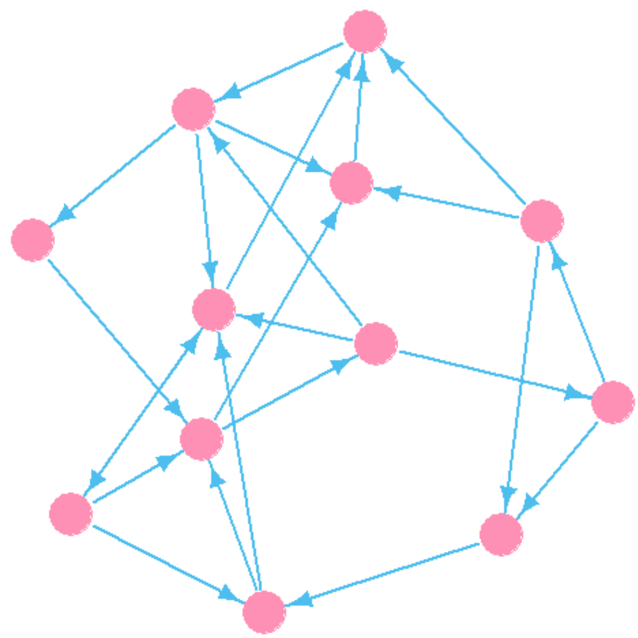

Figure 4.5: $\mathcal{G}^*$: The underlying strongly-connected directed graph for the experiment.

The performance of TV-$\mathcal{AB}$ along with Push-DIGing [84], and subgradient-push [76] (with constant and diminishing stepsizes) is shown in Fig. 4.6 with the average residual $1/n \sum_{i=1}^{n} \|\mathbf{x}_k^i - \mathbf{x}^*\|_2$ as the comparison metric. The stepsizes follow a similar regime as in Experiment 4.5.1. This numerical experiment, once again, confirms the linear convergence of TV-$\mathcal{AB}$ to the optimal solution provided the stepsize is sufficiently small.

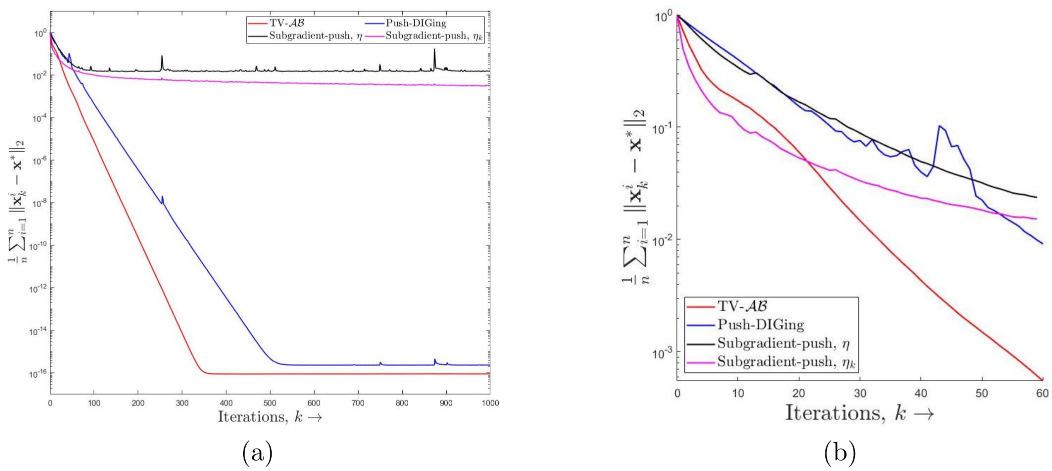

Figure 4.6: Distributed least squares: Performance comparison with the transients magnified.

4.6 Conclusions

In this chapter, we introduce the algorithm TV-$\mathcal{AB}$ to minimize a sum of smooth and strongly-convex functions over time-varying and possibly random digraphs. We show that TV-$\mathcal{AB}$ converges linearly to the optimal solution when underlying time-varying graphs satisfy the standard bounded connectivity assumption, i.e., a union of every $\mathcal{C}$ consecutive graphs is strongly-connected. We derive the convergence result based on the stability analysis of a linear system of inequalities along with a matrix perturbation argument. We further provide simulations that confirm the findings in this chapter.

Chapter 5

Epilogue

In this thesis, we focus on problems in the modeling, analysis, and design of complex, distributed, and networked dynamical systems. In particular, we investigate three distinct problems in networked systems and control theory as summarized in the following. We also discuss some possible directions for future work.

- **Distributed Estimation** – We consider a network of agents tasked to estimate the state of a Continuous-Time, Linear Time-Invariant system under the assumption that no agent possesses enough measurements in its neighborhood to estimate the entire system state on its own. Designing static estimator gains, we provide a networked Kalman-type estimator that combines prediction and innovation with information fusion among the agents. The main contribution of this work is the analysis of the estimation error using the notions of dissipativity and the input-output approach, enabling us to formulate stability and performance arguments as quasiconvex optimization problems involving linear matrix inequalities. We show that the resulting estimation error is stable and further ensures a given level of performance regarding noise rejection. Our approach serves as the foundation of future investigation towards extending the current work to the case of dynamical systems driven by external forces $\mathbf{v}(t) \in \mathbb{R}^p$ and to dynamic estimator design meeting certain frequency-dependent performance objectives in addition to stability and noise rejection.

- **Control of Spreading Processes** – We study a variant of the viral marketing phenomenon over heterogeneous social networks. The marketing objective investigated in this framework is product adoption. Borrowing concepts from the theory of epidemic processes, we introduce a simple yet insightful product adoption model, i.e., the potential-adopting-dormant-potential model and propose an optimal control scheme to simultaneously optimize the population of the adopting and dormant compartments under given time and resource constraints. We prove the existence of the solution to the optimal control problem and provide both analytical and numerical solutions using the Pontryagin Maximum Principle and Forward-Backward Sweep Method, respectively. Future directions include extending the current work to networks with time-varying links as well as a discrete-time model of the adoption process which seems to be more realistic.

- **Distributed Optimization** – We aim to solve the distributed optimization problem over multi-agent networks, where each agent has a local objective function derived from private information. The goal is to have agents collaborate with each other to optimize the sum of these local objective functions. Existing algorithms mostly deal with the corresponding problems under the assumption that the underlying network topology is strongly-connected, static, and undirected. The contribution of this work lies in the relaxation of such assumptions on the network topology. In particular, we assume that agents communicate according to a dynamic directed graph and present a computationally efficient fast distributed optimization algorithm. Contrary to the existing work, our proposed algorithm, rather than estimating the Perron eigenvector of the weight matrices, relies on a novel information mixing approach exploiting both row and column-stochastic weights to achieve agreement towards the optimal solution. We show that our algorithm converges linearly to the optimal solution when the global objective is smooth and strongly-convex, and the underlying time-varying graph exhibit bounded connectivity. Obtaining convergence rates for non-strongly-convex functions and extending current convergence results to random graphs are potential future directions to be explored.

Bibliography

[1] R. E. Kalman. “A New Approach to Linear Filtering and Prediction Problems”. In: *Transactions of the ASME–Journal of Basic Engineering* 82.D (1960), pp. 35–45.

[2] R. A. Horn and C. R. Johnson. *Topics in Matrix Analysis*. Cambridge University Press, 1994.

[3] R. A. Horn and C. R. Johnson. *Matrix Analysis*. Cambridge University Press, 2013.

[4] B. Brogliato et al. *Dissipative Systems Analysis and Control: Theory and Applications*. Communications and Control Engineering. Springer, 2006.

[5] K. Zhou and J. C. Doyle. *Essentials of Robust Control*. Prentice Hall, 1997.

[6] A. Kolmogoroff. “Zur Theorie der Markoffschen Ketten”. In: *Mathematische Annalen* 112 (1936), pp. 155–160.

[7] E. Seneta. *Non-negative Matrices and Markov Chains*. Springer Science & Business Media, 2006.

[8] A. Korniienko et al. "Performance control for interconnection of identical systems: Application to PLL network design". In: *International Journal of Robust and Nonlinear Control* 26.1 (2016), pp. 3–27.

[9] S. Boyd et al. *Linear Matrix Inequalities in System and Control Theory*. SIAM, 1994.

[10] D. P. Bertsekas, A. Nedić, and A. E. Ozdaglar. *Convex Analysis and Optimization*. Athena Scientific, 2003.

[11] D. P. Bertsekas. *Nonlinear Programming*. Athena Scientific, 1999.

[12] F. Saadatniaki et al. "On the input-output approach towards distributed estimation". In: *IEEE European Control Conference*. 2018, pp. 2152–2157.

[13] F. Saadatniaki and U. A. Khan. "Product adoption in heterogeneous networks: An epidemiological perspective". In: *52nd Asilomar Conference on Signals, Systems, and Computers*. 2018, pp. 1043–1047.

[14] F. Saadatniaki, R. Xin, and U. A. Khan. "Distributed Training with Mobile Agents: Optimization over Dynamic Directed Graphs". In: *IEEE Data Science Workshop*. in press.

[15] F. Saadatniaki, R. Xin, and U. A. Khan. “Optimization over time-varying directed graphs with row and column-stochastic matrices”. In: *arXiv preprint arXiv:1810.07393* (2018).

[16] S. Boyd and L. Vandenberghe. *Convex Optimization*. Cambridge University Press, 2004.

[17] H. R. Hashemipour, S. Roy, and A. J. Laub. “Decentralized Structures for Parallel Kalman Filtering”. In: *IEEE Transactions on Automatic Control* 33.1 (1988), pp. 88–94.

[18] A. G. O. Mutambara. *Decentralized Estimation and Control for Multisensor Systems*. CRC Press, 1998.

[19] U. A. Khan and A. Jadbabaie. “On the stability and optimality of distributed Kalman filters with finite-time data fusion”. In: *IEEE American Control Conference*. 2011, pp. 3405–3410.

[20] M. Doostmohammadian and U. A. Khan. “Graph-Theoretic Distributed Inference in Social Networks”. In: *IEEE Journal of Special Topics in Signal Processing–Issue on Signal Processing for Social Networks* 8.4 (2014), pp. 613–623.

[21] S. Park and N. C. Martins. “Design of Distributed LTI Observers for State Omniscience”. In: *IEEE Transactions on Automatic Control* 62.2 (2017), pp. 561–576.

[22] S. Oh et al. “Tracking and Coordination of Multiple Agents Using Sensor Networks: System Design, Algorithms and Experiments”. In: *Proceedings of the IEEE* 95.1 (2007), pp. 234–254.

[23] U. A. Khan, M. D. Ilić, and J. M. F. Moura. “Cooperation for aggregating complex electric power networks to ensure system observability”. In: *1st International Conference on Infrastructure Systems and Services: Building Networks for a Brighter Future*. 2008, pp. 1–6.

[24] M. A. Rahimian and A. Jadbabaie. “Group Decision Making and Social Learning”. In: *55th IEEE Conference on Decision and Control*. 2016, pp. 6783–6794.

[25] D. W. Casbeer and R. Beard. “Distributed Information Filtering using Consensus Filters”. In: *IEEE American Control Conference*. 2009, pp. 1882–1887.

[26] U. A. Khan and A. Jadbabaie. “Collaborative scalar-gain estimators for potentially unstable social dynamics with limited communication”. In: *Automatica* 50.7 (2014), pp. 1909 –1914.

[27] G. Battistelli and L. Chisci. “Kullback-Leibler average, consensus on probability densities, and distributed state estimation with guaranteed stability”. In: *Automatica* 50.3 (2014), pp. 707 –718.

[28] S. S. Stanković, M. S. Stanković, and D. M. Stipanović. “Decentralized Parameter Estimation by Consensus Based Stochastic Approximation”. In: *IEEE Transactions on Automatic Control* 56.3 (2011), pp. 531–543.

[29] R. Olfati-Saber and P. Jalalkamali. “Coupled Distributed Estimation and Control for Mobile Sensor Networks”. In: *IEEE Transactions on Automatic Control* 57.10 (2012), pp. 2609–2614.

[30] V. H. Nascimento and A. H. Sayed. “Continuous-Time Distributed Estimation”. In: *45th Asilomar Conference on Signals, Systems and Computers*. 2011, pp. 1761–1765.

[31] Z. Zhou, H. Fang, and Y. Hong. “Distributed Estimation for Moving Target Based on State-Consensus Strategy”. In: *IEEE Transactions on Automatic Control* 58.8 (2013), pp. 2096–2101.

[32] P. J. Moylan and D. J. Hill. “Stability criteria for large-scale systems”. In: *IEEE Transactions on Automatic Control* 23.2 (1978), pp. 143–149.

[33] G. Scorletti and G. Duc. “An LMI approach to decentralized H_∞ control”. In: *International Journal of Control* 74.3 (2001), pp. 211–224.

[34] A. Korniienko et al. *Control Law Design for Distributed Multi-Agent Systems*. Tech. rep. Laboratoire Ampère, Ecole Centrale de Lyon, 2011.

[35] U. A. Khan et al. “On connectivity, observability, and stability in distributed estimation”. In: *49th IEEE Conference on Decision and Control*. 2010, pp. 6639–6644.

[36] S. Skogestad and I. Postlethwaite. *Multivariable Feedback Control: Analysis and Design*. Wiley, 2005.

[37] H. K. Khalil. *Nonlinear Systems*. Prentice Hall, 2002.

[38] A. Barabási and R. Albert. “Emergence of Scaling in Random Networks”. In: *Science* 286.5439 (1999), pp. 509–512.

[39] J. Tang, X. Tang, and J. Yuan. “Profit Maximization for Viral Marketing in Online Social Networks: Algorithms and Analysis”. In: *IEEE Transactions on Knowledge and Data Engineering* 30.6 (2018), pp. 1095–1108.

[40] J. Kleinberg and D. Easley. *Networks, Crowds, and Markets: Reasoning about a Highly Connected World*. Cambridge University Press, 2010.

[41] P. Domingos and M. Richardson. “Mining the Network Value of Customers”. In: *7th ACM SIGKDD International Conference on Knowledge Discovery and Data Mining*. 2001, pp. 57–66.

[42] A. Fazeli, A. Ajorlou, and A. Jadbabaie. “Competitive Diffusion in Social Networks: Quality or Seeding?” In: *IEEE Transactions on Control of Network Systems* 4.3 (2017), pp. 665–675.

[43] K. Kandhway and J. Kuri. “Campaigning in Heterogeneous Social Networks: Optimal Control of SI Information Epidemics”. In: *IEEE/ACM Transactions on Networking* 24.1 (2016), pp. 383–396.

[44] G. C. Chasparis and J. S. Shamma. “Control of Preferences in Social Networks”. In: *49th IEEE Conference on Decision and Control*. 2010, pp. 6651–6656.

[45] C. Ballester, A. Calvó-Armengol, and Y. Zenou. “Who’s who in networks. Wanted: The key player”. In: *Econometrica* 74.5 (2006), pp. 1403–1417.

[46] D. Godes and D. Mayzlin. “Using Online Conversations to Study Word-of-Mouth Communication”. In: *Marketing Science* 23.4 (2004), pp. 545–560.

[47] N. A. Ruhi and B. Hassibi. “SIRS Epidemics on Complex Networks: Concurrence of Exact Markov Chain and Approximated Models”. In: *54th IEEE Conference on Decision and Control*. 2015, pp. 2919–2926.

[48] C. Nowzari, V. M. Preciado, and G. J. Pappas. “Analysis and Control of Epidemics: A Survey of Spreading Processes on Complex Networks”. In: *IEEE Control Systems* 36.1 (2016), pp. 26–46.

[49] H. J. Ahn and B. Hassibi. “Global Dynamics of Epidemic Spread over Complex Networks”. In: *52nd IEEE Conference on Decision and Control*. 2013, pp. 4579–4585.

[50] A. Khanafer, T. Başar, and B. Gharesifard. “Stability Properties of Infection Diffusion Dynamics over Directed Networks”. In: *53rd IEEE Conference on Decision and Control*. 2014, pp. 6215–6220.

[51] A. Khanafer and T. Başar. “An Optimal Control Problem Over Infected Networks”. In: *1st International Conference of Control, Dynamic Systems, and Robotics*. 2014.

[52] F. Liu and M. Buss. “Optimal Control for Information Diffusion over Heterogeneous Networks”. In: *55th IEEE Conference on Decision and Control*. 2016, pp. 141–146.

[53] F. Liu and M. Buss. “Node-Based SIRS Model on Heterogeneous Networks: Analysis and Control”. In: *IEEE American Control Conference*. 2016, pp. 2852–2857.

[54] E. Ismagilova. *Electronic Word of mouth (eWOM) in the Marketing Context : A State of the Art Analysis and Future Directions*. SpringerBriefs in Business. 2017.

[55] F. Blanchini. “Set invariance in control”. In: *Automatica* 35.11 (1999), pp. 1747–1767.

[56] W.H. Fleming and R.W. Rishel. *Deterministic and stochastic optimal control*. Applications of mathematics. Springer-Verlag, 1975.

[57] E. Asano et al. "Optimal control of vaccine distribution in a rabies metapopulation model". In: *Mathematical Biosciences and Engineering* 5.2 (2008), pp. 219–238.

[58] T. T. Yusuf and F. Benyah. "Optimal control of vaccination and treatment for an SIR epidemiological model". In: *World Journal of Modeling and Simulation* 8.3 (2012), pp. 194–204.

[59] G. Birkhoff and G.C. Rota. *Ordinary Differential Equations*. Wiley, 1989.

[60] P. Erdős and A. Rényi. "On Random Graphs I." In: *Publicationes Mathematicae (Debrecen)* 6 (1959), pp. 290–297.

[61] M. G. Rabbat and R. Nowak. "Distributed Optimization in Sensor Networks". In: *3rd International Symposium on Information Processing in Sensor Networks*. 2004, pp. 20–27.

[62] H. Raja and W. U. Bajwa. "Cloud K-SVD: A Collaborative Dictionary Learning Algorithm for Big, Distributed Data". In: *IEEE Transactions on Signal Processing* 64.1 (2016), pp. 173–188.

[63] K. Yuan et al. “Exact Diffusion for Distributed Optimization and Learning—Part I: Algorithm Development”. In: *IEEE Transactions on Signal Processing* 67.3 (2019), pp. 708–723.

[64] S. Safavi et al. “Distributed Localization: A Linear Theory”. In: *Proceedings of the IEEE* 106.7 (2018), pp. 1204–1223.

[65] C. C. Moallemi and B. V. Roy. “Distributed optimization in adaptive networks”. In: *16th Advances in Neural Information Processing Systems Conference*. 2004, pp. 887–894.

[66] A. Agarwal, M. J. Wainwright, and J. C. Duchi. “Distributed Dual Averaging In Networks”. In: *23rd Advances in Neural Information Processing Systems Conference*. 2010, pp. 550–558.

[67] S. Shahrampour, S. Rakhlin, and A. Jadbabaie. “Online Learning of Dynamic Parameters in Social Networks”. In: *26th Advances in Neural Information Processing Systems Conference*. 2013, pp. 2013–2021.

[68] J. Tsitsiklis, D. P. Bertsekas, and M. Athans. “Distributed Asynchronous Deterministic and Stochastic Gradient Optimization Algorithms”. In: *IEEE Transactions on Automatic Control* 31.9 (1986), pp. 803–812.

[69] A. Nedić and A. Ozdaglar. “Distributed Subgradient Methods for Multi-Agent Optimization”. In: *IEEE Transactions on Automatic Control* 54.1 (2009), pp. 48–61.

[70] J. C. Duchi, A. Agarwal, and M. J. Wainwright. "Dual Averaging for Distributed Optimization: Convergence Analysis and Network Scaling". In: *IEEE Transactions on Automatic control* 57.3 (2012), pp. 592–606.

[71] K. Yuan, Q. Ling, and W. Yin. "On the Convergence of Decentralized Gradient Descent". In: *SIAM Journal on Optimization* 26.3 (2016), pp. 1835–1854.

[72] E. Wei and A. Ozdaglar. "Distributed Alternating Direction Method of Multipliers". In: *51st IEEE Conference on Decision and Control*. 2012, pp. 5445–5450.

[73] J. F. C. Mota et al. "D-ADMM: A Communication-Efficient Distributed Algorithm for Separable Optimization". In: *IEEE Transactions on Signal Processing* 61.10 (2013), pp. 2718–2723.

[74] K. I. Tsianos, S. Lawlor, and M. G. Rabbat. "Push-Sum Distributed Dual Averaging for convex optimization". In: *51st IEEE Conference on Decision and Control*. 2012, pp. 5453–5458.

[75] K. I. Tsianos. "The Role of the Network in Distributed Optimization Algorithms: Convergence Rates, Scalability, Communication/Computation Tradeoffs and Communication Delays". PhD thesis. Department of Electrical and Computer Engineering, McGill University, 2013.

[76] A. Nedić and A. Olshevsky. "Distributed Optimization Over Time-Varying Directed Graphs". In: *IEEE Transactions on Automatic Control* 60.3 (2015), pp. 601–615.

[77] D. Kempe, A. Dobra, and J. Gehrke. "Gossip-Based Computation of Aggregate Information". In: *44th IEEE Symposium on Foundations of Computer Science*. 2003, pp. 482–491.

[78] F. Benezit et al. "Weighted Gossip: Distributed Averaging Using Non-Doubly Stochastic Matrices". In: *IEEE International Symposium on Information Theory*. 2010, pp. 1753–1757.

[79] C. Xi, Q. Wu, and U. A. Khan. "On the distributed optimization over directed networks". In: *Neurocomputing* 267 (2017), pp. 508–515.

[80] C. Xi and U. A. Khan. "Distributed Subgradient Projection Algorithm Over Directed Graphs". In: *IEEE Transactions on Automatic Control* 62.8 (2016), pp. 3986–3992.

[81] K. Cai and H. Ishii. "Average consensus on general strongly connected digraphs". In: *Automatica* 48.11 (2012), pp. 2750–2761.

[82] J. Xu et al. "Augmented Distributed Gradient Methods for Multi-agent Optimization Under Uncoordinated Constant Stepsizes". In: *54th IEEE Conference on Decision and Control*. 2015, pp. 2055–2060.

[83] G. Qu and N. Li. “Harnessing Smoothness to Accelerate Distributed Optimization”. In: *IEEE Transactions on Control of Network Systems* 5.3 (2018), pp. 1245–1260.

[84] A. Nedić, A. Olshevsky, and W. Shi. “Achieving Geometric Convergence for Distributed Optimization over Time-Varying Graphs”. In: *SIAM Journal on Optimization* 27.4 (2017), pp. 2597–2633.

[85] M. Zhu and S. Martínez. “Discrete-time dynamic average consensus”. In: *Automatica* 46.2 (2010), pp. 322–329.

[86] C. Xi, R. Xin, and U. A. Khan. “ADD-OPT: Accelerated Distributed Directed Optimization”. In: *IEEE Transactions on Automatic Control* 63.5 (2018), pp. 1329–1339.

[87] C. Xi et al. “Linear Convergence in Optimization Over Directed Graphs With Row-Stochastic Matrices”. In: *IEEE Transactions on Automatic Control* 63.10 (2018), pp. 3558–3565.

[88] R. Xin, C. Xi, and U. A. Khan. “FROST – Fast row-stochastic optimization with uncoordinated step-sizes”. In: *EURASIP Journal on Advances in Signal Processing* 2019.1 (2019).

[89] W. Shi et al. “EXTRA: An Exact First-Order Algorithm for Decentralized Consensus Optimization”. In: *SIAM Journal on Optimization* 25.2 (2015), pp. 944–966.

[90] C. Xi and U. A. Khan. “DEXTRA: A Fast Algorithm for Optimization Over Directed Graphs”. In: *IEEE Transactions on Automatic Control* 62.10 (2017), pp. 4980–4993.

[91] R. Xin and U. A. Khan. “A Linear Algorithm for Optimization Over Directed Graphs With Geometric Convergence”. In: *IEEE Control Systems Letters* 2.3 (2018), pp. 325–330.

[92] G. Qu and N. Li. “Accelerated distributed Nesterov gradient descent”. In: *arXiv preprint arXiv:1705.07176* (2017).

[93] P. Richtárik N. Loizou. “Momentum and Stochastic Momentum for Stochastic Gradient, Newton, Proximal Point and Subspace Descent Methods”. In: *arXiv preprint arXiv:1712.09677* (2017).

[94] R. Xin and U. A. Khan. “Distributed heavy-ball: A generalization and acceleration of first-order methods with gradient tracking”. In: *arXiv preprint arXiv:1808.02942* (2018).

[95] Y. Tian et al. “ASY-SONATA: Achieving geometric convergence for distributed asynchronous optimization”. In: *arXiv preprint arXiv:1803.10359* (2018).

[96] I. Lobel and A. Ozdaglar. “Distributed Subgradient Methods for Convex Optimization Over Random Networks”. In: *IEEE Transactions on Automatic Control* 56.6 (2011), pp. 1291–1306.

[97] A. Nedic and A. Olshevsky. "Distributed optimization of strongly convex functions on directed time-varying graphs". In: *IEEE Global Conference on Signal and Information Processing*. 2013, pp. 329–332.

[98] Q. Lü, H. Li, and D. Xia. "Geometrical convergence rate for distributed optimization with time-varying directed graphs and uncoordinated stepsizes". In: *Information Sciences* 422 (2018), pp. 516–530.

[99] J. Xu et al. "Convergence of Asynchronous Distributed Gradient Methods Over Stochastic Networks". In: *IEEE Transactions on Automatic Control* 63.2 (2018), pp. 434–448.

[100] I. Lobel, A. Ozdaglar, and D. Feijer. "Distributed multi-agent optimization with state-dependent communication". In: *Mathematical Programming* 129.2 (2011), pp. 255–284.

[101] D. Jakovetić, J. M. F. Xavier, and J. M. F. Moura. "Convergence Rates of Distributed Nesterov-Like Gradient Methods on Random Networks". In: *IEEE Transactions on Signal Processing* 62.4 (2014), pp. 868–882.

[102] D. Jakovetić et al. "Convergence rates for distributed stochastic optimization over random networks". In: *arXiv preprint arXiv:1803.07836* (2018).

[103] M. Eisen, A. Mokhtari, and A. Ribeiro. "Decentralized Quasi-Newton Methods". In: *IEEE Transactions on Signal Processing* 65.10 (2017), pp. 2613–2628.

[104] M.J.D. Powell. "Some global convergence properties of a variable metric algorithm for minimization without exact line searches". In: *Nonlinear Programming, SIAM-AMS Proceedings* 9.1 (1976).

[105] R. Byrd, J. Nocedal, and Y. Yuan. "Global Convergence of a Class of Quasi-Newton Methods on Convex Problems". In: *SIAM Journal on Numerical Analysis* 24.5 (1987), pp. 1171–1190.

[106] J. Nocedal and S. J. Wright. *Numerical Optimization.* Springer Series in Operation Research and Financial Engineering, 2006.

[107] T. Wu et al. "Decentralized Consensus Optimization With Asynchrony and Delays". In: *IEEE Transactions on Signal and Information Processing over Networks* 4.2 (2018), pp. 293–307.

[108] M. Assran and M. G. Rabbat. "Asynchronous Subgradient-Push". In: *arXiv preprint arXiv:1803.08950* (2018).

[109] J. N. Tsitsiklis. "Problems in Decentralized Decision Making and Computation". PhD thesis. Massachusetts Institute of Technology, 1984.

[110] A. Nedić and J. Liu. “On convergence rate of weighted-averaging dynamics for consensus problems”. In: *IEEE Transactions on Automatic Control* 62.2 (2017), pp. 766–781.

[111] P. D. Powell. “Calculating Determinants of Block Matrices”. In: *arXiv preprint arXiv:1112.4379* (2011).

[112] C.M. Bishop. *Pattern Recognition and Machine Learning*. Information Science and Statistics. Springer, 2016.

[113] Y. LeCun and C. Cortes. *The MNIST database of handwritten digits*. `http://yann.lecun.com/exdb/mnist/`. 1998.

[114] T. Hastie, R. Tibshirani, and J. H. Friedman. *The Elements of Statistical Learning: Data Mining, Inference, and Prediction*. Springer Series in Statistics. Springer, 2009.